EVALUATION OF FLOOR VIBRATION IN AN EXISTING BUILDING

A THESIS SUBMITTED TO
THE GRADUATE SCHOOL OF NATURAL AND APPLIED SCIENCES
OF
MIDDLE EAST TECHNICAL UNIVERSITY

BY

YAVUZ SEMERDÖKEN

IN PARTIAL FULFILLMENT OF THE REQUIREMENTS
FOR
THE DEGREE OF MASTER OF SCIENCE
IN
CIVIL ENGINEERING

SEPTEMBER 2019

Approval of the thesis:

EVALUATION OF FLOOR VIBRATION IN AN EXISTING BUILDING

submitted by **YAVUZ SEMERDÖKEN** in partial fulfillment of the requirements for the degree of **Master of Science in Civil Engineering Department, Middle East Technical University** by,

Prof. Dr. Halil Kalıpçılar
Dean, Graduate School of **Natural and Applied Sciences**   _____

Prof. Dr. Ahmet Türer
Head of Department, **Civil Engineering**   _____

Prof. Dr. Ahmet Yakut
Supervisor, **Civil Engineering, METU**   _____

Assoc. Prof. Dr. Ozan Cem Çelik
Co-Supervisor, **Civil Engineering, METU**   _____

Examining Committee Members:

Prof. Dr. Kağan Tuncay
Civil Engineering, METU   _____

Prof. Dr. Ahmet Yakut
Civil Engineering, METU   _____

Assoc. Prof. Dr. Ozan Cem Çelik
Civil Engineering, METU   _____

Assoc. Prof. Dr. Alper Aldemir
Civil Engineering, Hacettepe University   _____

Assist. Prof. Dr. Abdullah Dilsiz
Civil Engineering, Ankara Yıldırım Bayazıt University   _____

Date: 05.09.2019

I hereby declare that all information in this document has been obtained and presented in accordance with academic rules and ethical conduct. I also declare that, as required by these rules and conduct, I have fully cited and referenced all material and results that are not original to this work.

Name, Surname: Yavuz Semerdöken

Signature:

ABSTRACT

EVALUATION OF FLOOR VIBRATION IN AN EXISTING BUILDING

Semerdöken, Yavuz
Master of Science, Civil Engineering
Supervisor: Prof. Dr. Ahmet Yakut
Co-Supervisor: Assoc. Prof. Dr. Ozan Cem Çelik

September 2019, 105 pages

Vibration serviceability is a major concern in the design of lighter floor systems of newer buildings. Floor vibrations due to walking and rhythmic movements of the occupants should not exceed threshold levels for the comfort of occupants and the protection of sensitive equipment in the buildings. The objective of this study is to evaluate the floor vibration problem reported in a six-story reinforced concrete with two basement floors office building. First, structural system dynamic properties of the building were identified using its available ambient vibration records. The finite element model of the building was developed and calibrated to match the identified natural vibration frequencies. Then, the vibration records of the floors at which the problem was reported were analyzed to examine if threshold levels stipulated in design codes had been exceed. Finally, finite element simulations and the in-situ floor vibration data for the floor response due to walking of the occupants were compared with the threshold levels recommended in the AISC Floor Vibrations Due to Human Activity.

Keywords: Dynamic Properties, Dynamic Tests, Existing Buildings, Floor Vibrations, System Identification

ÖZ

MEVCUT BİR BİNANIN DÖŞEME TİTREŞİMİNİN DEĞERLENDİRİLMESİ

Semerdöken, Yavuz
Yüksek Lisans, İnşaat Mühendisliği
Tez Danışmanı: Prof. Dr. Ahmet Yakut
Ortak Tez Danışmanı: Doç. Dr. Ozan Cem Çelik

Eylül 2019, 105 sayfa

Yeni binaların hafif döşeme sistemlerinin tasarımında titreşim esnasındaki kullanılabilirliği önemli bir sorundur. Bina sakinlerinin yürüme ve ritmik hareketlerinden dolayı oluşan döşeme titreşimleri, bu kişilerin konforu ve binalardaki hassas ekipmanların korunması için limit değerleri aşmamalıdır. Bu çalışmanın amacı, iki bodrum kata sahip altı katlı betonarme bir ofis binasında rapor edilmiş olan döşeme titreşim probleminin değerlendirilmesidir. İlk olarak, binanın yapısal sistem dinamik özellikleri mevcut ortam titreşim kayıtları kullanılarak belirlenmiştir. Binanın sonlu elemanlar modeli geliştirilmiş ve belirlenmiş olan doğal titreşim frekanslarını elde etmek için model kalibre edilmiştir. Daha sonra, problemin bildirildiği döşemelerin titreşim kayıtları yönetmeliklerde öngörülen limit değerlerin aşılıp aşılmadığını belirlemek için analiz edilmiştir. Son olarak, bina sakinlerinin yürümesinden dolayı meydana gelen döşeme tepkisi için sonlu elemanlar simülasyonları ve yerinde alınan döşeme titreşim kayıtları AISC'de tavsiye edilen limit değerler ile karşılaştırılmıştır.

Anahtar Kelimeler: Dinamik Özellikler, Dinamik Testler, Döşeme Titreşimleri, Mevcut Binalar, Sistem Tanımlaması

Dedicated to the strongest persons I know: my mother and father.

ACKNOWLEDGEMENTS

First of all, I would like to express my sincere gratitude to my supervisor Dr. Ahmet Yakut for his guidance, advice, criticism, encouragements, and insight throughout the research.

Besides my advisor, I would like to thank my co-supervisor Dr. Ozan Cem Çelik for his support, motivation, guidance, and many other things. You have set an example of excellence as a researcher, mentor, instructor, and role model.

Moreover, I would like to thank the rest of my thesis committee: Dr. Kağan Tuncay, Dr. Alper Aldemir, and Dr. Abdullah Dilsiz for their insightful comment, advice, and encouragement.

I thank my friends and colleagues: Erhan Budak, İsmail Ozan Demirel, Oğuzhan Gümüş, Okan Koçkaya, and Casim Yazıcı for their friendship and the times we spent together.

My special thanks go to Dr. Eren Yağmur, Yunus İşıkli, and my brother Selim Semerdöken for their supports, constant encouragements, and devoting precious times.

Finally and most of all, I would like to thank to my family for providing me with unfailing support and continuous encouragement throughout my life. This accomplishment would not have been possible without you.

TABLE OF CONTENTS

LIST OF TABLES

TABLES

LIST OF FIGURES

FIGURES

CHAPTER 1

INTRODUCTION

1.1. Background

Vibration serviceability is a major concern in the design of buildings with flexible floor systems. Floor vibrations due to machinery in such buildings and daily human activities such as walking, dancing and jumping should remain below the tolerance limits for human comfort and sensitive equipment (Bachmann and Ammann, 1987; Murray, 1991). Otherwise, floor vibrations can cause serviceability as well as safety problems. For example, the Broughton Suspension Bridge in Manchester, England collapsed due to the structural vibrations caused by marching soldiers on April, 1831 (Prakash and Anil, 2014). The Techno Mart, a 39-story shopping mall, in Seoul, Korea had to be evacuated due to the floor vibrations caused by people training in a fitness center in the building (Chung et al., 2016). Excessive vibrations due to rhythmic activities such as people dancing and jumping simultaneously, which even led to collapse of floors, have also been reported in other buildings.

Today, buildings have been designed and constructed with thinner slabs with the developing construction technology. These flexible floors make people feel insecure and uncomfortable due to unwanted vibrations (Gajalakshmi et al., 2015). Floor vibration problems are not limited to steel or composite floor systems (Debney and Willford, 2009). It is imperative to control both the deflection under existing loads and the level of vibration caused by dynamic loads in engineering structures. The state-of-the-art finite element platforms can be used to simulate the behavior of floor systems under dynamic loads. However, the assumptions in developing the finite element structural models have to be verified with the experimental data. The dynamic properties of the floor systems (natural vibration frequencies, vibration mode shapes,

1

and modal damping ratios) identified from in-situ dynamic tests can be used to validate the assumptions in material properties, boundary conditions, and cross sectional dimensions of the members.

Dynamic tests are divided into three groups as forced vibration (Shabbir and Omenzetter, 2008; Yu et al., 2008; Celik et al., 2015; Celik, 2016), ambient vibration (Crawford and Ward, 1964; Ivanovic et al., 2000; Skolnik et al., 2006), and seismic monitoring (Foutch et al., 1975; Trifunac et al., 2001; Celebi, 2013) depending on the source of vibration. In ambient vibration tests, structural vibrations due to wind, road traffic, and human activity are recorded, and upon signal processing of the records both in time and frequency domain (Brincker et al., 2001), structural system dynamic properties are identified. Ambient vibration tests do not interfere with the daily use of the structure (Ventura and Horyna, 2000). In forced vibration tests, a sinusoidal excitation is applied to the building by a shaker mounted on upper floors. These tests are more straightforward and costly than ambient vibration tests.

1.2. Objectives and Scope

This study focuses on the floor vibration problem reported in a six-story reinforced concrete (RC) office building in Ankara, Turkey. The building was strengthened by replacing the interior hollow-brick partition walls with structural walls and by jacketing of interior columns in 2004. Ambient vibration records of the building were taken in 2017.

The objectives of this study are to identify the structural system and floor system dynamic properties of the case study building using its available ambient vibration records and to compare the level of human-induced floor vibrations with the tolerance limit for human comfort. The critical steps to achieve these objectives are listed below:

(1) Identify the structural system dynamic properties of the building using its available ambient vibration records.

(2) Develop a three-dimensional finite element structural model of the building and calibrate the model with the system identification data.

(3) Identify the dynamic properties of the floor system where the vibration problem was reported using the available floor vibration records.

(4) Perform an assessment of the floor vibration problem using AISC (2016) design guidelines.

(5) Simulate the walking-induced floor vibrations using the developed structural model.

(6) Recommend retrofit strategies for the floor system to reduce the excessive vibrations.

1.3. Thesis Outline

This chapter has presented the context of the research and the objectives and scope of the study.

Chapter 2 presents the critical appraisal of the state of the art on system identification from ambient vibration records and assessment of floor vibrations.

Chapter 3 describes the case study building and its instrumentation scheme.

Chapter 4 presents the analysis of the ambient vibration records, the finite element structural model of the building, and the eigenvalue analysis. The identified structural system dynamic properties from the ambient vibration records are compared with those determined from the eigenvalue analysis.

Chapter 5 presents the evaluation of floor vibration based on measurements and analyses under the walking load on the ground and second floors. It also presents floor vibration calculations and comparisons with limits after modifications applied to reduce the floor vibration.

Finally, Chapter 6 presents the major conclusions drawn from this study.

CHAPTER 2

LITERATURE REVIEW

2.1. Overview

This chapter summarizes and discusses the previous experimental and analytical studies in the areas of ambient vibration testing and floor vibrations.

2.2. Ambient Vibration Testing

Dynamic properties of structural systems — natural vibration frequencies, vibration mode shapes, and modal damping ratios — can be identified from their ambient vibration records. These modal properties are crucial for researchers and engineers for structural health monitoring, understanding the structural behavior of the as-built and retrofitted buildings, evaluating the seismic risk of structures, improving the modeling of structural systems, and advancing the building codes (Michel et al., 2008; Celik et al., 2015).

Structural analyses of various structures including buildings, stadiums, dams, nuclear power plants, and historical palaces have been performed by different researchers using various modeling methods. The ambiguities in structural modeling were resolved by making different assumptions, which are usually validated through experimental data. In the literature, there are various studies in updating the analytical models of engineered structures based on their identified structural system dynamic properties from ambient vibration records. The acceleration values for ambient vibration tests are expected to range from 10^{-7} to 10^{-4} g. Therefore, information about the elastic behavior of the structure can be obtained from the low level of the shaking.

In-situ dynamic tests such as ambient and forced vibration tests have been performed for almost a decade in California. The U.S. Coast and Geodetic Survey determined the

fundamental periods of several buildings from their ambient vibration records in the early 1930s (Carder, 1936). Ambient vibration testing was used to identify higher vibration modes after 30 years (Crawford and Ward, 1964; Ward and Crawford, 1966).

Trifunac (1970a, 1970b) identified the structural system dynamic properties of a 22- and a 39-story steel frame building from ambient vibration records. These properties agree quite well with those identified from their previous forced vibration tests (Trifunac, 1972).

Udwadia and Trifunac (1973) compared the dynamic properties of four buildings (a 22-story moment-resisting steel frame, a 39-story moment-resisting steel frame, a 9-story reinforced concrete building with a central core wall, and a 9-story moment-resisting steel frame) identified from their pre- and post-earthquake ambient vibration records. Forced vibration tests show frequencies about 4% smaller than those obtained from ambient vibration tests for the first building. After the San Fernando earthquake, the reduction of the natural frequencies of the second building is approximately 15%, 19%, and 17% in the first translational mode along the EW, NS directions and first torsional mode, respectively. For the third building, the reduction of the natural frequencies were also calculated as 14% and 9% in the first and second EW modes while 5% for the first mode in the stiffer NS direction.

Celebi and Safak (1991) measured translational, torsional, and rocking motions of the Transamerica Building. This building is a vertically tapered multi-story steel structure. The instrumentation system consisted of 13 uniaxial accelerometers and 3 triaxial accelerometers According to analysis results of recorded earthquake response data, the dominant frequency is 0.28 Hz in both the NS and EW directions. The rocking frequency is 1.8 Hz in the EW direction and 2.0 Hz in the NS direction.

Ivanovic et al. (2000) reported the results of two ambient vibration records after the 1994 Northbridge earthquake and aftershocks of this earthquake to a seven-story reinforced concrete building in California. Changes in the modal frequencies were expected due to differences in the state of the structure like addition of wooden braces.

Three out of four modal frequencies in the EW directions were increased about 10% according to the first state of the structure. The first transverse and torsional mode frequencies did not change while the frequency of the second transverse mode in the NS direction increased approximately 10%.

Ventura et al. (2002) performed an ambient vibration test on the One Wall Center Tower, the tallest building in Vancouver, Canada. Dynamic properties associated with the first eight vibration modes were identified using the frequency domain decomposition (FDD) method (Brincker et al., 2001). A finite element model was developed using commercially computer program. The first model demonstrates that the fundamental frequencies differed by approximately 15%. The model was therefore updated by modeling the façade and comparable modal frequencies were determined.

Ventura et al. (2003) investigated the dynamic properties of a 52- and a 54-story instrumented steel frame building by analyzing their ambient vibration records using the FDD method. They obtained the first six modes and damping ratios of both structures using the FDD method. The damping values are determined below 5%. This research demonstrates that comparable ground shaking at the base of two neighboring tall structures of similar height and floor area can generate considerably distinct reaction based on the type of lateral force resisting system (52-story building builds on a perimeter tube system, 54-story building builds on a spine structure with outrigger frames.

Gentile and Sais (2007) performed ambient vibration studies on a historic masonry tower to evaluate its structural condition and to determine the presence of major cracks in the load-bearing walls. Five vibration modes within the frequency range 0-10 Hz were determined in this study.

Baspolat et al. (2013) determined the dynamic properties of the Deriner Dam, the highest concrete arch dam in Turkey, from its ambient vibration records. The first five natural frequencies of the dam (1.7–4.5 Hz), mode shapes and damping ratios were determined. The damping ratios were below 5%.

Soyoz et al. (2013) performed ambient vibration tests on a six-story reinforced concrete building at Bogazici University to investigate the impact of seismic retrofitting on its modal properties. Ambient vibrations were recorded before, during, and after the seismic retrofit. They also performed forced vibration tests on the building and compared the results with those from ambient vibration tests after the retrofit. After the retrofit, the modal frequencies increased about 96%, 90%, and 88% for the first, second, and third mode while damping ratios did not change significantly.

Sampaio and Souza (2015) performed four ambient vibration tests on different days to determine the vibration problems that occurred during pile driving for a 17-story residential building. In this study, the first test was performed to obtain the dynamic properties of the building. The second test was conducted for modal analysis of the 11th floor slabs. Comfort analysis was performed according to ISO 2301 in the second and third ambient vibration tests. The analyses indicated that vibrations were disturbing for the residents.

2.3. Floor Vibrations

Vibration occurs in the floor systems of many engineering structures such as stadiums, gymnasiums, and office buildings due to human activities. In some cases, these vibrations are annoying for building users and become unacceptable for their safety. Floor vibrations occur due to human activity, longer floor spans, lower natural frequency, etc. (Allen, 1990).

The first study on vibration problems in floor systems caused by human activities was made by Tredgold in 1828. Tredgold (1828) suggested that long-span beams be deep enough to avoid shaking of objects while walking on the floor.

The sensitivity level varies with the method and suggestions have been released by various authors. Reiher and Meister (1931) recorded one of the earliest. These were human reactions determined by standing topics on a shaker table with topics and subjecting them to steady-state motion. From this data, the chart called the Reiher-Meister scale was created.

Lenzen (1966) stated that the floor vibrations under dynamic loads are related to the damping and mass of the system. In addition to deflection control, Lenzen pioneered the creation of a new calculation method based on the floor acceleration. He also proposed that the amplitudes of the Reiher-Meister scale be lowered by a factor of ten to account for the transient nature of floor vibrations and modified the Reiher-Meister scale as shown in Figure 2.1. The difference between the scales is due to the difference in human perception to transient vibrations as compared to steady state vibrations.
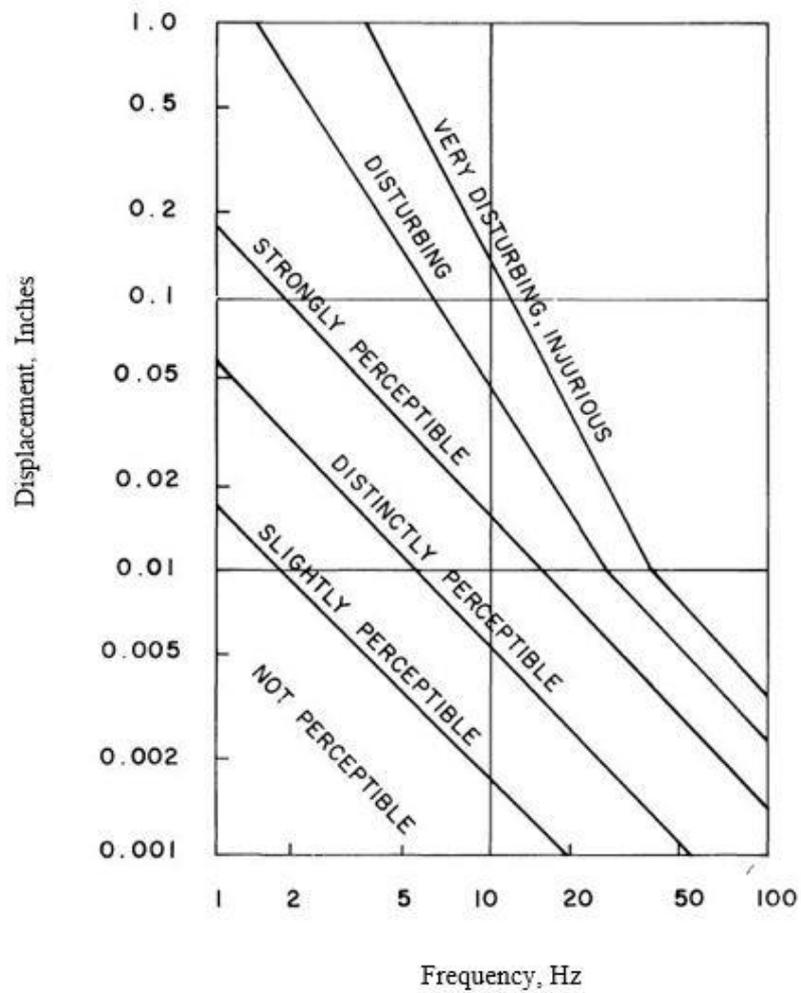
Figure 2.1. Modified Reiher-Meister Scale (Lenzen, 1966)

In 1976, Allen and Rainer published impact-response experiments on floor systems. Allen and Rainer (1976) developed an empirical equation for the effects of mass and damping on vibration of the floor system based on these experiments. Murray (1981; 1991) later expanded this subject by examining on many different kinds of floor systems.

International Organization for Standardization (ISO, 1989) provided the acceleration limits for floor vibration in terms of frequency of floor as shown in Figure 2.2. This plot demonstrates the suggested limits of maximum acceleration for human toleration due to walking.
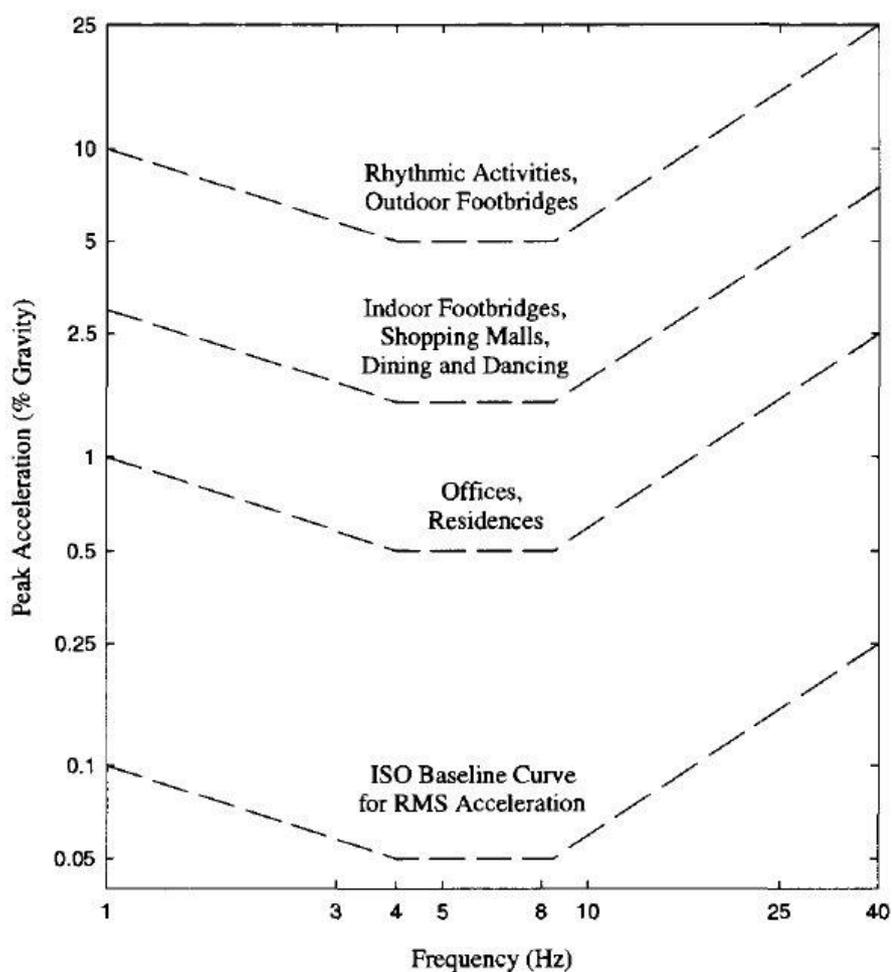
Figure 2.2. Recommended peak acceleration for human tolerance (ISO 2631-2)

In 1991, the US Structural Steel Education Council published a guide for preventing floor vibration. In this study, human-induced vibrations were defined, the types of human activities were classified, factors affecting the vibration response of floors were determined, and floor structural system parameters were calculated (Naeim, 1991).

In 1993, Allen and Murray suggested a method for designing floor systems under the influence of walking (Allen and Murray, 1993).

In addition to these two regulations, the guidelines of AISC (2016) and EN suggested techniques for calculating under the impact of human activity to prevent vibration in the floor system. These two guidelines are currently being used as the latest techniques for vibration problems.

In 2001, Murray presented precautions for avoiding excessive floor vibrations in office buildings (Murray, 2001).

Davenny established that vibration originated by footfall is frequently the basic reason of floor vibration compared to machine vibration. Building floor vibrates at its natural frequency in response to a footstep impulse, and the vibration is maximum at the middle of the floor while it is minimum near the supporting columns (Davenny, 2010). The vibrations originated by footfalls are also associated with the speed of walking. The suggested values for walking frequency and speed are given by Arup (2004) as shown in Table 2.1.

Table 2.1. *Footfalls rate (Arup, 2004)*

Frequency (Hz)	Designation
1.5–1.8	"Normal walking" for cellular areas
1.8–2.0	Someone who is in hurry
2.0–2.4	"A very brisk pace" considered likely in corridors

In recent years, studies have been carried out on the effects of vibrations caused by rhythmic activities and investigations have been made to compare the analytical and theoretical methods proposed in guidelines. Examples are the investigation of the vibrations in the floors of the Tin Shui Wai Public Library (Li et al., 2011) and the reaction of a slab subjected to forced transient vibration caused by rhythmic dance (Smith and Korman, 2012).

CHAPTER 3

DESCRIPTION OF THE BUILDING AND ITS INSTRUMENTATION

3.1. Introduction

Within the scope of this thesis, available ambient and human-induced vibration records of a reinforced concrete (RC) building were analyzed. This chapter presents the description of the building and its instrumentation scheme.

3.2. Building Description

The investigated building is a six-story RC office building with two basement floors (see Fig. 3.1), located in Cankaya district of Ankara, Turkey. It is 23.5 m tall (including the first basement floor; see Fig. 3.2) and has a nearly square floor plan (21 × 22 m; see Fig. 3.3). The building was a four-story moment-resisting frame building with a basement floor when its construction was completed in 1952. In 1972, two floors and a partial basement floor were added. The building was strengthened with 0.25 m thick cast-in-place RC shear walls which were located four in the EW direction and four in the NS direction (see Fig. 3.3), which are continuous from the foundation to the top of the building. The interior columns were strengthened by RC jacketing. Total column cross-sectional area to floor area ratio is 1.8 percent for the first five floors whereas it is 2.2 percent for the ground floor and 2.8 percent for the basement floor. During the strengthening, the interior hollow clay brick walls were removed for reducing the mass of the building. Figure 3.3 presents the floor plans of the building after strengthening. Elevator shaft walls are 0.20 m thick. The floor slabs are 0.14 m thick and the roof slab is 0.12 m thick.

(a)   (b)

(c)

Figure 3.1. External view of the building (a) front view, (b) NW view, (c) back view
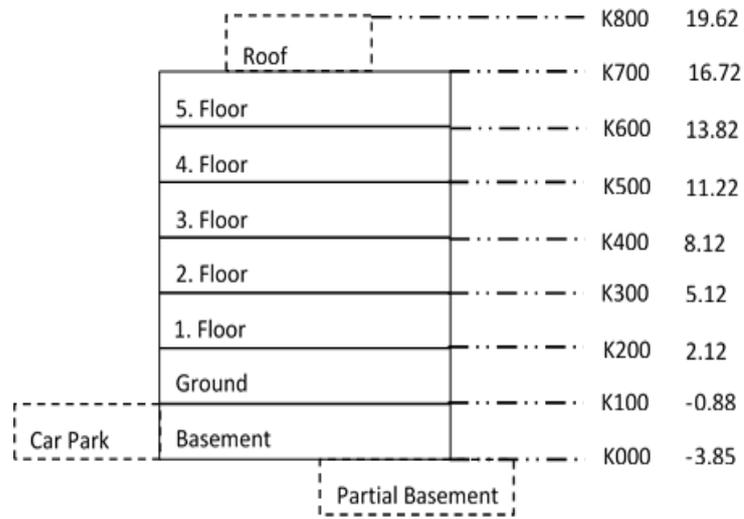
Figure 3.2. Floor labels and elevations (in m)
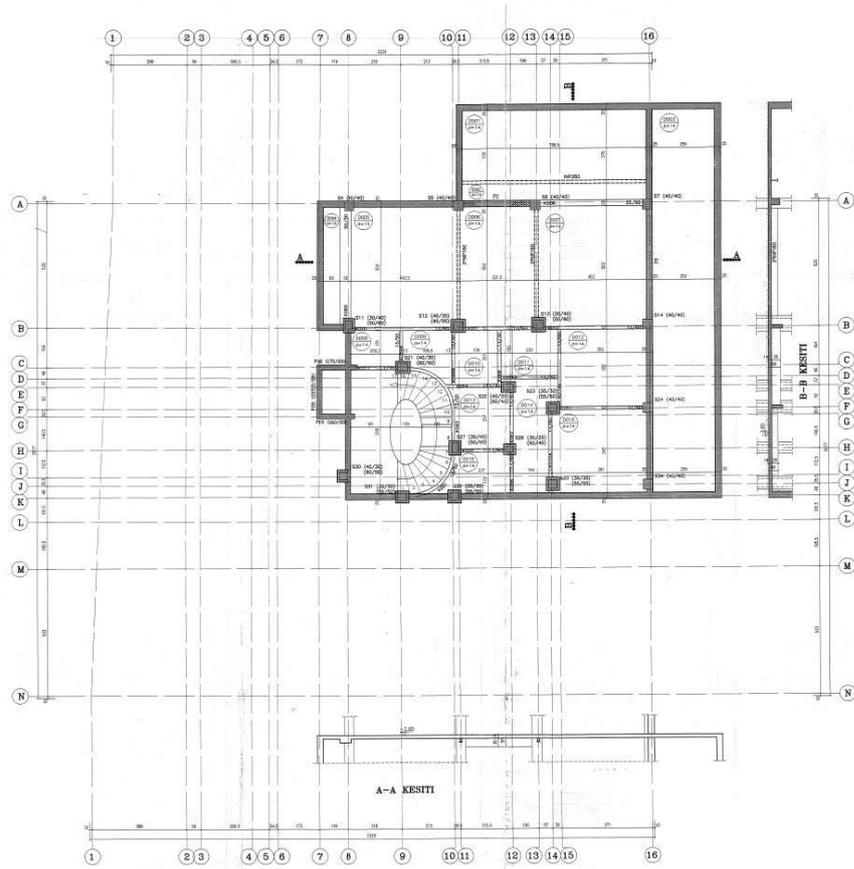
(a) partial basement floor (-3.85)

Figure 3.3. Plan views

15
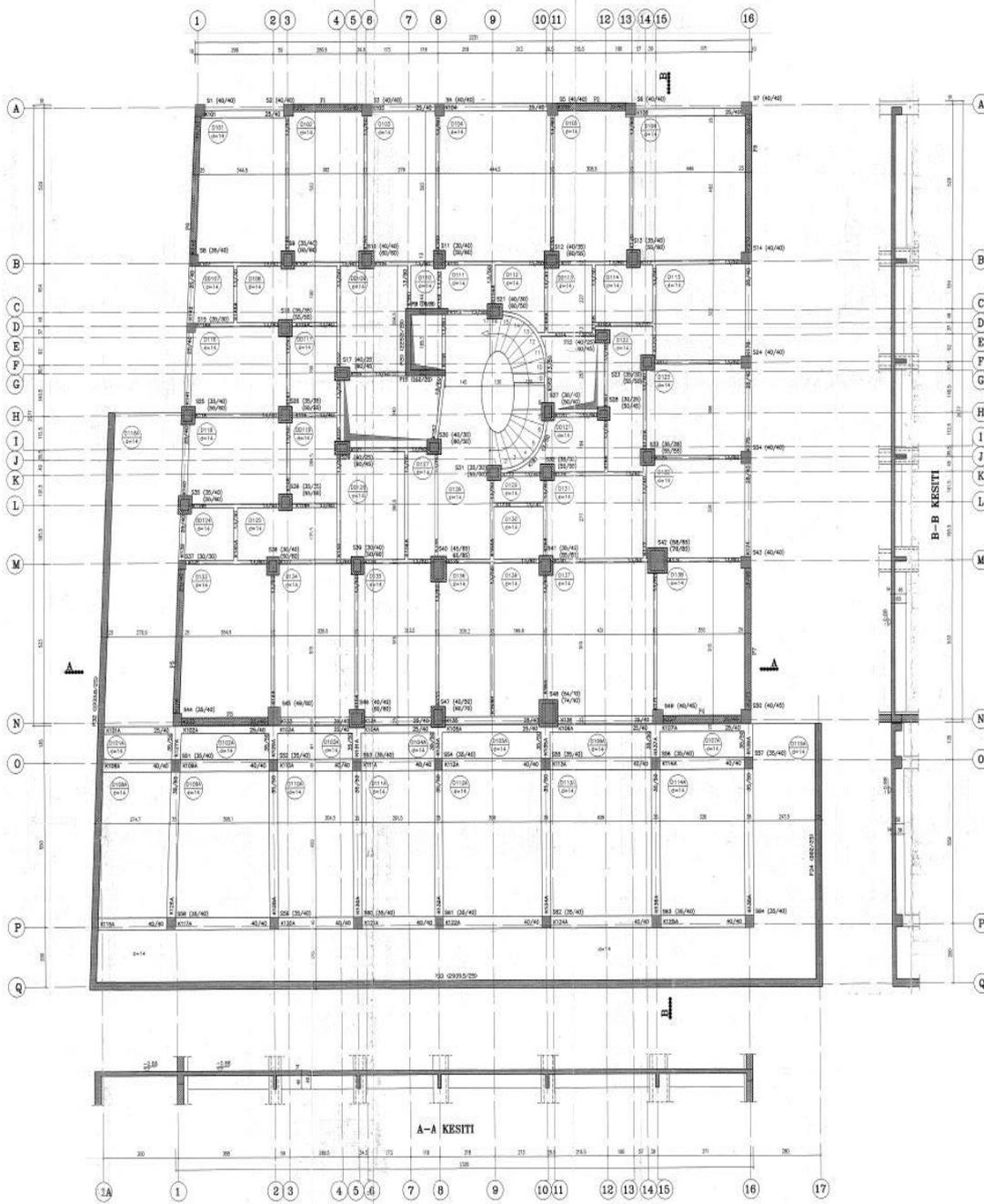
(b) basement floor (-0.88)

Figure 3.3. Plan views (continued)

16
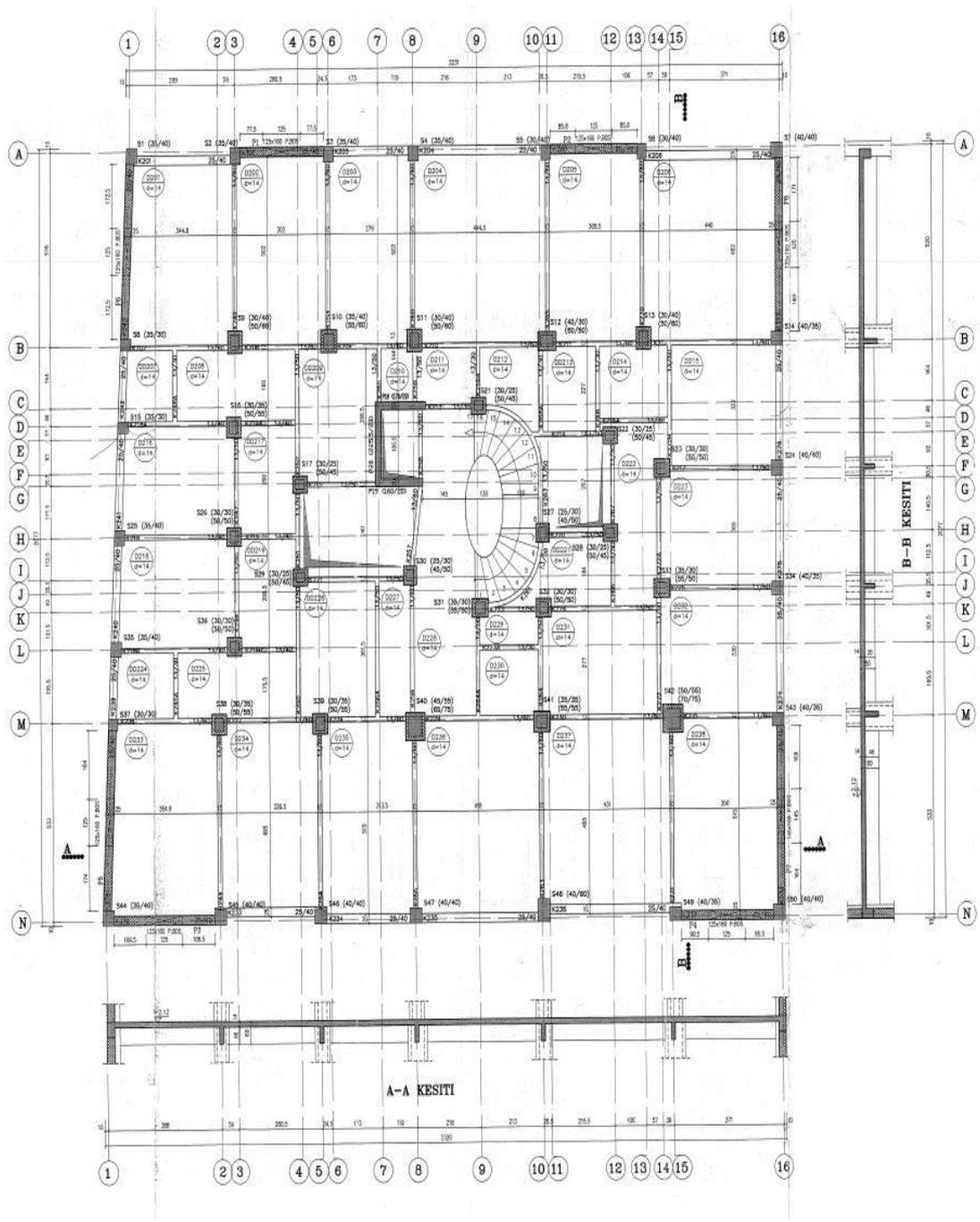
(c) ground floor (+2.12)

Figure 3.3. Plan views (continued)

17
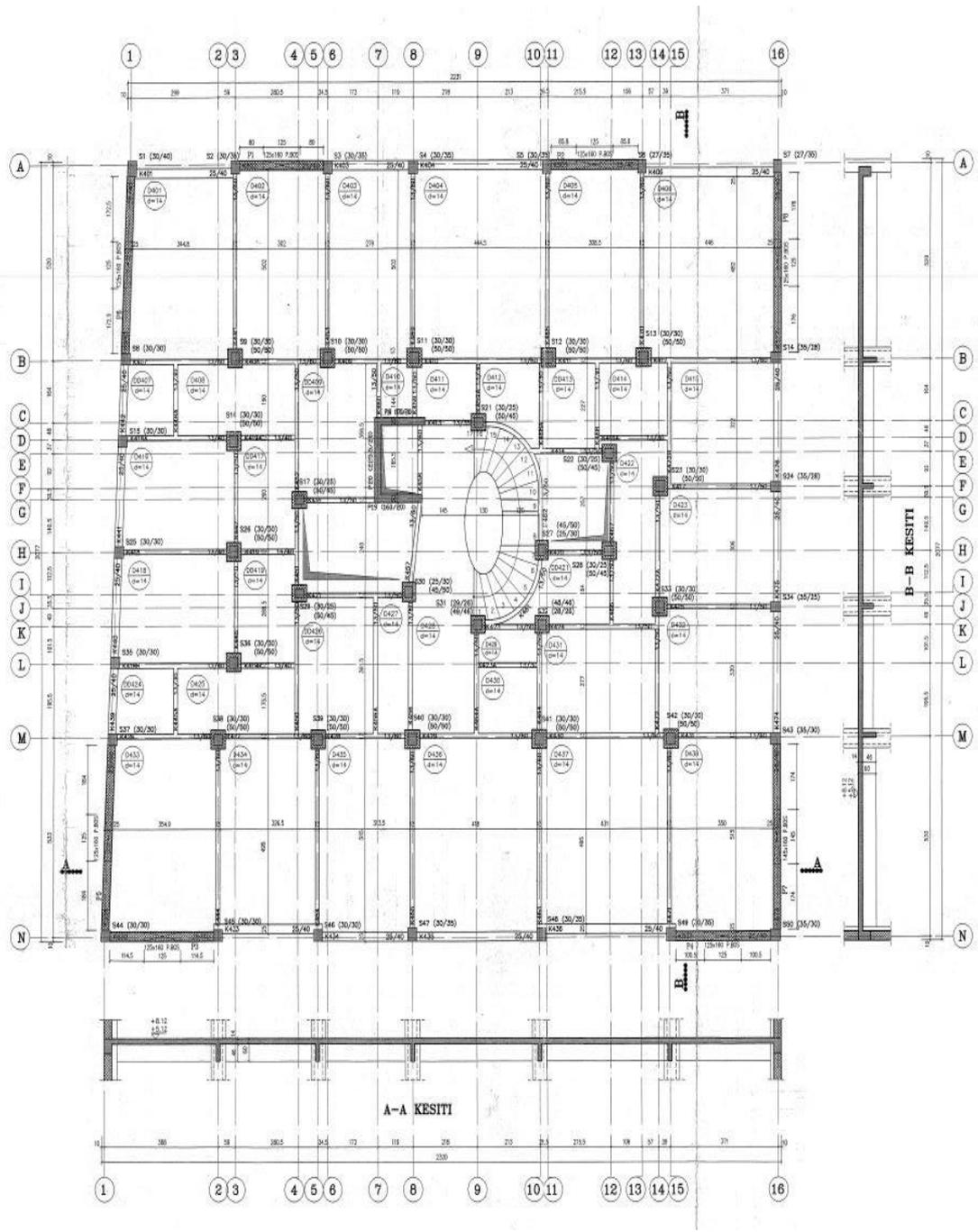
(d) first and second floors (+5.12 and +8.12)

Figure 3.3. Plan views (continued)

18
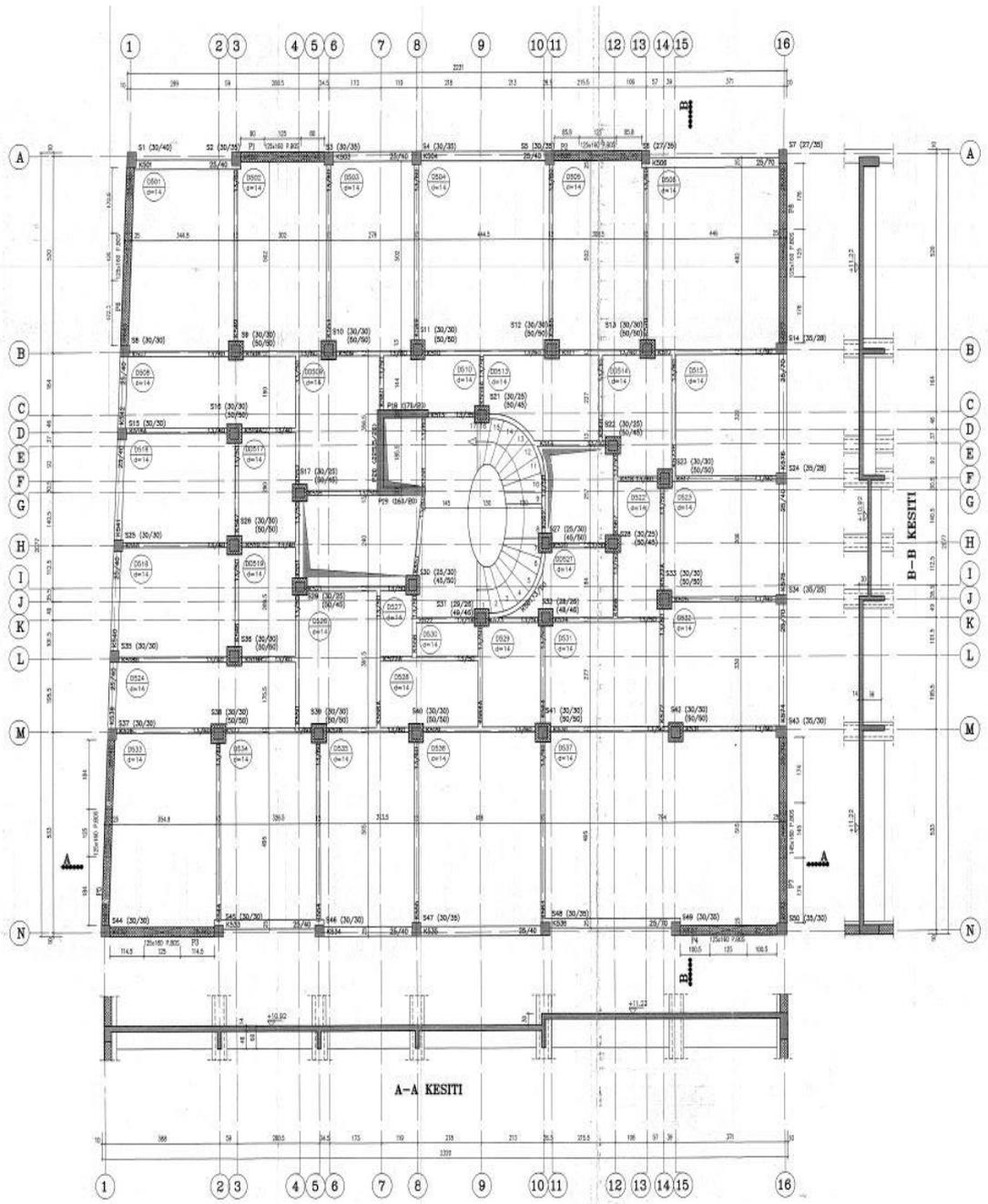
(e) third floor (+11.22)

Figure 3.3. Plan views (continued)

19
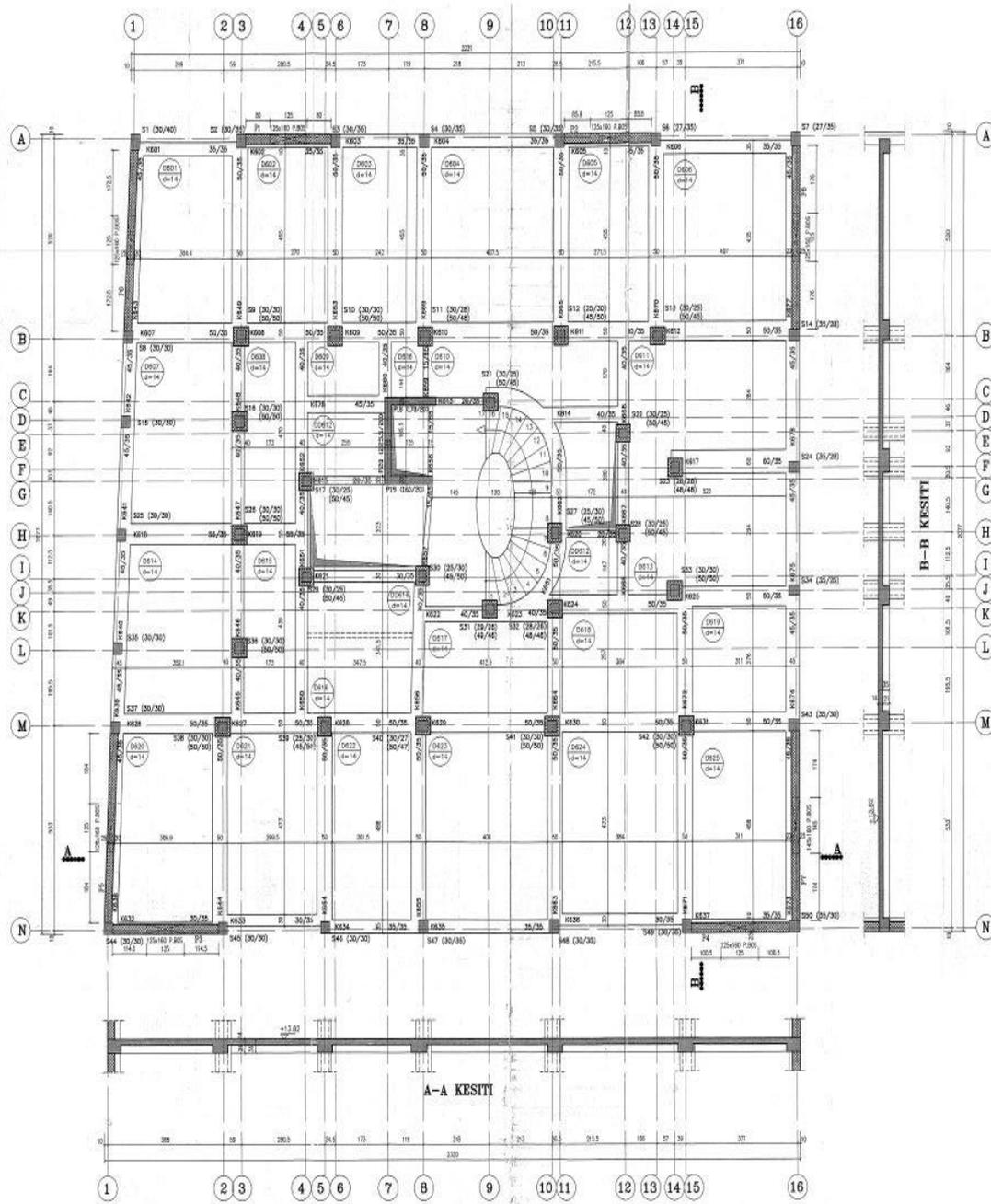
(f) fourth floor (+13.82)

Figure 3.3. Plan views (continued)

20
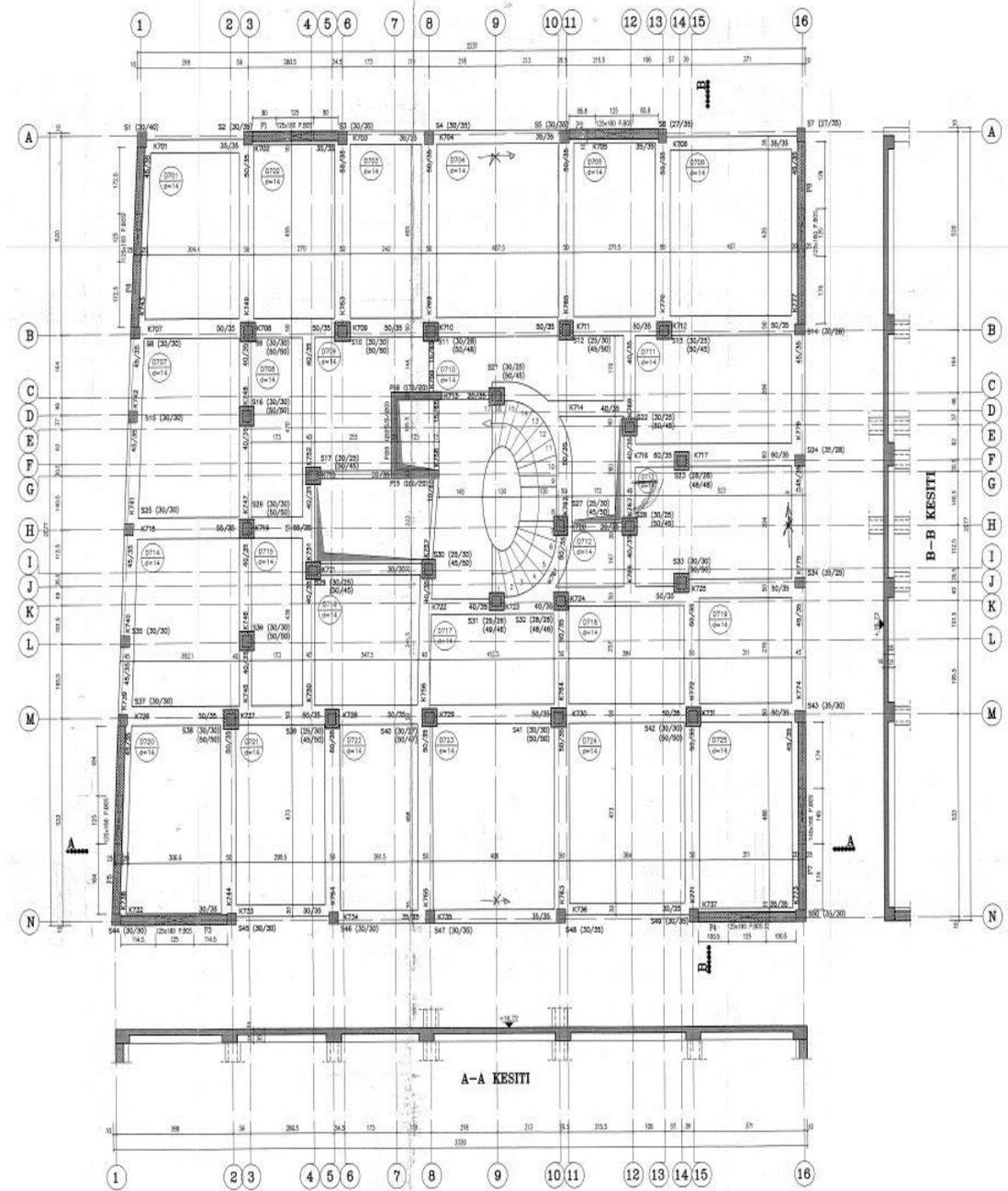
(g) fifth floor (+16.72)

Figure 3.3. Plan views (continued)

21
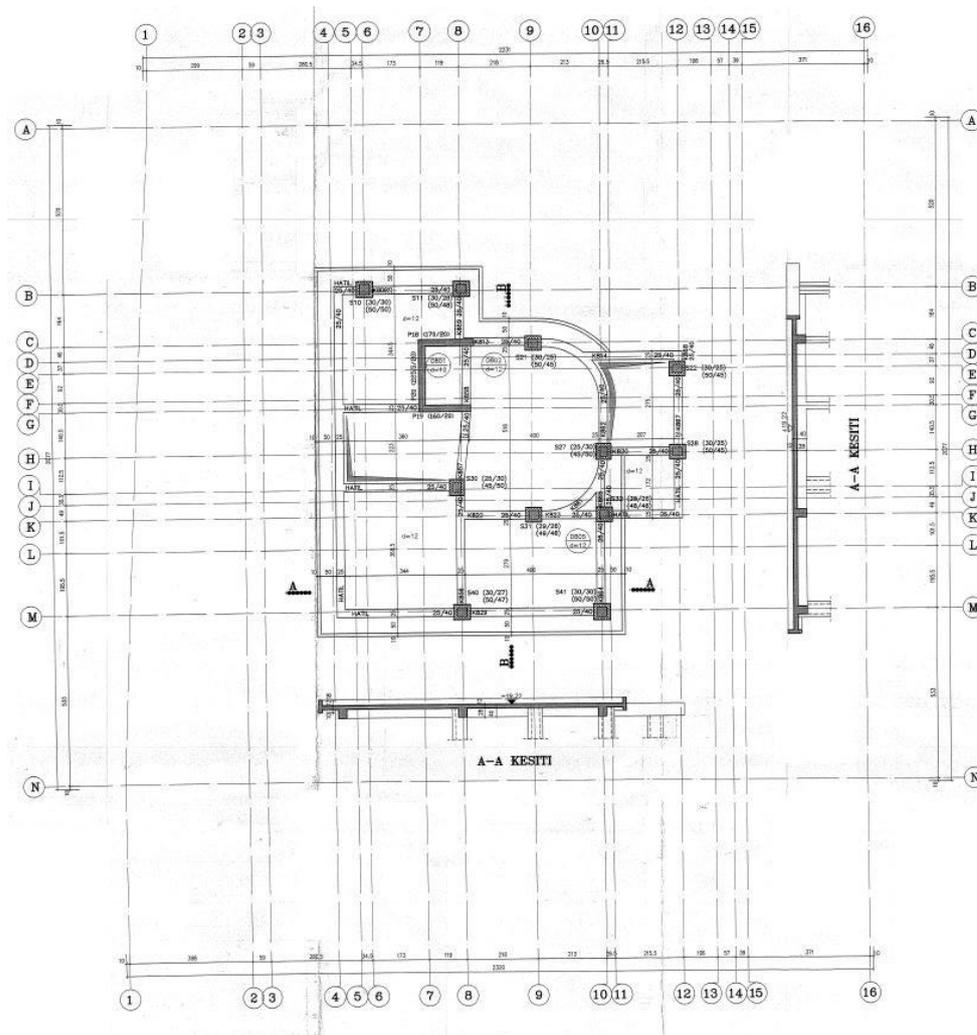
(h) roof floor (+19.22)

Figure 3.3. Plan views (continued)

Column dimensions were reduced at the upper floors as they were designed for gravity loads only. The cross-sectional dimensions of all the columns and shear walls are given in Appendices A and B.

Although the spans are relatively long reaching 5.3 m, 250 × 400 mm size spandrel beams were used on typical stories. Beams having various depths (30, 40, 50 cm, etc.) and a width of 13 cm were used at the interior frames. Wide beams with a depth of 35 cm and different widths were used on the fourth and fifth floors as shown in Figure 3.4.
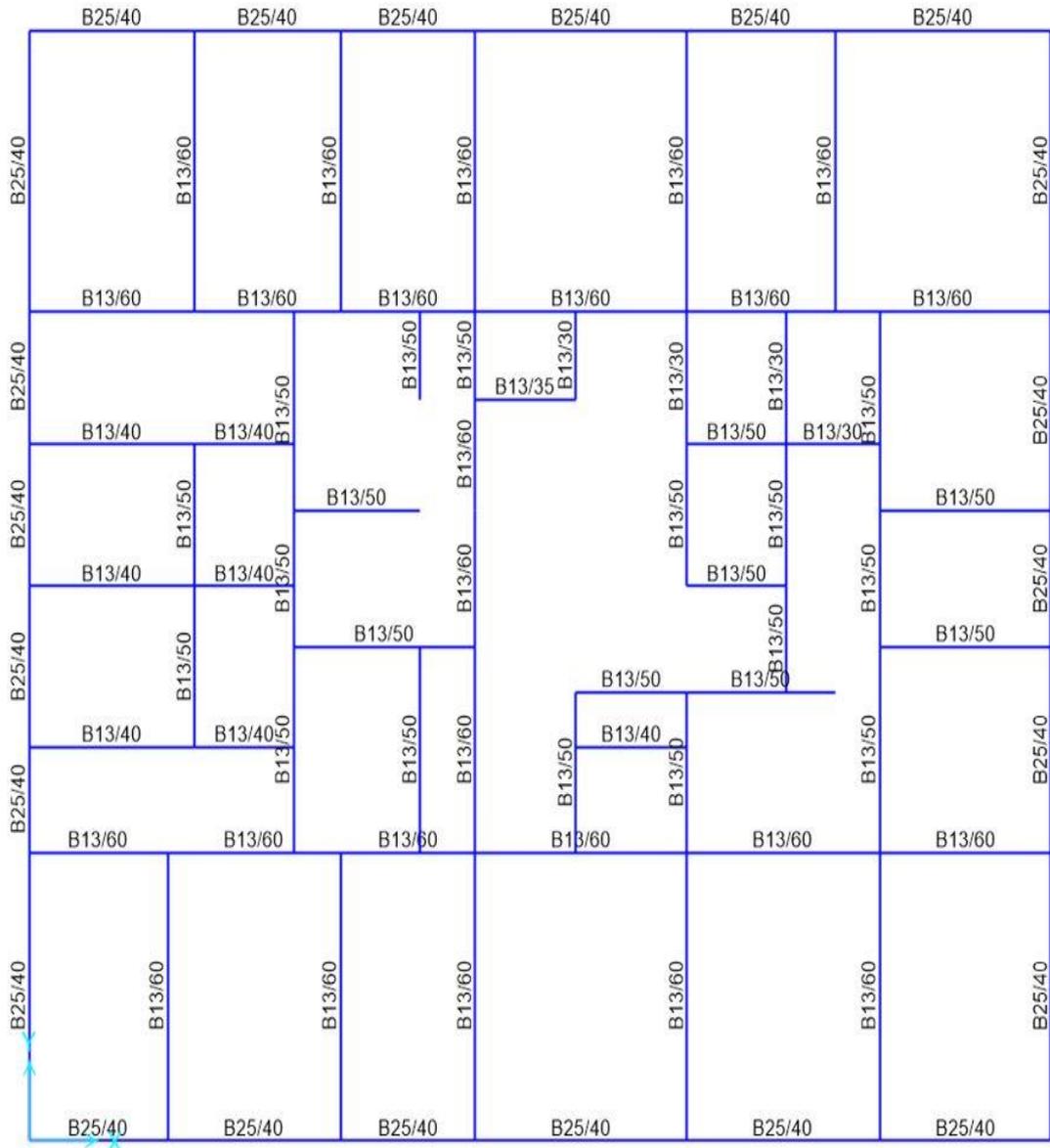
(a) first, second, and third floors

Figure 3.4. Beam sections

23
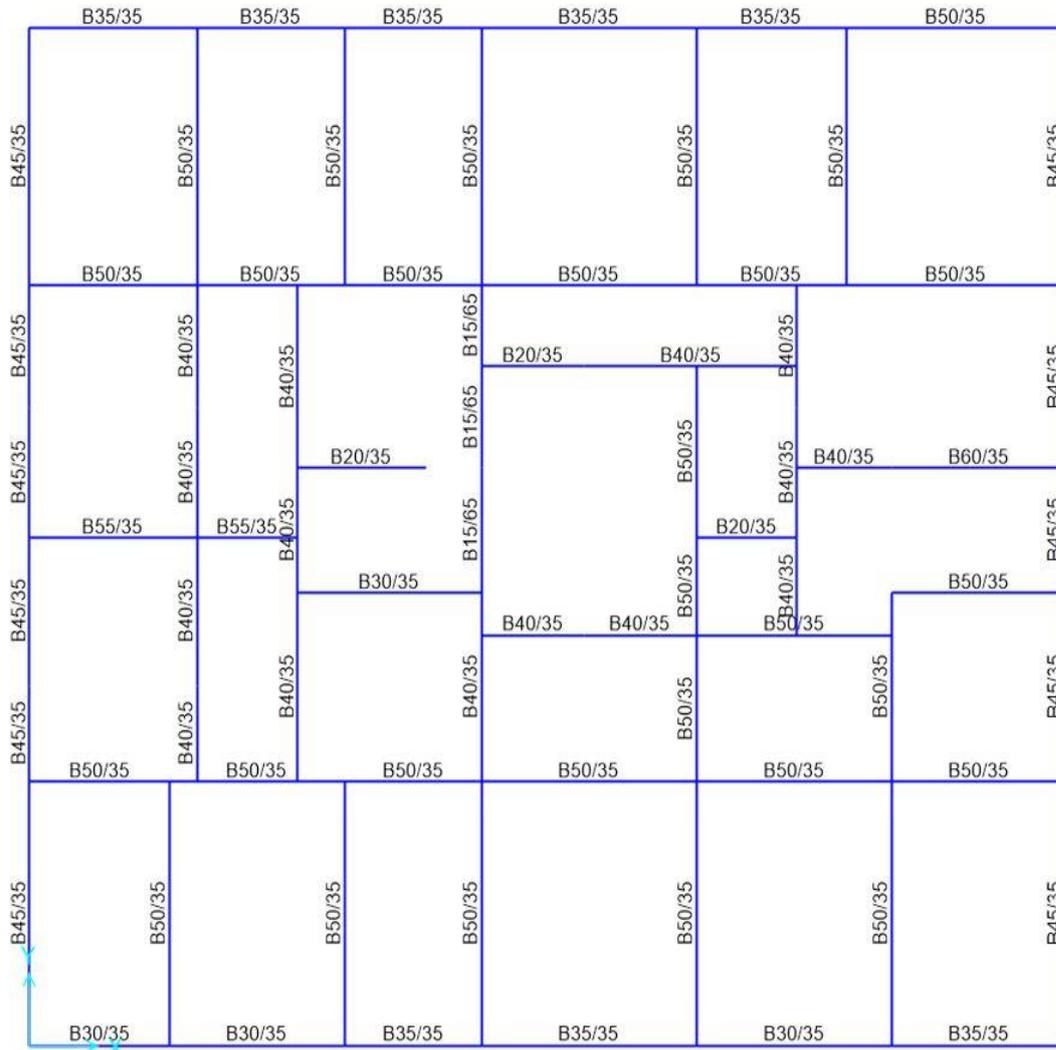
(b) fourth and fifth floors

Figure 3.4. Beam sections

The concrete compressive strength was determined as 12 MPa and the steel yield strength was determined as 220 MPa in the experiments performed at the METU Structural Mechanics Laboratory. Grade C20 concrete and S420 steel (the characteristic compressive and yield strengths, respectively, are 20 MPa and 420 MPa [Turkish Standards Institute, 2000]) were used for the retrofit. Local site class was determined as Z4 according to the Turkish Earthquake Code [Ministry of Public Work and Settlement, 2007].

24

3.3. Building Instrumentation

To determine the dynamic properties of the building, twelve uniaxial accelerometers (see Fig. 3.5) were placed throughout the building (basement, first, fourth, fifth floor ceilings) as shown in Figure 3.6. The measurements taken from the building lasted for seven days. In the first five days, accelerometers were oriented in the horizontal direction (see Fig. 3.7), whereas in the last two days they were oriented in the vertical direction (see Fig. 3.8). The sampling frequency was 100 Hz. The recorded data were divided into an-hour-long sets. The records in the horizontal direction were used for the system identification of the investigated building whereas records in the vertical direction were used for the analysis of floor vibration to determine whether the limit values were exceeded. During the experimental measurements, a multi-channel digitizer was used. Detailed information related to the accelerometers and the data acquisition system can be found in relevant documents (Guralp, 2009).
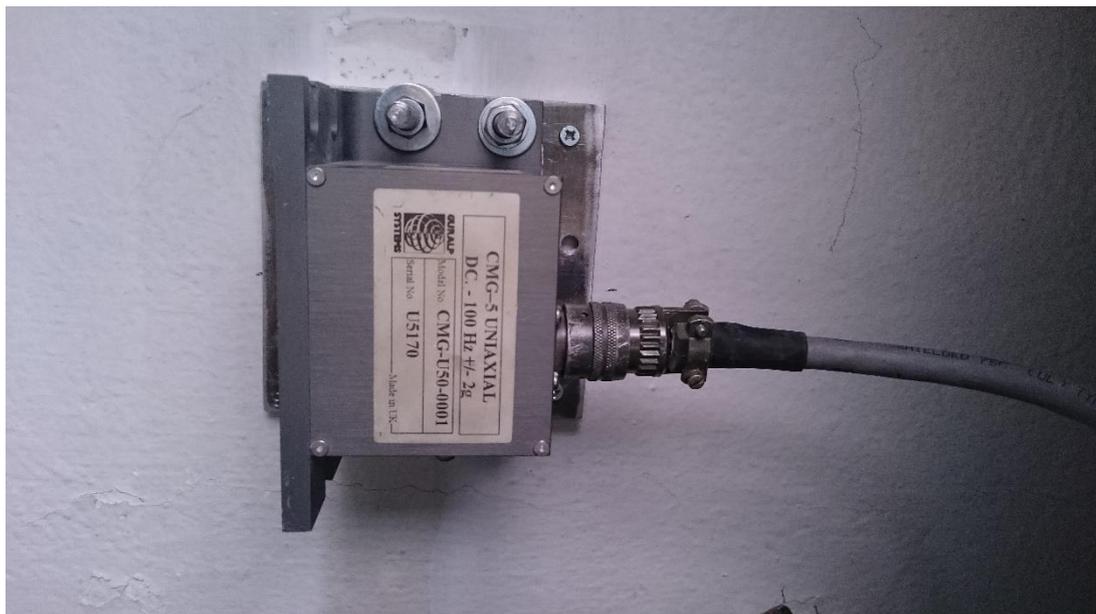
Figure 3.5. Uniaxial accelerometer
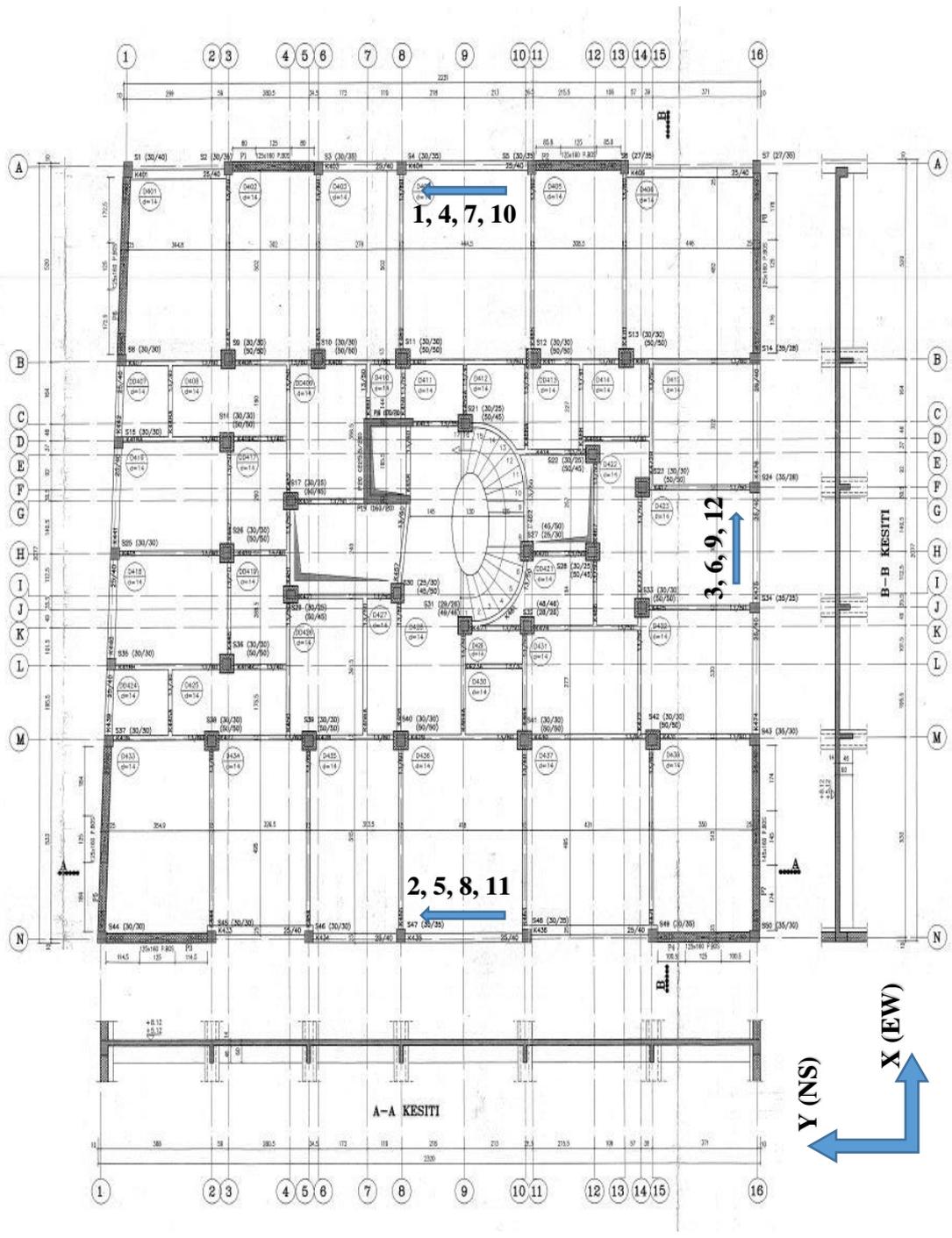
Figure 3.6. Instrumentation scheme and the location of the accelerometers on the plan
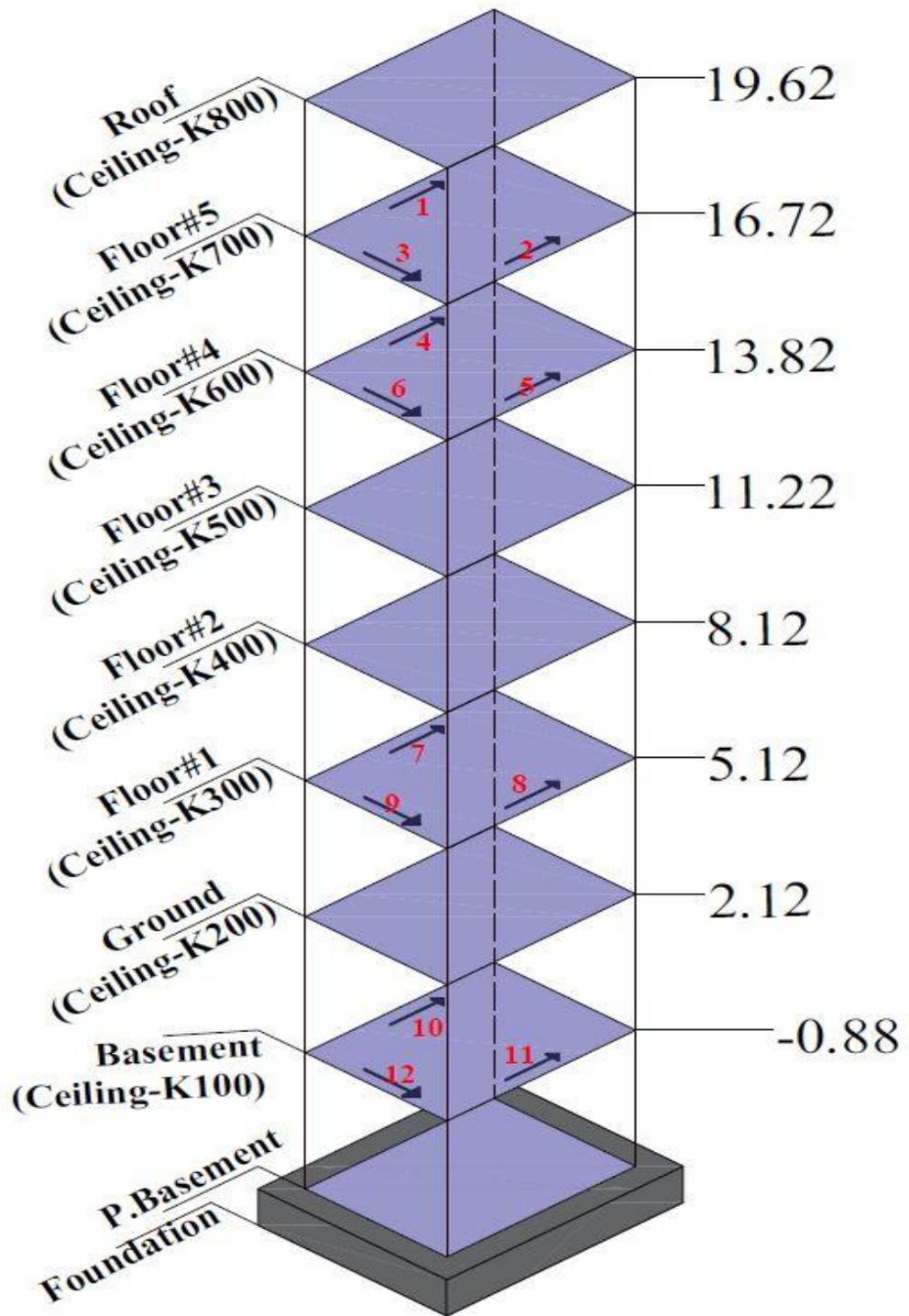
Figure 3.7. Instrumentation scheme for the horizontal direction
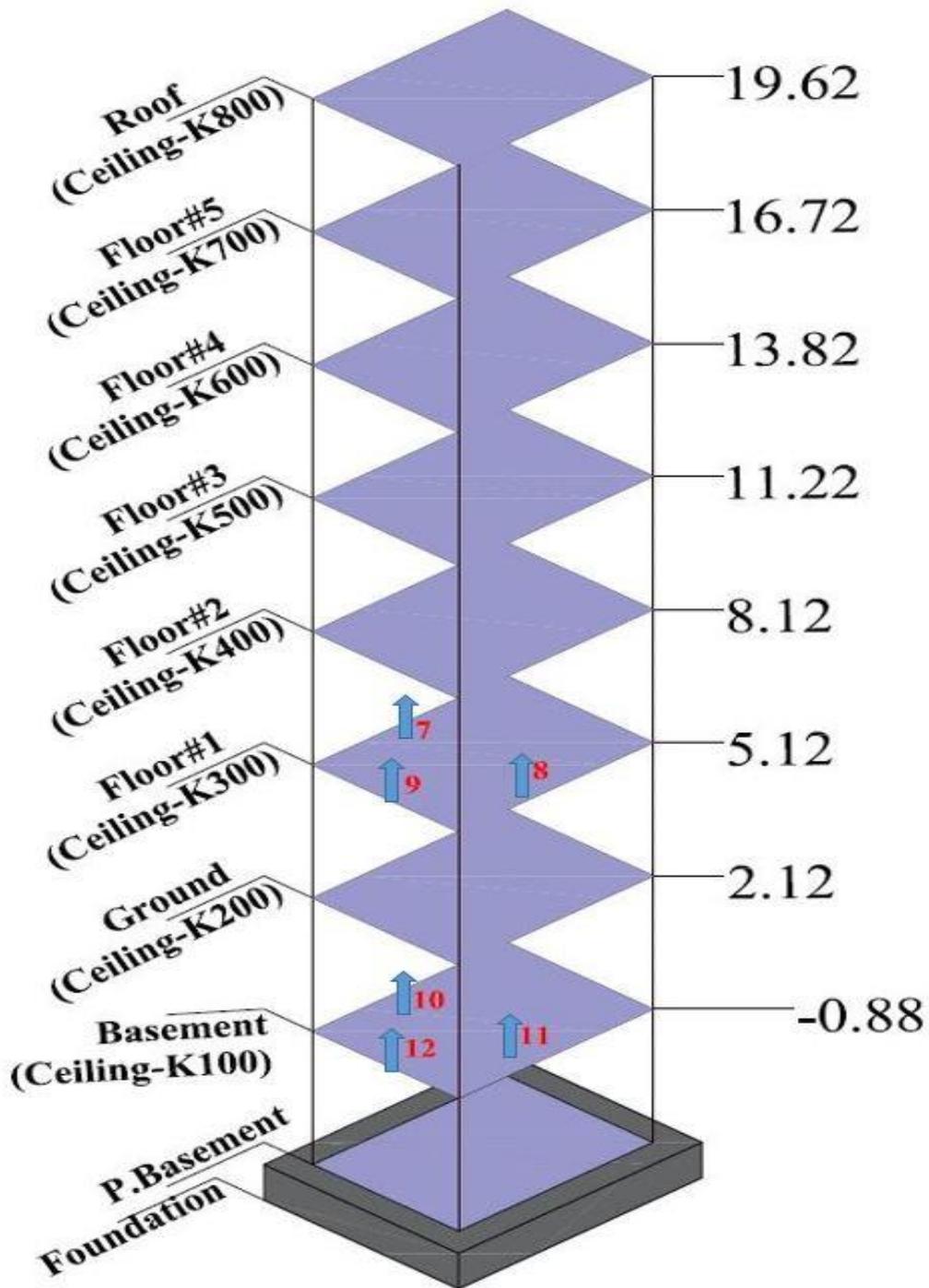
Figure 3.8. Instrumentation scheme for the vertical direction

CHAPTER 4

SYSTEM IDENTIFICATION OF THE BUILDING

4.1. Introduction

Dynamic properties of structures such as natural frequencies, mode shapes, and damping ratios can be determined by using experimental methods. These parameters are very important for engineers and researchers because they are used for estimating structural behavior under earthquakes, detecting the changes in structural behavior after retrofitting or damage, updating structural elastic properties for analytical modeling, and developing the building codes (Michel et al., 2008; Celik et al., 2015). Building responses are measured experimentally using accelerometers deployed throughout the building. It is generally very difficult to shake engineering structures (e.g. a building or a bridge) artificially due to their size. Therefore, using the recorded structural response under ambient loads is the most practical and economical approach for identifying the modal properties of these structures (Magalhaes et al., 2010). In ambient vibration testing, low-amplitude structural response of the building is measured by sensitive accelerometers. The recorded data are processed using output-only identification tools. Currently, there are a lot of robust methods, in time or in frequency domains, which are implemented in commercial software such as ARTeMIS (Svibs, 2014). A review of system identification methods in civil engineering applications can be found in Cunha and Caetano (2005).

Within the scope of this thesis, the available ambient vibration records were analyzed by using Fourier transforms and band-pass filters and by Enhanced FDD (EFDD; Jacobsen et al., 2006) method and the dynamic properties of the building were identified. Then, an analytical model of the building was developed to simulate its measured dynamic properties. This chapter presents the analysis of the ambient

vibration records, the finite element structural model of the building, and the eigenvalue analysis. The identified structural system dynamic properties from the ambient vibration records are compared with those determined from the eigenvalue analysis.

4.2. Fourier Analysis of the recorded Horizontal Accelerations

Algorithms of signal processing are summarized below:

- Row data is converted to acceleration data (see Fig. 4.1),
- In case of acceleration data, it is easier to obtain frequency peaks since amplitudes are higher.
- Apply band-pass filter for 0.05-50 Hz,,
- Compute the Fourier Amplitude Spectrum (FAS) of the filtered signals,
- Smooth the data by using moving average method for twenty-one points (see Figs. 4.2 and 4.3),
- Find the natural frequency and calculate damping with half-power bandwidth method (Rea and Bouwkamp, 1971; Trifunac et al., 2001; Safak and Cakti, 2014).

Natural vibration frequencies of the building were determined as 2.73 Hz and 3.11 Hz for the first translational modes along the X (EW direction) and Y (NS direction) directions, respectively, and 5.00 Hz for the first torsional mode. The fourth and fifth modes were also determined as 8.54 Hz and 9.23 Hz which are the second modes in the X and Y directions, respectively (see Figs. 4.2 and 4.3). In order to identify torsional modes, the recordings of two sensors (Acc #4 and Acc#5, locations shown in Fig. 3.6) installed on the fourth floor are analyzed. The FAS are calculated for the recordings at the two accelerometers, as well as the sum and the difference of both recordings (see Fig. 4.4). This makes it possible to separate the bending modes (sum) from the torsional modes (difference) (Safak and Celebi, 1990a).
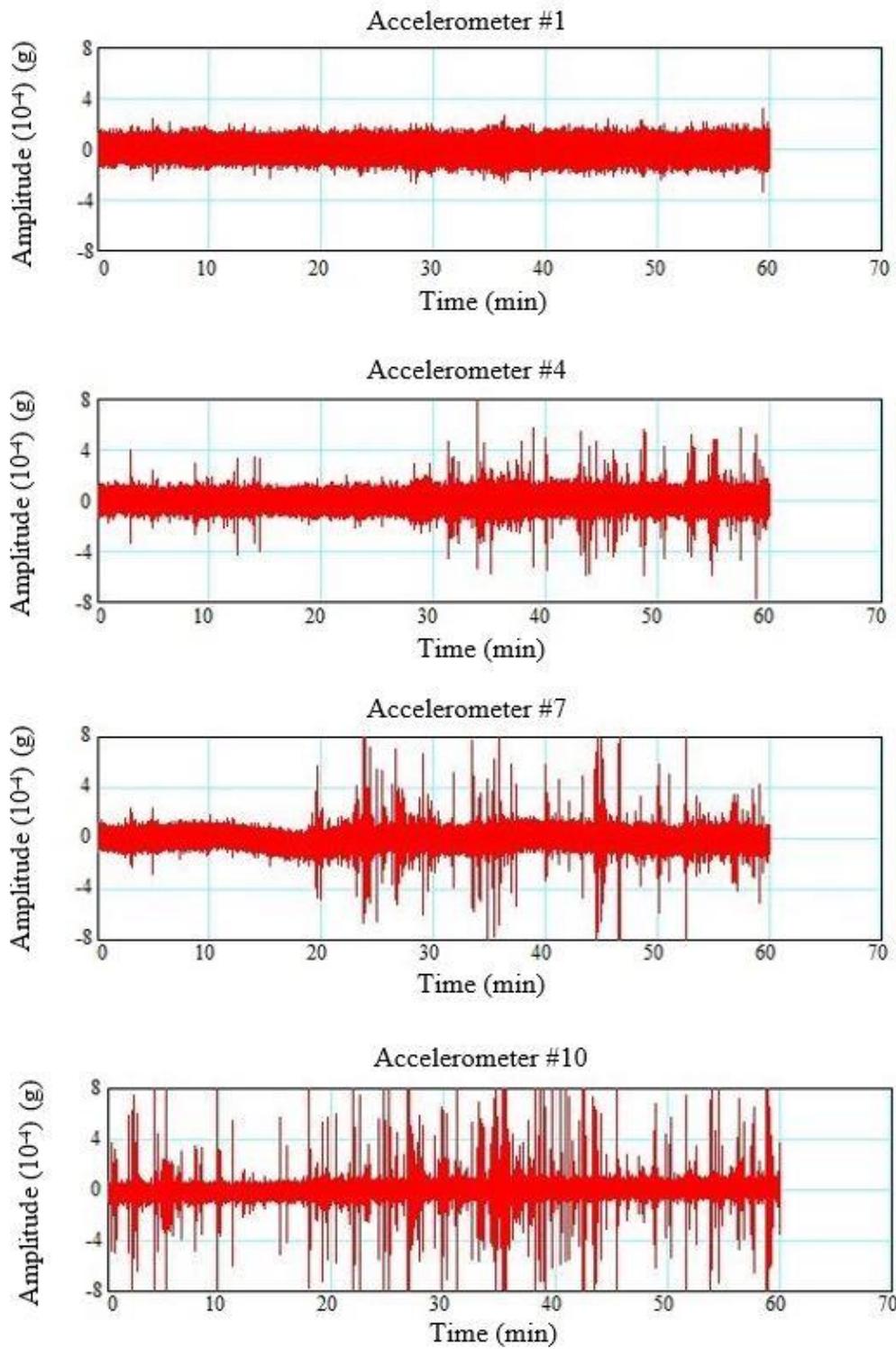
Figure 4.1. Time domain
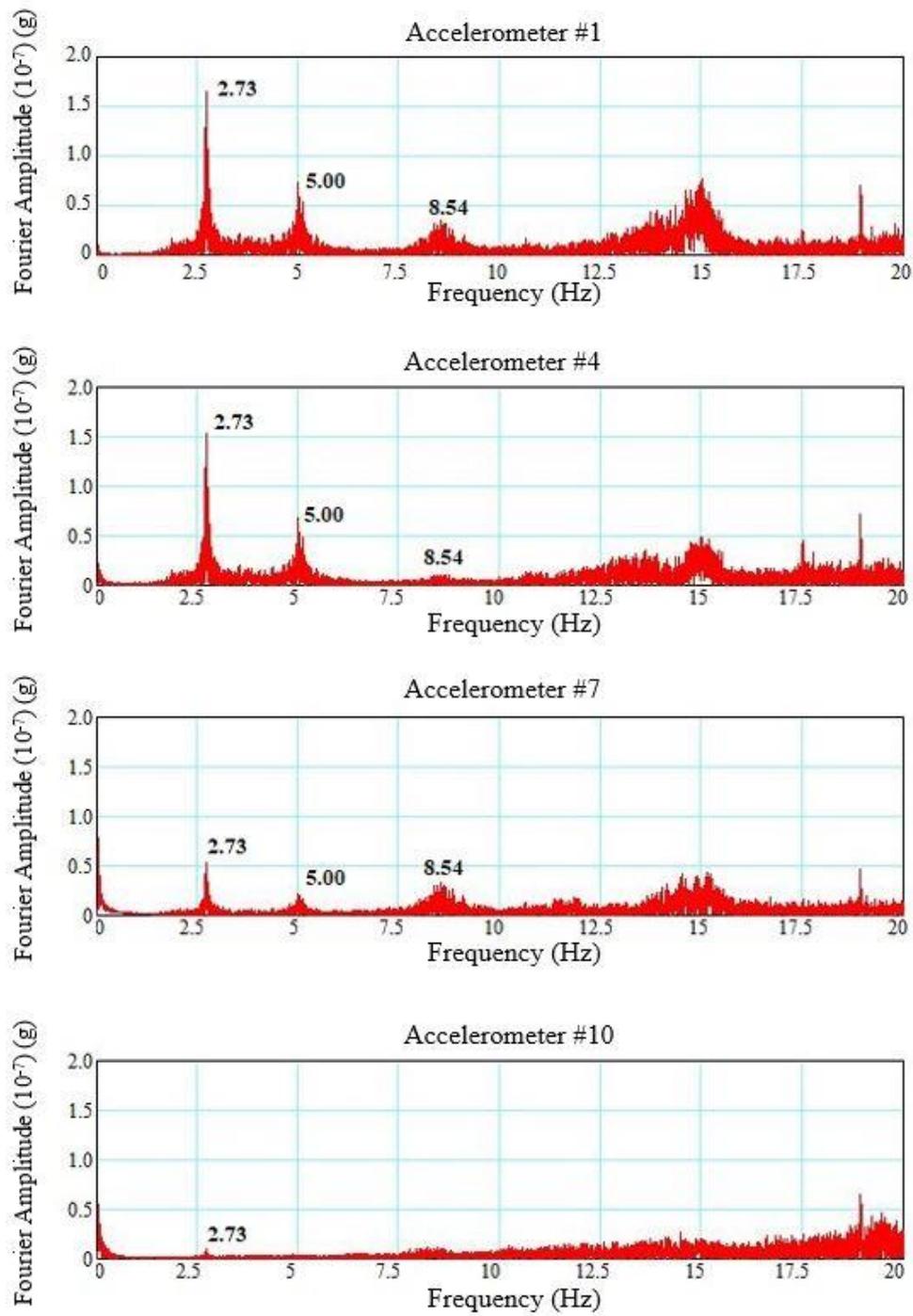
31

Figure 4.2. Fourier amplitude spectra for the EW direction

32
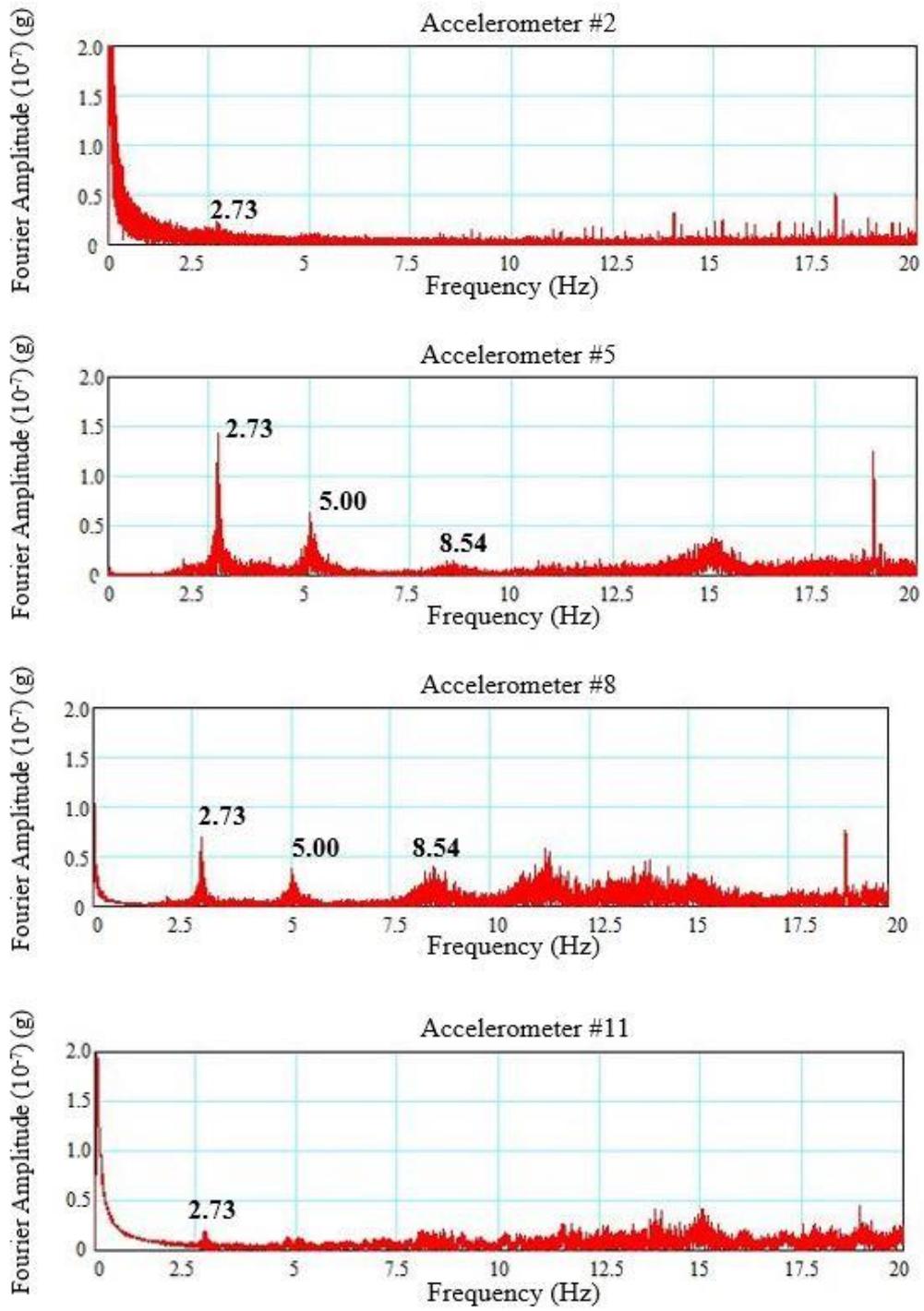
Figure 4.2. Fourier amplitude spectra for the EW direction (continued)

33
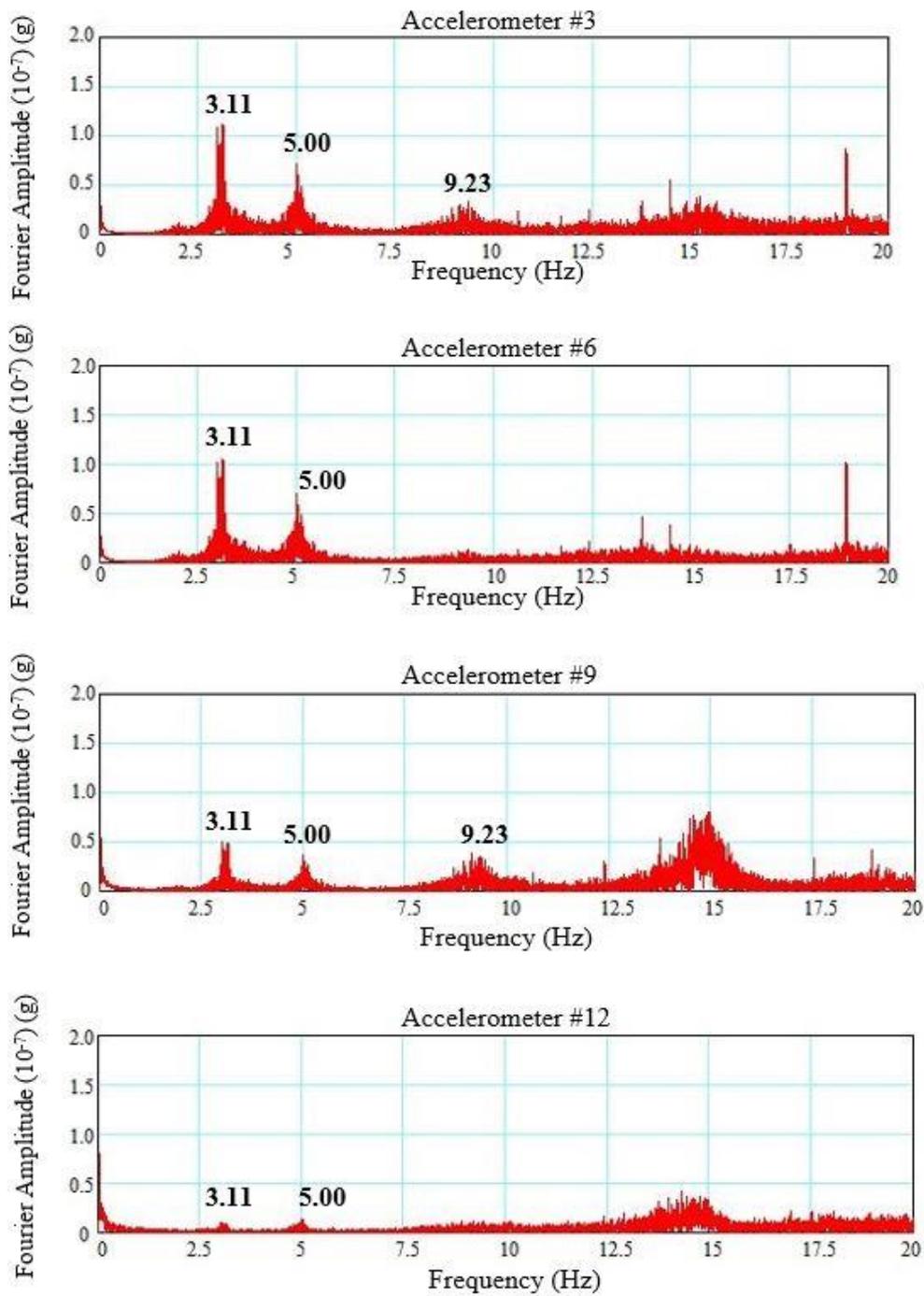
Figure 4.3. Fourier amplitude spectra for the NS direction

34
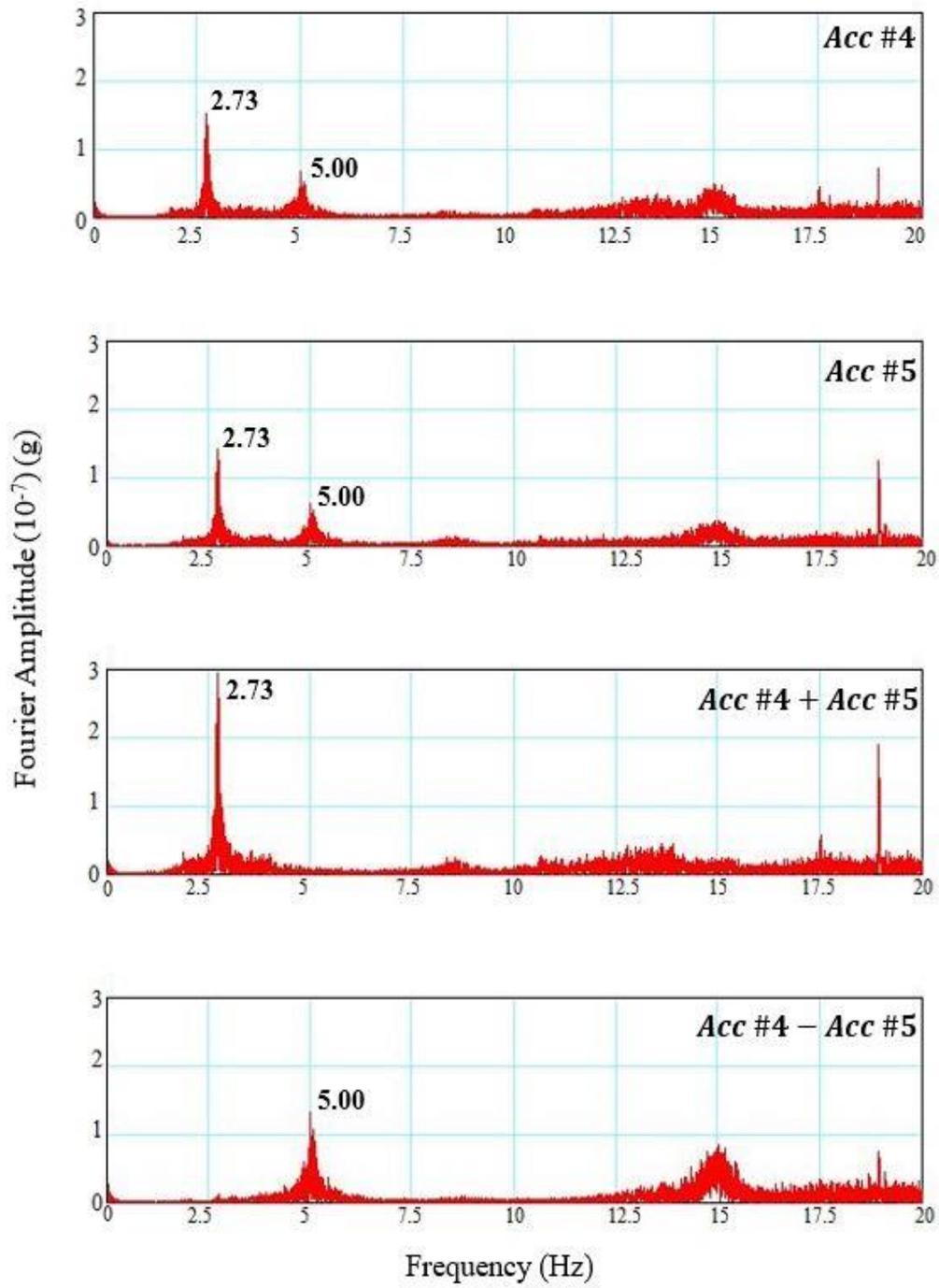
Figure 4.4. Fourier amplitude spectra for two parallel accelerometers

35

Provided all records are time-synchronized, it is possible to detect mode shapes from the modal displacement time histories. Modal displacements were calculated by narrow band-pass filtering the accelerations around the modal frequencies and double integrating the accelerations. The location and amplitude of each sampling stage can be described at that point by plotting modal displacement time records (e.g. from top to bottom) (see Figs. 4.5 and 4.6). Torsional responses are calculated from the difference between two parallel horizontal accelerometers (see Fig. 4.7).
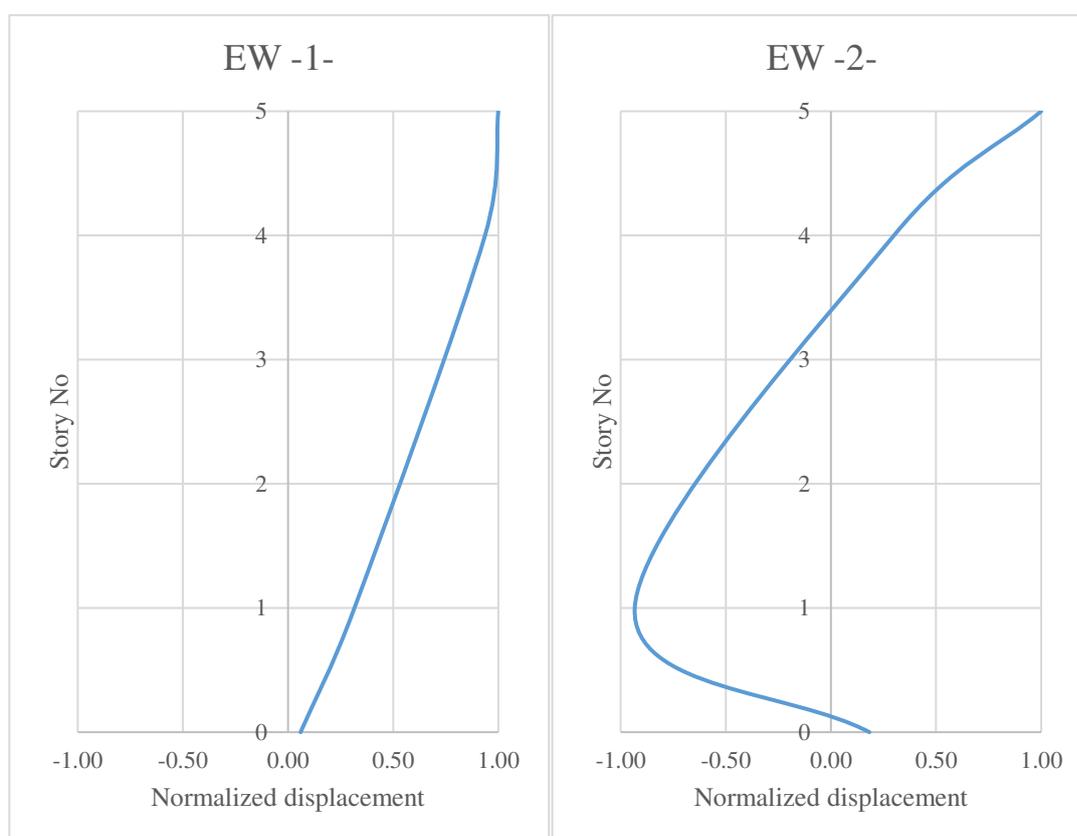
Figure 4.5. The first and second translational mode shapes for the EW direction
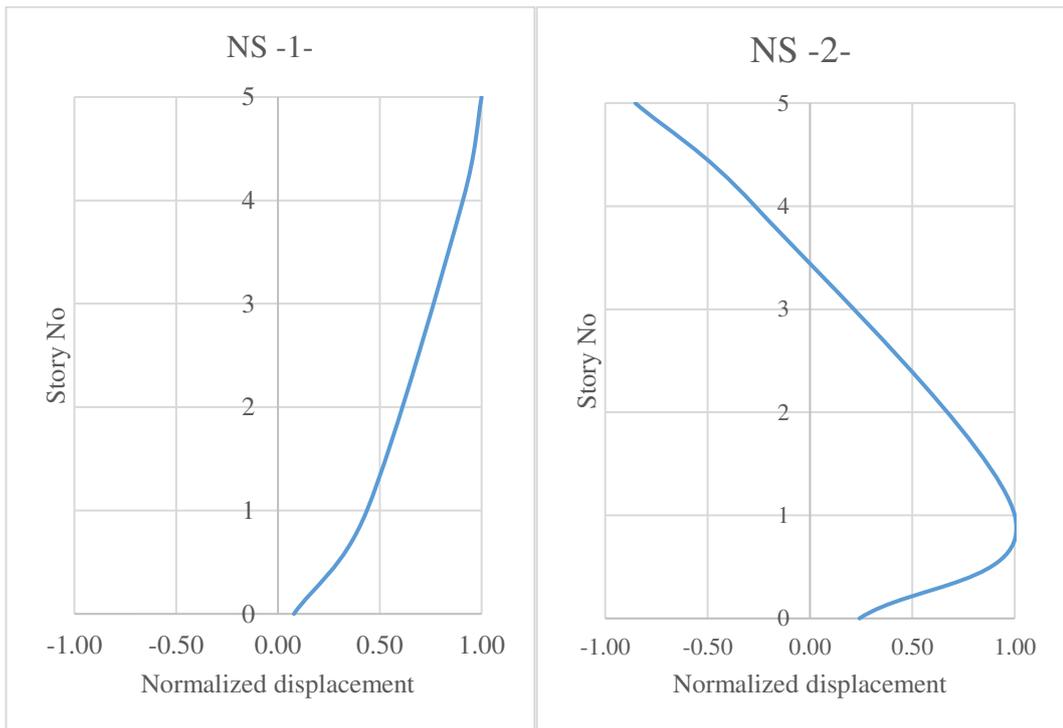
Figure 4.6. The first and second translational mode shapes for the NS direction
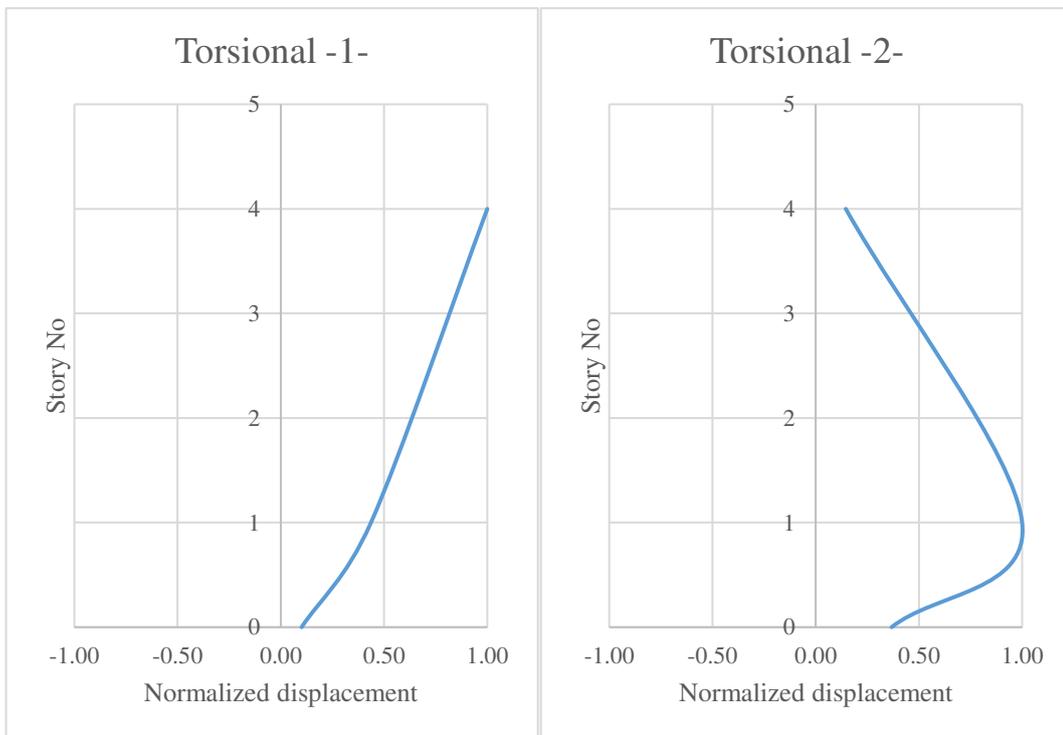
Figure 4.7. The first and second torsional mode shapes

37

Modal damping ratios, ζ, were calculated using the half-power bandwidth method (Chopra, 1995):

$$\zeta = \frac{f_b - f_a}{f_b + f_a} = \frac{f_b - f_a}{2f_n} \qquad (4.2)$$

where f_a and f_b are half-power frequency points and f_n is the natural frequency. Figure 4.8 illustrates this calculation for mode #1. The identified natural frequencies, and damping ratios are summarized in Table 4.1.
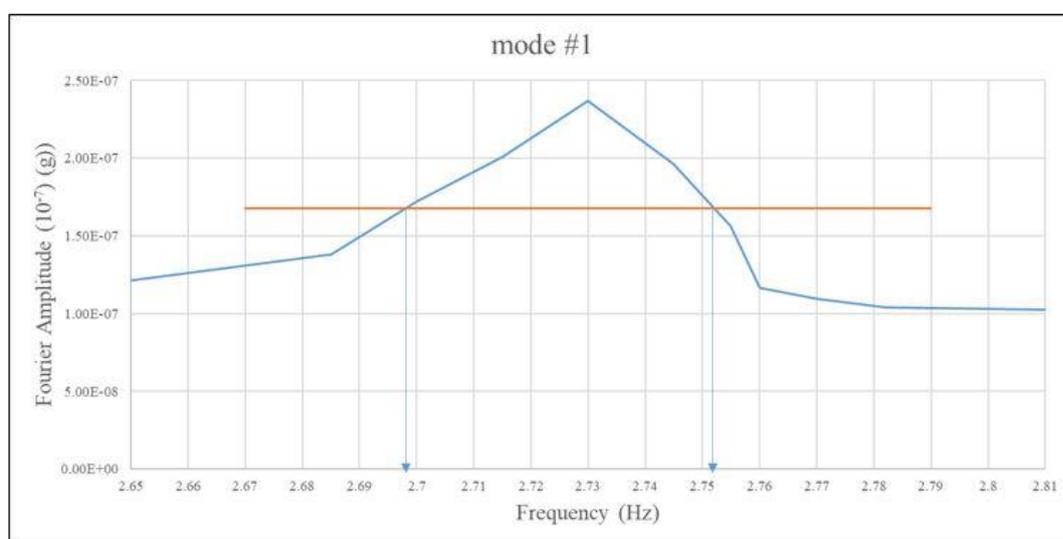
Figure 4.8. Damping ratio for mode #1

$$\zeta = \frac{2.79 - 2.67}{2.79 + 2.67} = \frac{2.79 - 2.67}{2 \times 2.73} = 0.022$$

Table 4.1. *Fourier analysis results*

Mode Number	Description	Frequency (Hz)	Damping Ratio (%)
1	X–Longitudinal	2.73	2.2
2	Y–Longitudinal	3.11	2.1
3	Torsion	5.00	1.5
4	X–Translational	8.54	1.9
5	Y–Translational	9.23	2.2

38

Figures 4.9 and 4.10 show hourly variation of the vibration frequencies on different days.

Figure 4.9 demonstrates the hourly variation of measurements of ambient vibrations collected during working day. During operating hours there is a rise in frequencies while after operating hours the natural vibration frequencies are about the same. There is an increase in the natural frequencies due to hot weather (Clinton et al., 2006). During the day, the ambient excitation is an order of magnitude larger than at night.

Figure 4.10 demonstrates the hourly variation of measurements of ambient vibrations collected during holiday. There is no major change in the first and second translational frequencies due to very low human activities and environmental factors (Clinton et al., 2006).
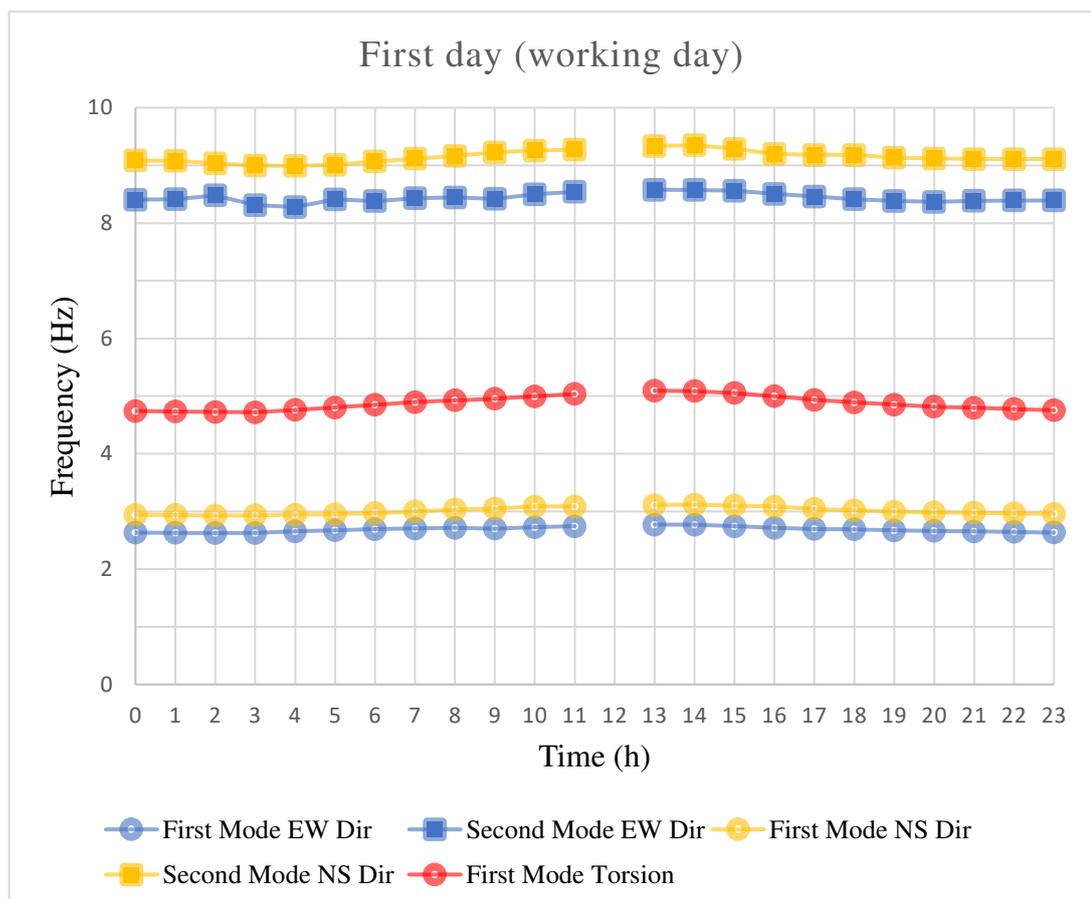
Figure 4.9. Hourly variation of frequencies (28/04/2017)
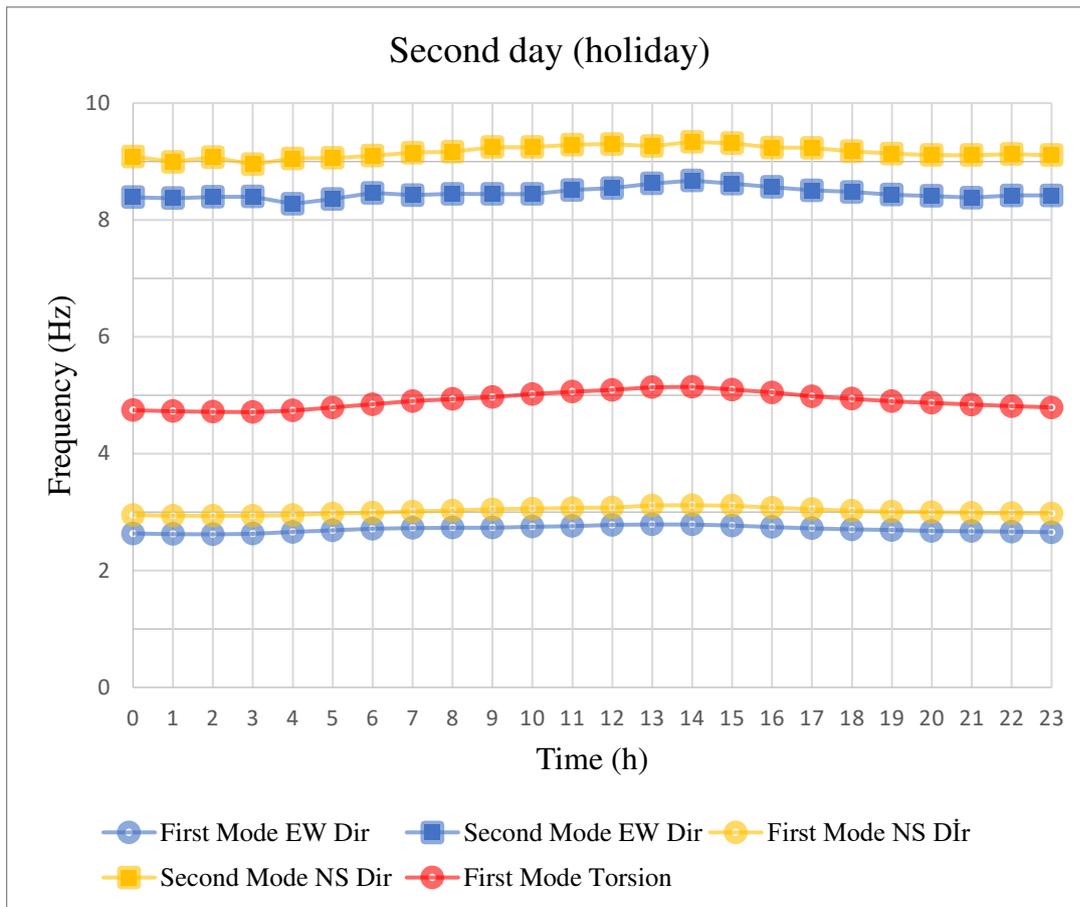
Figure 4.10. Hourly variation of frequencies (29/04/2017)

4.3. Enhanced Frequency Domain Decomposition

Natural frequencies, mode shapes and modal damping ratios can also be identified by using the EFDD method (Jacobsen et al. 2006).

In the EFDD method, the natural frequency is obtained by determining the number of zero transition which is time-dependent, and damping is acquired with the logarithmic reduction of the single degree of freedom normalized auto-correlation function. In this method, the peak points of the Power Spectral Density function corresponds to the natural frequencies. The singular vectors that compose the peak points correspond to the mode shapes (Brincker et al., 2000).

Structural system dynamic properties were identified by the EFDD method using the ARTeMIS (Svibs, 2014). So, the modal and the dynamic parameters were examined using this program. First, the geometry of the building was created by entering the coordinates of the accelerometers (see Fig. 4.11). Nodal points and frame elements were used to develop the representative model. Then, the vibration data (acceleration-time) obtained from experimental studies were transferred to the program. The software calculates the spectral density functions.

The peaks were investigated by selecting many points and the frequency values which are possible as the mode shapes were selected. Then, the graphical representations which in the motions were not observed together with the mode shape had been eliminated, and the five frequency values were extracted as shown in Figure 4.12. Frequencies, and damping ratios are summarized in Table 4.2 and also the vibration mode shapes are given in Figure 4.13.
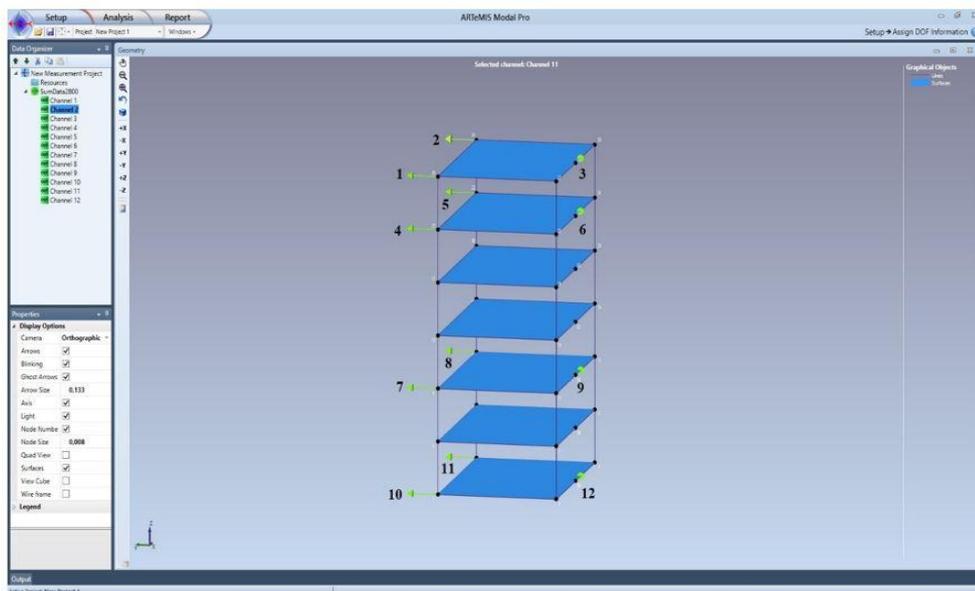
Figure 4.11. ARTeMIS model geometry
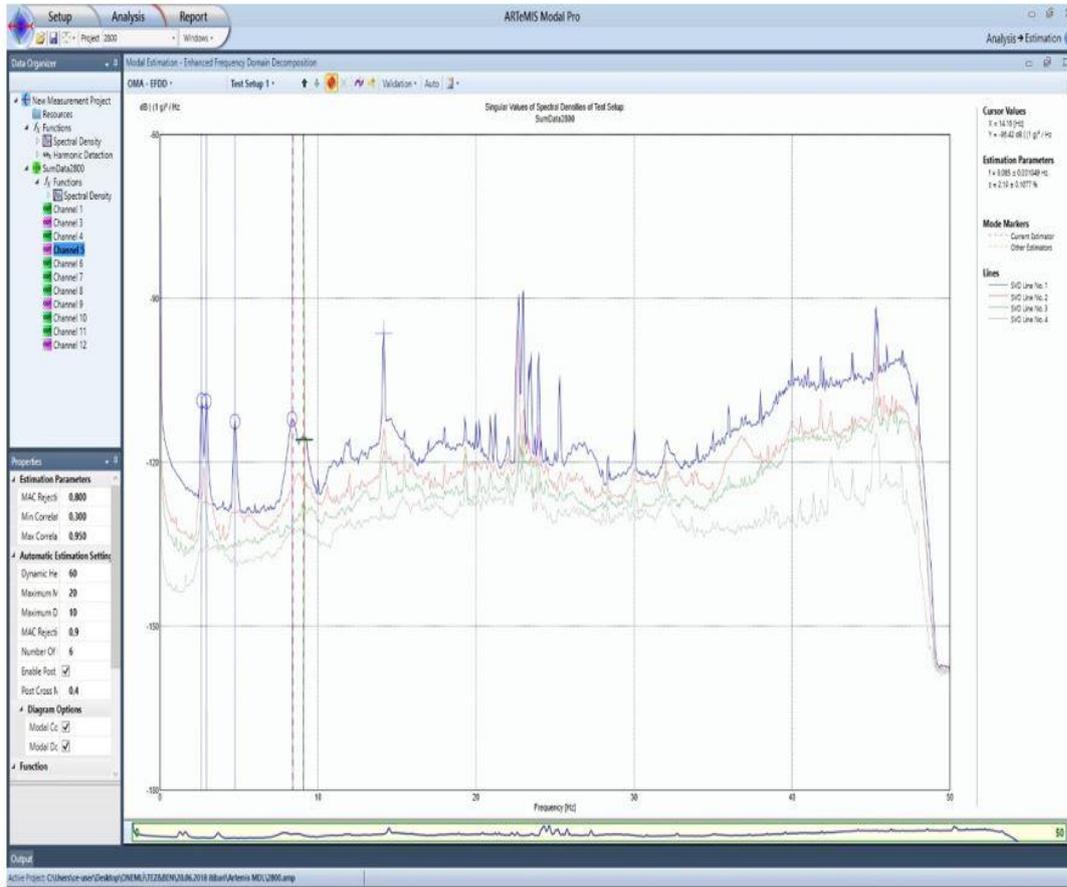
Figure 4.12. Singular values of spectral densities of the test setup

Table 4.2. *EFDD analysis results*

Mode Number	Description	Frequency (Hz)	Damping Ratio (%)
1	X–Longitudinal	2.73	2.1
2	Y–Longitudinal	3.09	2.0
3	Torsion	5.00	1.5
4	X–Translational	8.50	1.7
5	Y–Translational	9.26	2.1

42
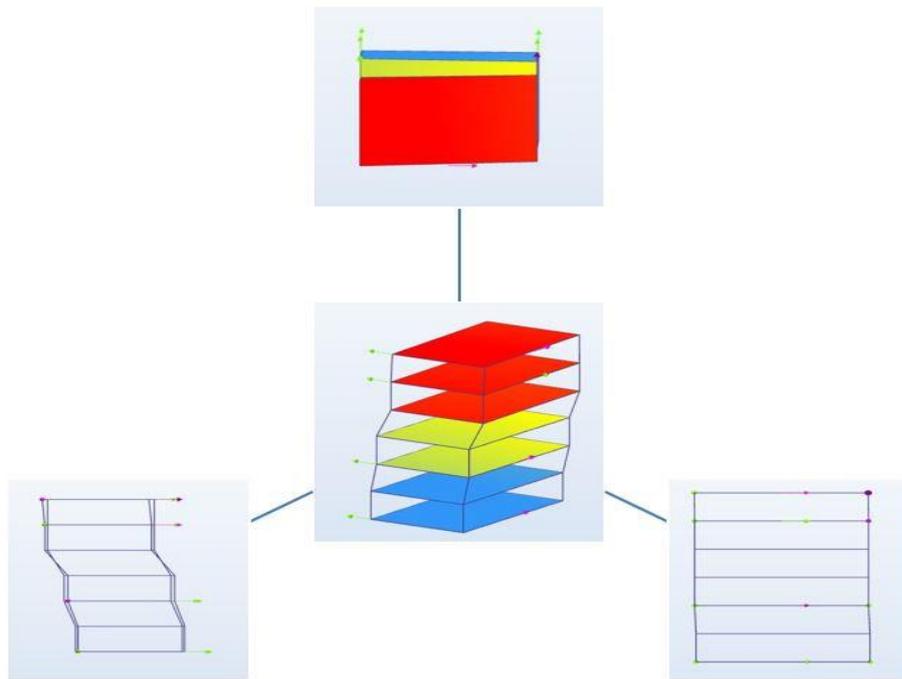
(a) First translational mode in the EW direction
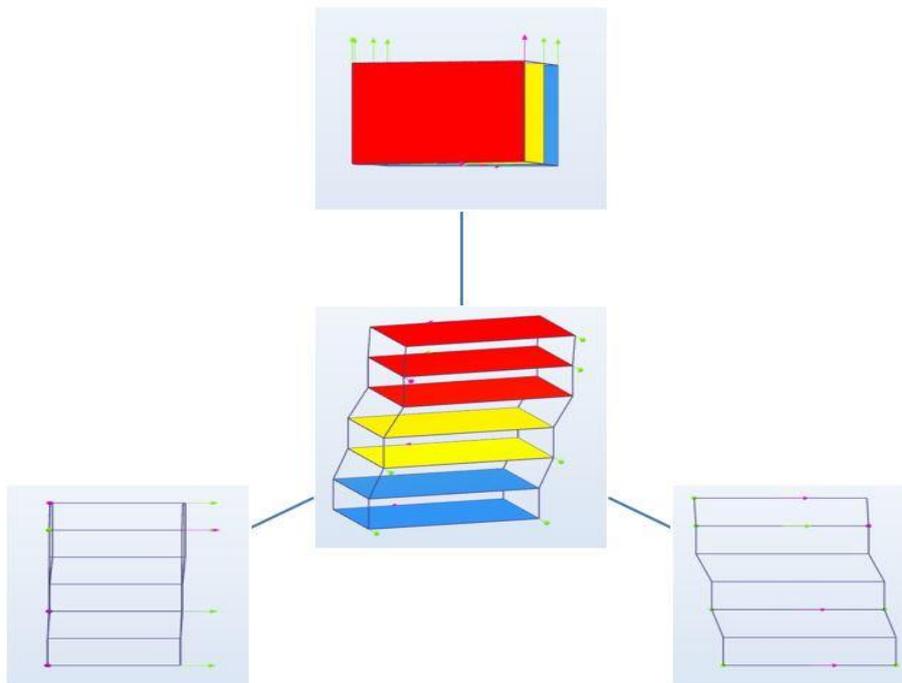
(b) First translational mode in the NS direction

Figure 4.13. Mode shapes
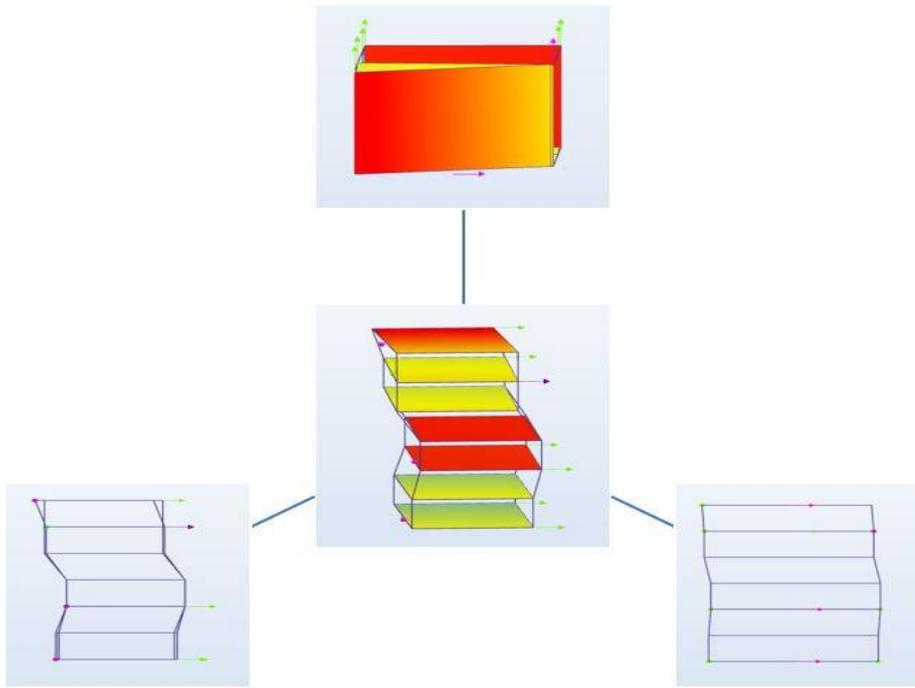
(c) Second translational mode in the EW direction
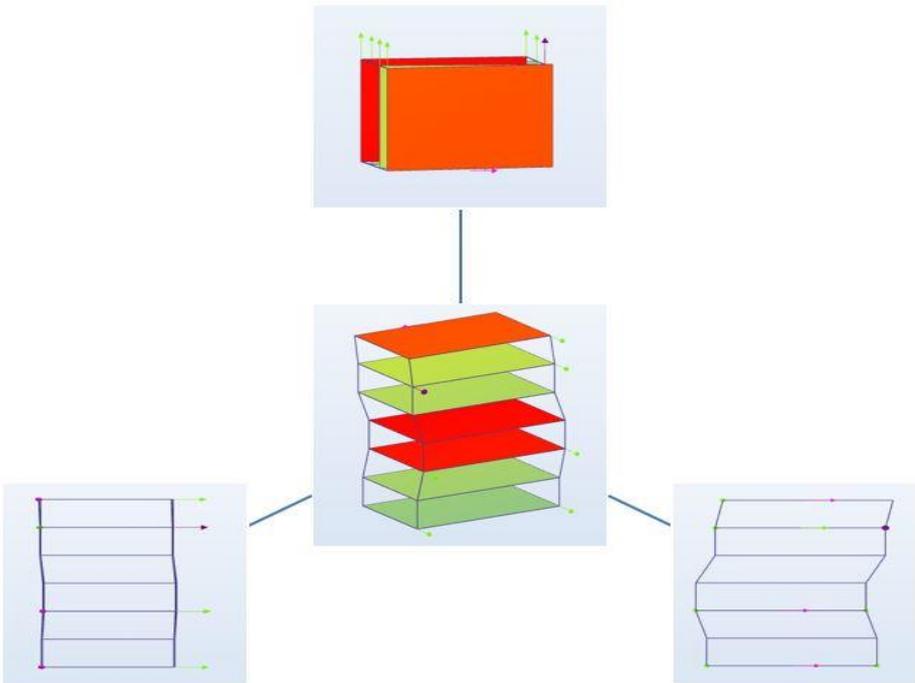
(d) Second translational mode in the NS direction

Figure 4.13. Mode shapes (continued)
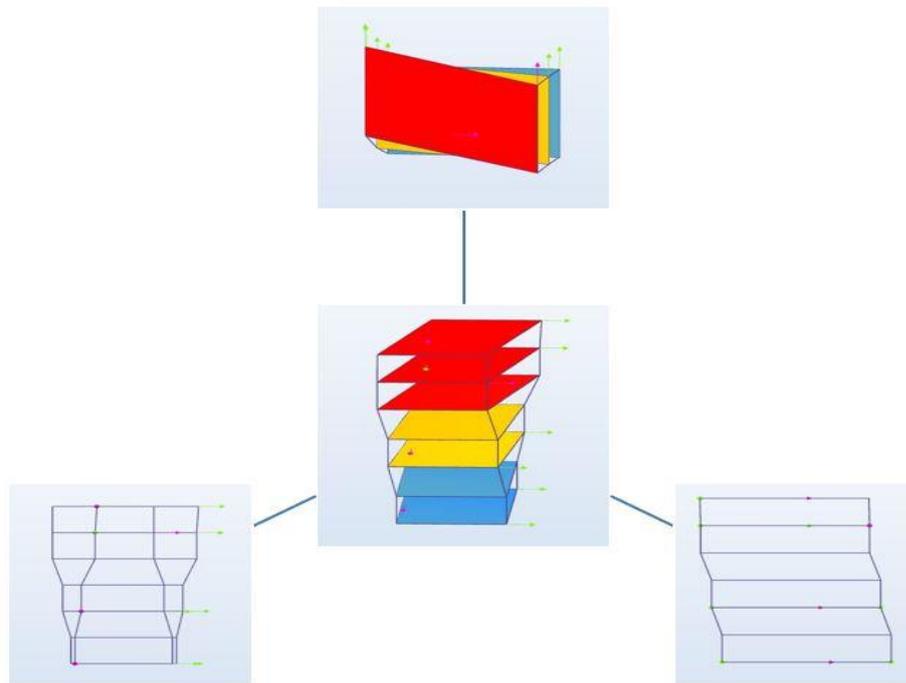
(e) First torsional mode

Figure 4.13. Mode shapes (continued)

4.4. Finite Element Modeling

In addition to determination of dynamic properties of the building using Fourier analysis and ARTeMIS software, finite element model of the building is also used to analytically determine these properties. In this study, two analytical models of the building were developed. The first model, called the initial model, represents the existing structural system of the building consisting of columns, beams, shear walls, and slabs. In the second model, infill walls were incorporated and the modeling parameters such as the elastic moduli and width of infill walls were calibrated to match the dynamic properties identified from the ambient vibration test.

The three-dimensional linear elastic finite element structural model of the building was developed using SAP2000 (Computers and Structures, 2019). The dimensions of the structural members after the strengthening of the building in 2016 were used. Figure 4.14 shows the three-dimensional view of the finite element model (FEM), the

45

plan view, and views of the axes strengthened by the shear walls with openings in EW and NS directions.
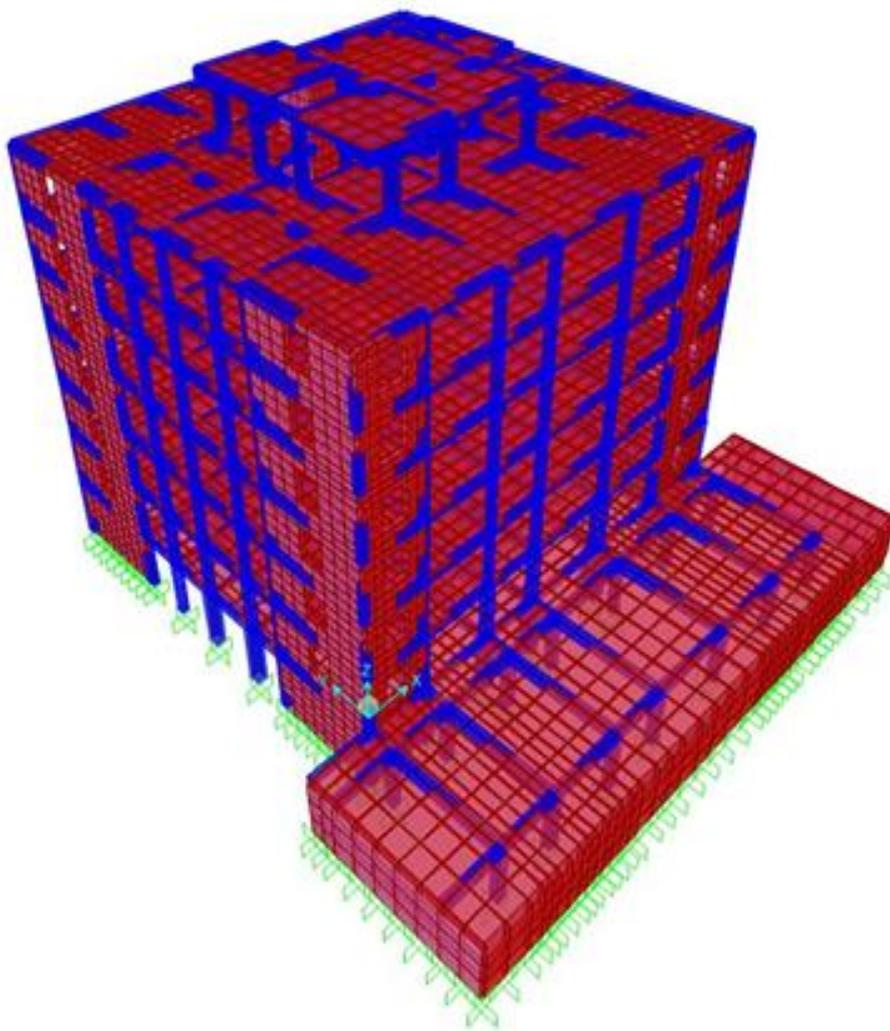
(a) 3D view

Figure 4.14. View of the analytical model of the investigated building
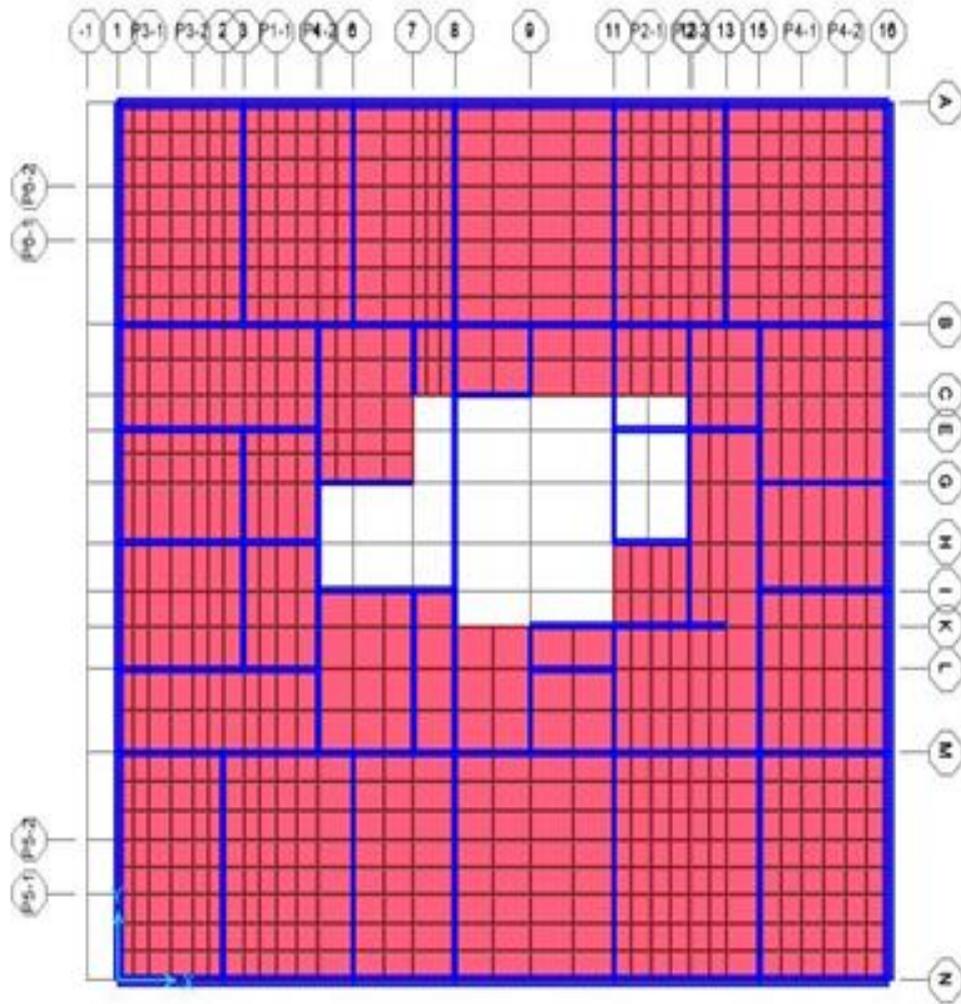
(b) Plan view

Figure 4.14. View of the analytical model of the investigated building (continued)
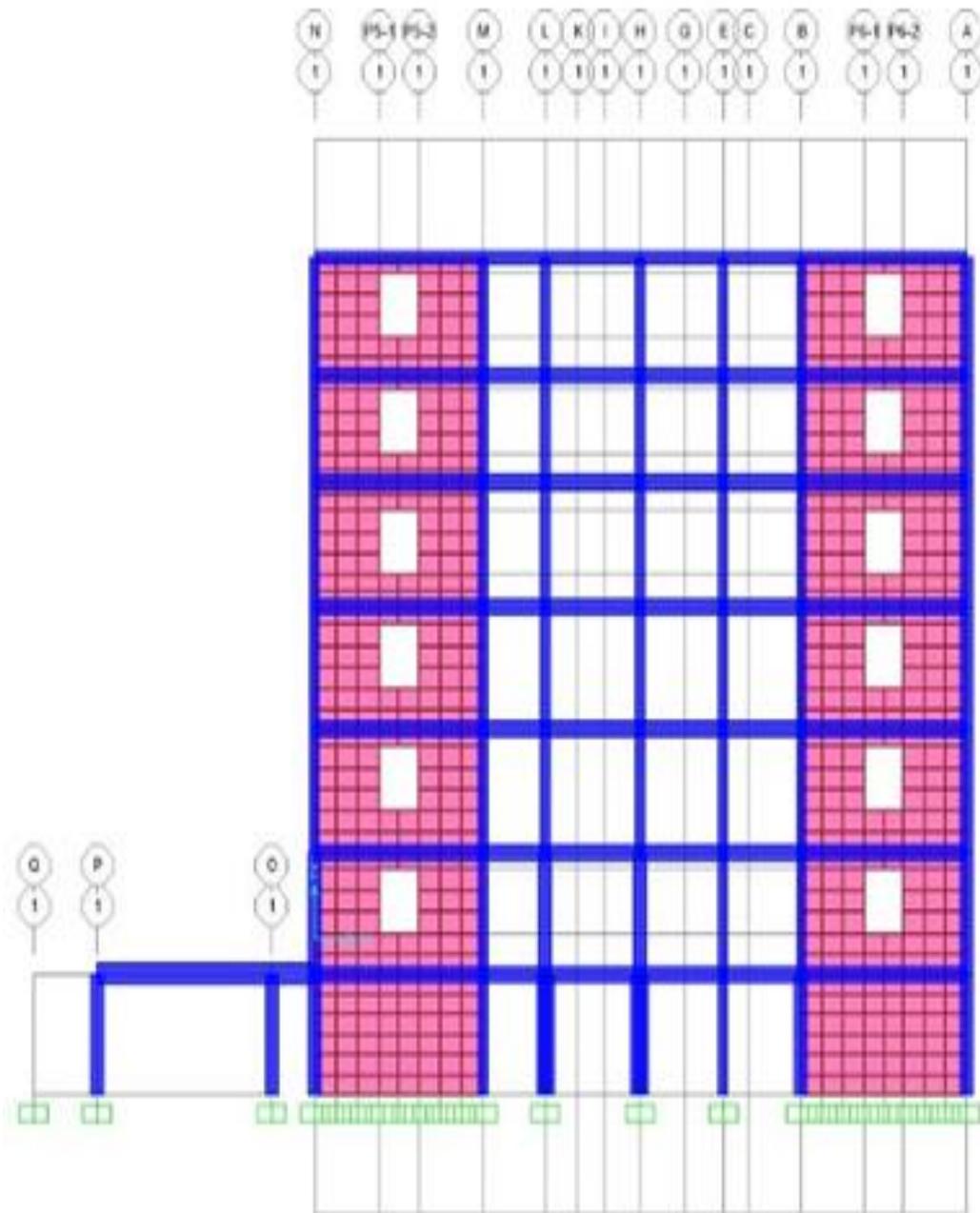
(c) 1-1 axis (EW direction)

Figure 4.14. View of the analytical model of the investigated building (continued)
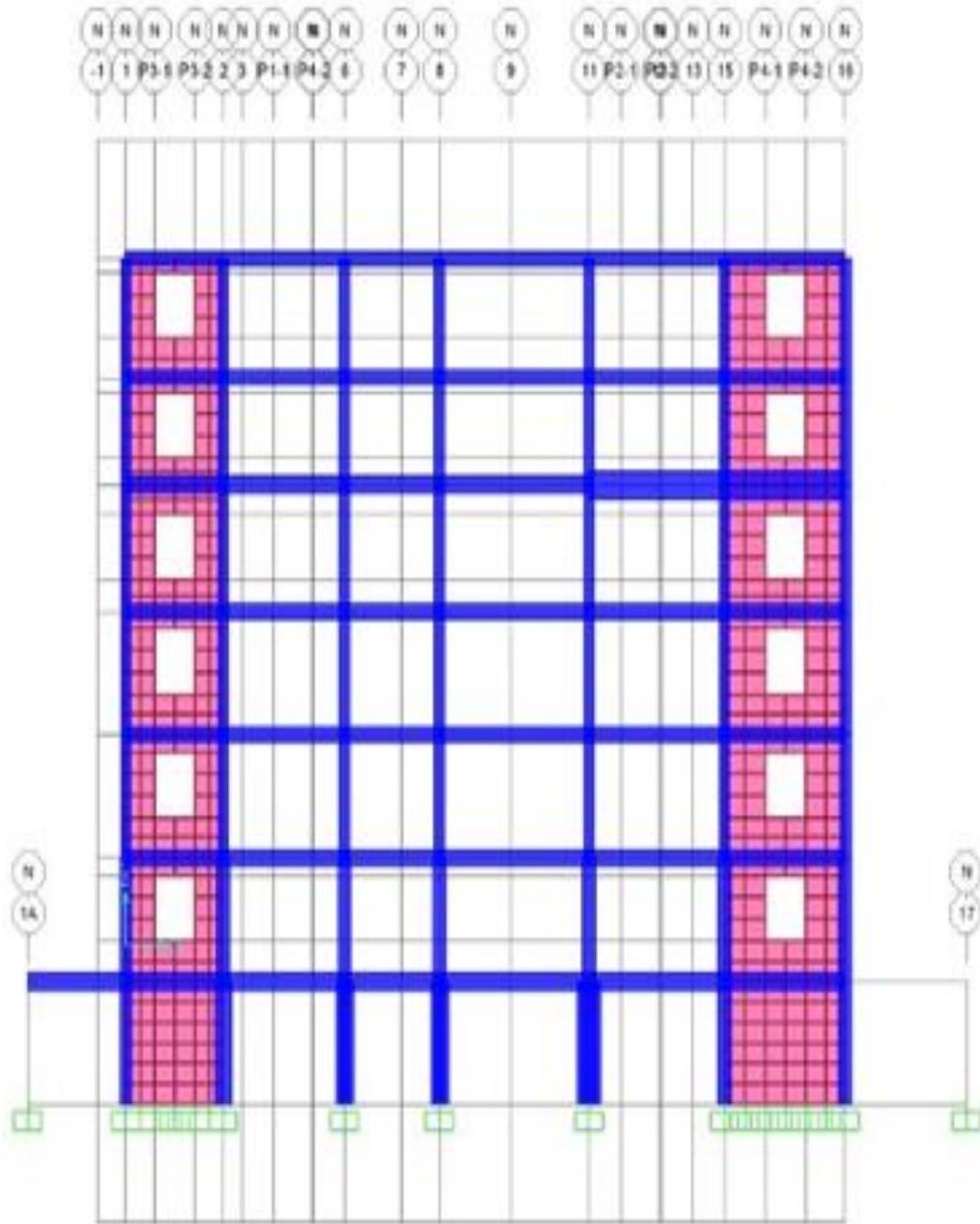
(d) N-N axis (NS direction)

Figure 4.14. View of the analytical model of the investigated building (continued)

Columns and beams were modeled using frame elements whereas shear walls and slabs were modeled using shell elements. Foundation-column joints were defined as moment connections in the design documents; hence fixed supports were defined. Soil-structure interaction effects were ignored. Rigid diaphragms were defined at all floors. Door and window openings in the shear walls were modeled.

The finite element meshes were used for the ground, typical, and roof floor slabs. The mass of the structural and non-structural components was defined as a distributed load using unit weights of the materials. The unit weight of structural concrete was taken as 24 kN/m^3. The Poisson's ratio for concrete was taken as 0.2 according to TS 500. The modulus of elasticity, *E*, for concrete is given by

$$E_{cj} = 3250 \sqrt{f_{cj}} + 14000 \tag{4.3}$$

in Turkish Standards (TS 500, 2000). Moduli of elasticity for grade C12 and C20 concrete were taken as 25,000 MPa and 28,000 MPa, respectively, according to TS 500.

Four different loads were considered. The first load was the dead weight of the building. The second load was the live loads determined according to TS 498 (1997). The third load was superimposed load for non-structural components (cladding, furniture, etc.) on floor slabs. The fourth load was a point load equal to the walking load described in Chapter 5.

In order to determine the dynamic properties of the investigated building, an eigenvalue analysis was performed. Dynamic masses were defined based on the load combination DL + 0.3LL (DL and LL stand for dead and live loads, respectively). Eigenvalue analysis of the structural model yielded the natural vibration frequencies of the building as 1.5 Hz and 2.3 Hz for the first translational modes along the X (EW) and Y (NS) directions, respectively, and 3.0 Hz for the first torsional mode. The fourth mode was determined as 6.29 Hz with 15% mass participation in X direction. Table 4.3 shows mass participation ratios for the first four modes.

Table 4.3. *Natural vibration frequencies and mass participation ratios*

Mode Number	Description	Frequency (Hz)	Modal Participating Mass Ratio (%)
1	X–Longitudinal	1.59	57
2	Y–Longitudinal	2.43	59
3	Torsion	3.29	48
4	X–Translational	6.67	15

4.4.1. Modeling of Hollow-Brick Infill Walls

Infill walls are considered as non-structural members and ignored in the structural design. The reasons for neglecting the contribution of the infill walls to the building stiffness can be summarized as follow (Mainstone and Weeks, 1970; Dhanasekar and Page, 1986):

- Modeling of infill walls is relatively difficult and complicated.
- The strength of infill wall materials is variable.
- Construction quality significantly affects the wall strength and it is changeable and unreliable.
- Although the contribution to the capacity of energy absorption and stiffness of the building is generally known, the impact of the infills wall is not considered in order to remain on the safe side.

In the literature, equivalent diagonal strut members were proposed for modeling the infill walls (Mainstone and Weeks, 1970). All exterior hollow-brick partition walls in the building were modeled by using diagonal strut elements connected to the structural frame at beam-column joints according to the Turkish Earthquake Code (Ministry of Public Works and Settlement, 2007). Two diagonal struts were utilized for each infill panel, and the equivalent strut thickness (0.25 m) and modulus of elasticity (1875 MPa) were taken the same as those of the infill panels.

The width of equivalent diagonal strut is given by

$$\alpha = 0.175(\lambda h_{col})^{-0.4} L_{inf} \tag{4.4}$$

where

$$\lambda = \sqrt[4]{\frac{E_{inf} t_{inf} \sin 2\theta}{4 E_{fc} I_{col} h_{inf}}} \tag{4.5}$$

$$\theta = \tan^{-1}\left(h_{inf}/L_{inf}\right) \tag{4.6}$$

α is the width of the equivalent strut member, h_{col} is the height of the column, I_{col} is the moment of inertia of the column, L_{inf} is the length of the infill panel, t_{inf} is the thickness of the infill panel, h_{inf} is the height of the infill panel, E_{inf} is the modulus of elasticity of the infill panel material, E_{fc} is the modulus of elasticity of the frame material (Mainstone and Weeks, 1970).

Equivalent diagonal strut members on the outer perimeter of the building were placed as shown in Figure 4.15. Eigenvalue analysis of the structural model yielded the natural vibration frequencies of the building as 2.03 Hz and 2.61 Hz for the first translational modes along the X and Y directions, respectively, and 3.81 Hz for the first torsional mode. The fourth mode was 7.14 Hz with 12% mass participation in the X direction. The analysis results are given in Table 4.4.

Table 4.4. *Natural frequencies determined from the analytical model with strut members*

Mode Number	Description	Frequency (Hz)	Modal Participating Mass Ratio (%)
1	X–Longitudinal	2.10	61
2	Y–Longitudinal	2.91	60
3	Torsion	4.09	49
4	X–Translational	7.59	13
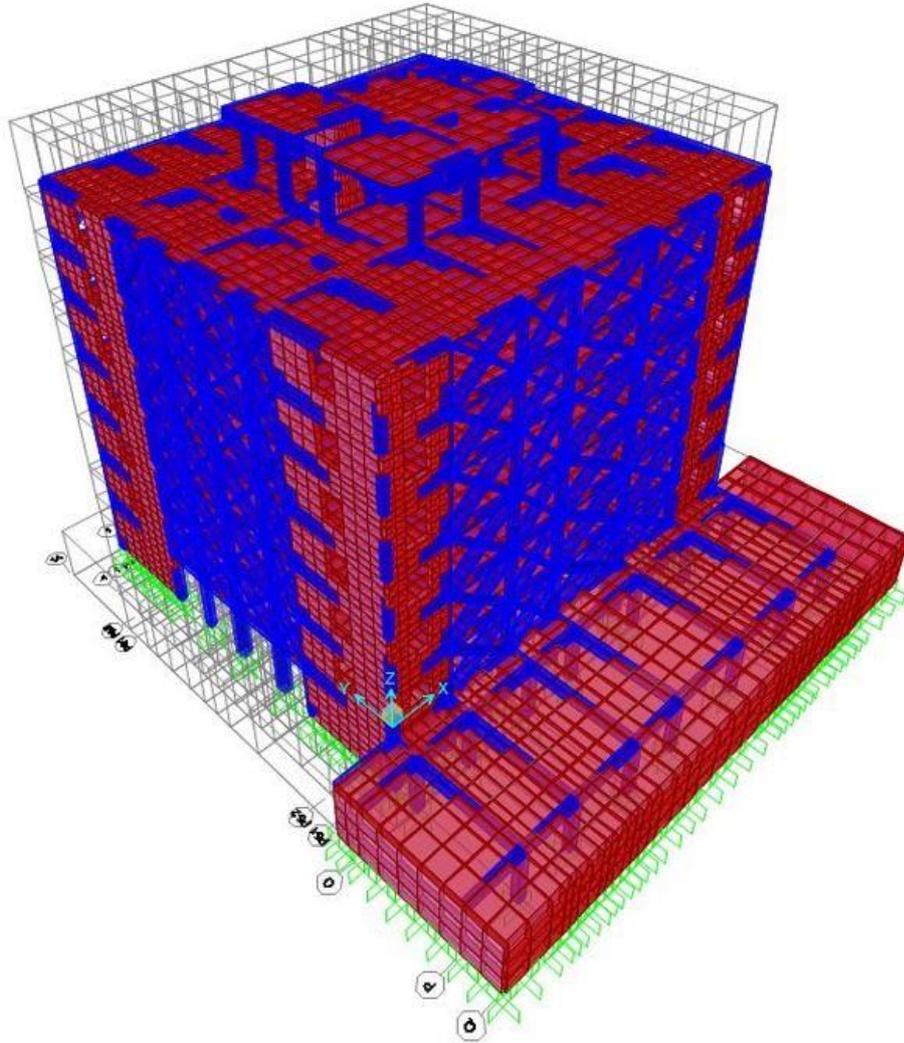
Figure 4.15. Finite element model with strut members

4.4.2. Validation of the Dynamic Properties and Calibration of the FEM

The dynamic properties of structural system that were determined from the FEM were validated using those identified from the ambient vibration records of the building. Thus, frequency values and mode shapes obtained in Fourier analysis (determined based on measurements) and SAP2000 software (determined from the FEM) are compared. As shown in Figure 4.16 and Table 4.5, the frequency values are different though the mode shapes are similar. Thus, it was imperative to update the analytical model.
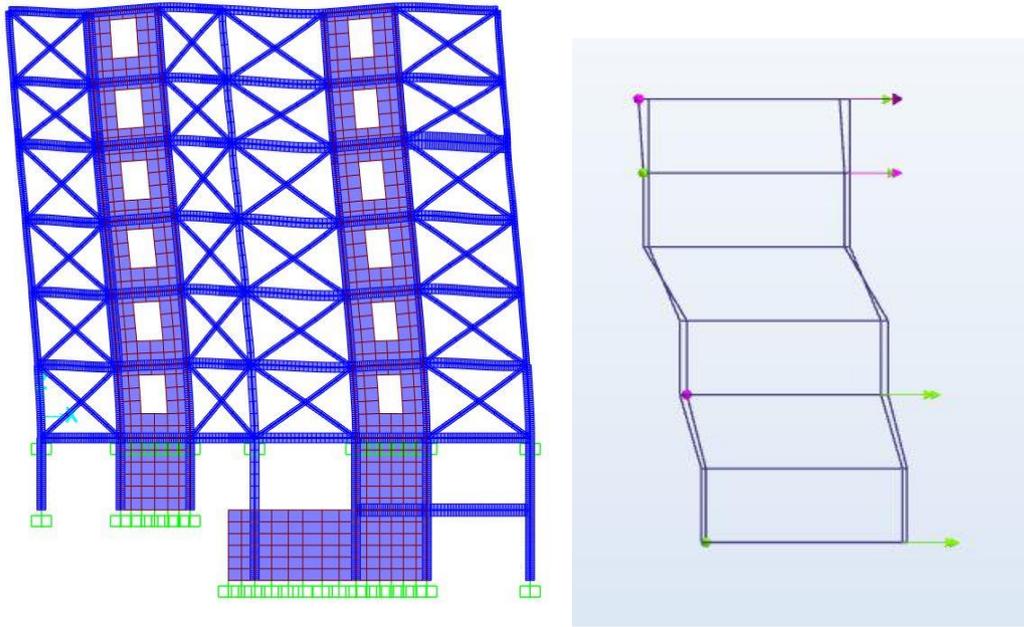
(a) First mode
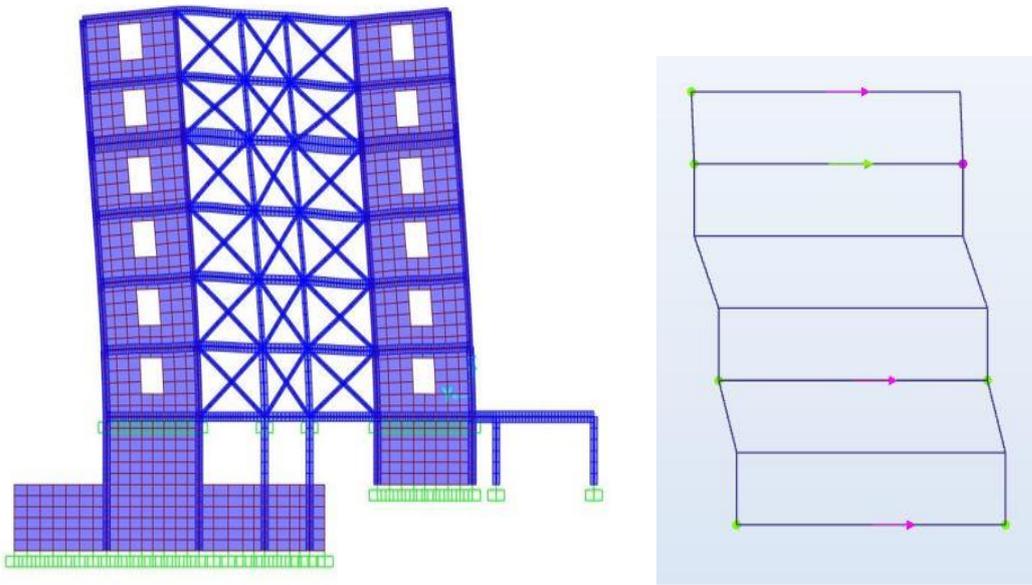
(b) Second mode

Figure 4.16. Comparison of the mode shapes between SAP2000 and Fourier analysis
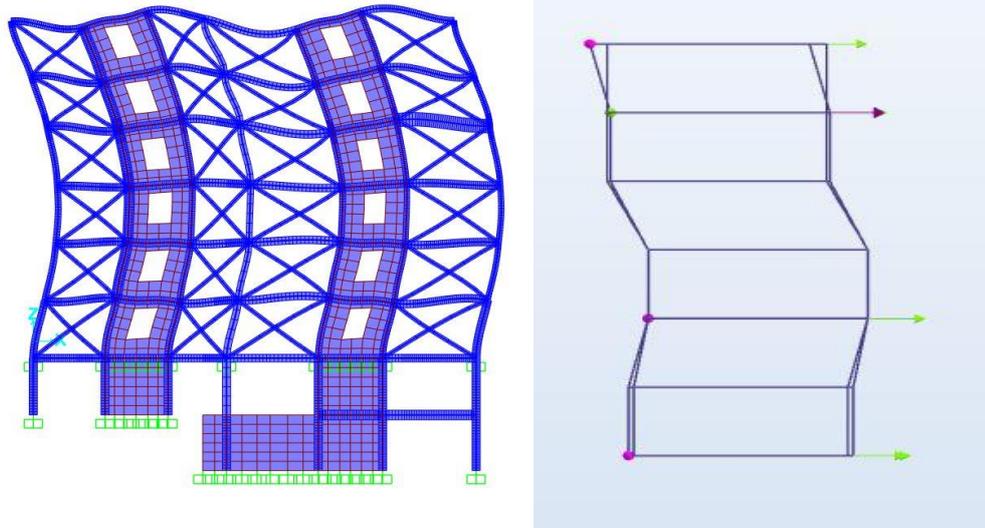
(c) Fourth mode
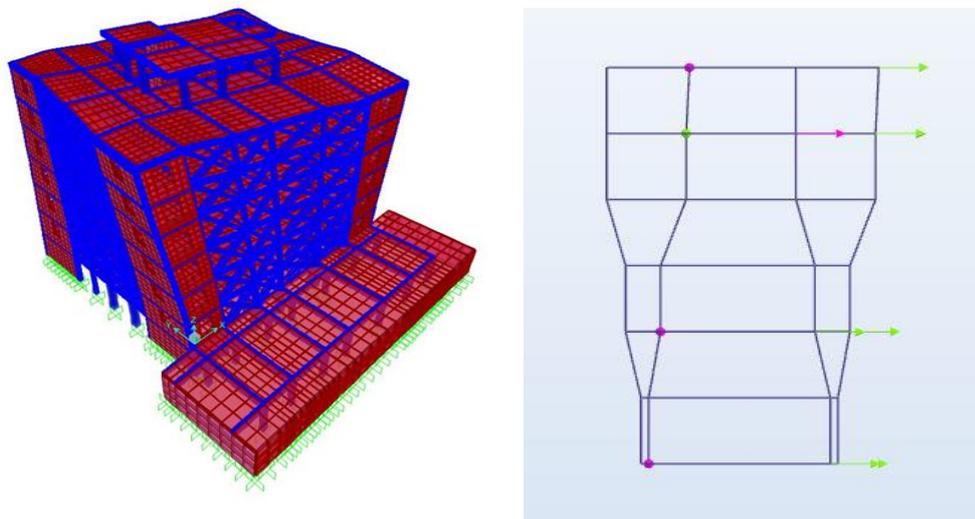
(d) Third mode

Figure 4.16. Comparison of the mode shapes between SAP2000 and Fourier analysis (continued)

Table 4.5. *Comparison of the analytical and experimental results*

Modes	Description	Frequency (Hz)		Differences (%)
		Fourier analysis	SAP2000	
1	X–Longitudinal	2.73	2.10	23
2	Y–Longitudinal	3.11	2.91	6
3	Torsion	5.00	4.09	18
4	X–Translational	8.54	7.59	11

The main purpose of the finite element model update is to calibrate and provide sufficient correlation with the results obtained from measurements in the actual structure. This is acquired by matching several pairs of analytical and experimental vibration modes in terms of natural frequencies and mode shapes. As a result, a more realistic finite element model can be obtained and can facilitate further studies on structural behavior. In the study of updating the analytical model, analysis was conducted on several models (shown in Table 4.6) considering various alternatives for some of the parameters selected. The model that gives closest modal properties to the experimental values was determined.

Table 4.6. General information related to alternative models

#of Model	Description					
	Openings (Door or Window)	First Floor	Strut Members	Roof	Sup. Dead Load (kN/m^2)	Live Load (kN/m^2)
#1	x	x	x	✓	x	2.0
#2	x	Fixed	x	✓	x	2.0
#3	x	Fixed	✓	✓	x	2.0
#4	x	Fixed	✓	x	x	2.0
#5, #5-1, #5-2, #5-3	x	Fixed	✓	✓	0.5 / 1.0 / 1.5 / 2.0	2.0
#6	✓	X	x	✓	x	2.0
#7	✓	Fixed	x	✓	x	2.0
#8	✓	Fixed	✓	✓	x	2.0
#9	✓	Fixed	✓	x	x	2.0
#10, #10-1, #10-2, #10-3	✓	Fixed	✓	✓	0.5 / 1.0 / 1.5 / 2.0	2.0

While developing alternative analytical models, the parameters related to the mass and stiffness of the structure were changed. The building mass depends on dead and live load cases. Hence, the effects of these load cases on building mass were investigated by trying different cases. The modulus of elasticity values of the diagonal strut elements were selected as another update parameter. The FEMA 356 (2000), TEC (2007), and Eurocode 6 (2005) suggested this value as $550f_k$, $750f_k$, and $1000f_k$, respectively. The following equation was utilized in order to calculate modulus of elasticity of infill walls to achieve a comparable result in this study:

$$E_{st} = 750f_k \qquad\qquad (4.7)$$

In addition, the equivalent strut width coefficient was taken 0.175 in Eq. (4.4). But in recent studies, this coefficient was used as 0.27 (Chrysostomou and Asteris, 2012). In this thesis, the analytical model was analyzed according to the widths determined by using both coefficient values and the results were summarized. Moreover, in the study conducted by Stafford Smith and Carter (1969), the equivalent diagonal strut width was stated to change with the applied load. In studies conducted by many researchers (Stafford and Carter, 1969; Mehrabi et al., 1996; Sattar and Liel, 2010; Celik, 2016) it has been shown that the initial stiffness of the infill wall corresponds to approximately twice of one strut stiffness. Based on these studies, two diagonal struts per infill wall were used in the elastic range in this study. Modal analysis of the alternative models was performed and frequency values of these models are presented in Tables 4.7 - 4.12. The model #10-3 (Analysis-4) was considered to give the closest results to the measured values because it gives closer frequency values for the first translational mode along the Y direction.

Table 4.7. *Modal analysis results for different analytical models (Analysis-1)*

MODEL [C12, C20, E_{b12}=25000MPa, E_{b20}=28000MPa, E_{st}=550*2,5=1375MPa, cf=0,175]

Mode Shapes	MDL #1 Freq (Hz)	MDL #2 Freq (Hz)	MDL #3 Freq (Hz)	MDL #4 Freq (Hz)	MDL #5 Freq (Hz)	MDL #5-1 Freq (Hz)	MDL #5-2 Freq (Hz)	MDL #5-3 Freq (Hz)	MDL #6 Freq (Hz)	MDL #7 Freq (Hz)	MDL #8 Freq (Hz)	MDL #9 Freq (Hz)	MDL #10 Freq (Hz)	MDL #10-1 Freq (Hz)	MDL #10-2 Freq (Hz)	MDL #10-3 Freq (Hz)
Mode #1 (X Dir.)	1.64	2.01	2.42	2.50	2.37	2.32	2.28	2.23	1.59	1.90	2.28	2.36	2.23	2.18	2.14	2.10
Mode #1 (Y Dir.)	2.57	3.24	3.44	3.58	3.37	3.30	3.24	3.18	2.43	2.96	3.16	3.28	3.09	3.03	2.97	2.91
Mode #1 (Tor.)	3.56	4.44	4.89	4.93	4.80	4.72	4.64	4.57	3.29	3.94	4.38	4.42	4.30	4.23	4.16	4.09
Mode #2 (X Dir.)	7.40	8.99	9.47	10.23	9.31	9.16	9.01	8.86	6.67	7.60	8.17	8.66	8.02	7.87	7.72	7.59
Mass	3935	3935	3935	3865	4107	4278	4450	4621	3875	3875	3875	3805	4047	4218	4390	4561

Table 4.8. *Modal analysis results for different analytical models (Analysis-2)*

MODEL [C12, C20, E_{b12}=25000MPa, E_{b20}=28000MPa, E_{st}=550*2,5=1375MPa, cf=0,27]

Mode Shapes	MDL #1 Freq (Hz)	MDL #2 Freq (Hz)	MDL #3 Freq (Hz)	MDL #4 Freq (Hz)	MDL #5 Freq (Hz)	MDL #5-1 Freq (Hz)	MDL #5-2 Freq (Hz)	MDL #5-3 Freq (Hz)	MDL #6 Freq (Hz)	MDL #7 Freq (Hz)	MDL #8 Freq (Hz)	MDL #9 Freq (Hz)	MDL #10 Freq (Hz)	MDL #10-1 Freq (Hz)	MDL #10-2 Freq (Hz)	MDL #10-3 Freq (Hz)
Mode #1 (X Dir.)	1.64	2.01	2.59	2.69	2.54	2.49	2.44	2.40	1.59	1.90	2.44	2.52	2.39	2.34	2.30	2.25
Mode #1 (Y Dir.)	2.57	3.24	3.54	3.69	3.47	3.40	3.34	3.28	2.43	2.96	3.25	3.38	3.19	3.12	3.06	3.00
Mode #1 (Tor.)	3.56	4.44	5.10	5.14	5.01	4.93	4.85	4.77	3.29	3.94	4.59	4.63	4.51	4.43	4.36	4.29
Mode #2 (X Dir.)	7.40	8.99	9.70	10.53	9.54	9.39	9.24	9.09	6.67	7.60	8.45	8.99	8.29	8.14	8.00	7.86
Mass	3935	3935	3935	3865	4107	4278	4450	4621	3875	3875	3875	3805	4047	4218	4390	4561

Table 4.9. *Modal analysis results for different analytical models (Anlysis-3)*

MODEL [C12, C25, E_{b12}=25000MPa, E_{b20}=28000MPa, E_{st}=750*2,5=1875MPa, cf=0,175]

Mode Shapes	MDL #1 Freq (Hz)	MDL #2 Freq (Hz)	MDL #3 Freq (Hz)	MDL #4 Freq (Hz)	MDL #5 Freq (Hz)	MDL #5-1 Freq (Hz)	MDL #5-2 Freq (Hz)	MDL #5-3 Freq (Hz)	MDL #6 Freq (Hz)	MDL #7 Freq (Hz)	MDL #8 Freq (Hz)	MDL #9 Freq (Hz)	MDL #10 Freq (Hz)	MDL #10-1 Freq (Hz)	MDL #10-2 Freq (Hz)	MDL #10-3 Freq (Hz)
Mode #1 (X Dir.)	1.64	2.01	2.52	2.61	2.47	2.42	2.38	2.33	1.59	1.90	2.38	2.46	2.33	2.28	2.24	2.19
Mode #1 (Y Dir.)	2.57	3.24	3.50	3.64	3.43	3.36	3.30	3.24	2.43	2.96	3.21	3.34	3.15	3.08	3.02	2.97
Mode #1 (Tor.)	3.56	4.44	5.01	5.06	4.93	4.84	4.77	4.69	3.29	3.94	4.51	4.54	4.43	4.35	4.28	4.21
Mode #2 (X Dir.)	7.40	8.99	9.61	10.40	9.45	9.30	9.15	9.00	6.67	7.60	8.34	8.85	8.18	8.03	7.89	7.75
Mass	3935	3935	3935	3865	4107	4278	4450	4621	3875	3875	3875	3805	4047	4218	4390	4561

58

Table 4.10. *Modal analysis results for different analytical models (Analysis-4)*

MODEL [C12, C25, E_{b12}=25000MPa, E_{b20}=28000MPa, E_{st}=750*2,5=1875MPa, cf=0,27]

Mode Shapes	MDL #1 Freq (Hz)	MDL #2 Freq (Hz)	MDL #3 Freq (Hz)	MDL #4 Freq (Hz)	MDL #5 Freq (Hz)	MDL #5-1 Freq (Hz)	MDL #5-2 Freq (Hz)	MDL #5-3 Freq (Hz)	MDL #6 Freq (Hz)	MDL #7 Freq (Hz)	MDL #8 Freq (Hz)	MDL #9 Freq (Hz)	MDL #10 Freq (Hz)	MDL #10-1 Freq (Hz)	MDL #10-2 Freq (Hz)	MDL #10-3 Freq (Hz)
Mode #1 (X Dir.)	1.64	2.01	2.74	2.84	2.68	2.63	2.58	2.53	1.59	1.90	2.58	2.66	2.52	2.47	2.42	2.38
Mode #1 (Y Dir.)	2.57	3.24	3.63	3.78	3.56	3.49	3.42	3.36	2.43	2.96	3.34	3.47	3.27	3.20	3.14	3.08
Mode #1 (Tor.)	3.56	4.44	5.28	5.33	5.19	5.10	5.02	4.94	3.29	3.94	4.77	4.80	4.68	4.60	4.52	4.45
Mode #2 (X Dir.)	7.40	8.99	9.89	10.8	9.74	9.59	9.43	9.32	6.67	7.60	8.69	9.27	8.53	8.38	8.23	8.09
Mass	3935	3935	3935	3865	4107	4278	4450	4621	3875	3875	3875	3805	4047	4218	4390	4561

Table 4.11. *Modal analysis results for different analytical models (Analysis-5)*

MODEL [C12, C20, E_{b12}=25000MPa, E_{b20}=28000MPa, E_{st}=1000*2,5=2500MPa, cf=0,175]

Mode Shapes	MDL #1 Freq (Hz)	MDL #2 Freq (Hz)	MDL #3 Freq (Hz)	MDL #4 Freq (Hz)	MDL #5 Freq (Hz)	MDL #5-1 Freq (Hz)	MDL #5-2 Freq (Hz)	MDL #5-3 Freq (Hz)	MDL #6 Freq (Hz)	MDL #7 Freq (Hz)	MDL #8 Freq (Hz)	MDL #9 Freq (Hz)	MDL #10 Freq (Hz)	MDL #10-1 Freq (Hz)	MDL #10-2 Freq (Hz)	MDL #10-3 Freq (Hz)
Mode #1 (X Dir.)	1.64	2.01	2.65	2.74	2.59	2.54	2.49	2.45	1.59	1.90	2.49	2.57	2.44	2.39	2.34	2.30
Mode #1 (Y Dir.)	2.57	3.24	3.57	3.72	3.50	3.43	3.37	3.31	2.43	2.96	3.28	3.41	3.21	3.15	3.09	3.03
Mode #1 (Tor.)	3.56	4.44	5.16	5.21	5.07	4.99	4.91	4.83	3.29	3.94	4.65	4.69	4.57	4.49	4.41	4.34
Mode #2 (X Dir.)	7.40	8.99	9.76	10.62	9.61	9.46	9.31	9.19	6.67	7.60	8.53	9.08	8.37	8.22	8.07	7.94
Mass	3935	3935	3935	3865	4107	4278	4450	4621	3875	3875	3875	3805	4047	4218	4390	4561

Table 4.12. *Modal analysis results for different analytical models (Analysis-6)*

MODEL [C12, C20, E_{b12}=25000MPa, E_{b20}=28000MPa, E_{st}=1000*2,5=2500MPa, cf=0,27]

Mode Shapes	MDL #1 Freq (Hz)	MDL #2 Freq (Hz)	MDL #3 Freq (Hz)	MDL #4 Freq (Hz)	MDL #5 Freq (Hz)	MDL #5-1 Freq (Hz)	MDL #5-2 Freq (Hz)	MDL #5-3 Freq (Hz)	MDL #6 Freq (Hz)	MDL #7 Freq (Hz)	MDL #8 Freq (Hz)	MDL #9 Freq (Hz)	MDL #10 Freq (Hz)	MDL #10-1 Freq (Hz)	MDL #10-2 Freq (Hz)	MDL #10-3 Freq (Hz)
Mode #1 (X Dir.)	1.64	2.01	2.90	3.01	2.84	2.79	2.73	2.68	1.59	1.90	2.72	2.81	2.66	2.61	2.56	2.51
Mode #1 (Y Dir.)	2.57	3.24	3.74	3.89	3.66	3.59	3.52	3.45	2.43	2.96	3.43	3.57	3.36	3.29	3.23	3.17
Mode #1 (Tor.)	3.56	4.44	5.49	5.54	5.39	5.30	5.22	5.14	3.29	3.94	4.96	5.00	4.88	4.79	4.71	4.64
Mode #2 (X Dir.)	7.40	8.99	10.09	11.11	9.95	9.80	9.69	9.54	6.67	7.60	8.96	9.59	8.80	8.64	8.49	8.35
Mass	3935	3935	3935	3865	4107	4278	4450	4621	3875	3875	3875	3805	4047	4218	4390	4561

59

4.5. Comparison of the Test Results with the FEM

Several trials were performed on the analytical model and the results were presented in the previous section. The calibrated models matched better the experimental mode frequencies. For this reason, calibrated analytical model #10-3 (Analysis-4) was chosen as the final updated model.

When the results of the selected analytical model from Analysis case 4 and the experimental ones were compared, the frequency values were found to be closer to the experimental results than the initial analytical model as shown in Table 4.13. The match of analytical and experimental mode shapes demonstrates that idealizations and assumptions made before for updating the model are reasonable.

During the comparison and calibration studies between the measurements and analytical results, one of the encountered problems was that the analytical model consisted of five normal stories, two basements, and roof floor, while the instrumentation merely covered the basement, first, fourth, and fifth floors. Therefore, the response of the roof and other floors was indirectly included in the dynamic measurements. These measurements were also influenced by the structural properties of these floors.

Table 4.13. *Comparisons of calibrated model and experimental analysis results*

Modes	Description	Frequency (Hz)		Differences (%)
		Fourier analysis	SAP2000	
1	X–Longitudinal	2.73	2.38	12.8
2	Y–Longitudinal	3.11	3.08	0.9
3	Torsion	5.00	4.45	11.0
4	X–Translational	8.54	8.09	5.3

CHAPTER 5

FLOOR VIBRATION ANALYSIS

5.1. Determining the Floor Vibration Threshold Level

At the design stage, vibrations should be regarded as one of the most important comfort conditions in buildings. Otherwise, they cause unrest and discomfort for residents and a loss use of the building. Allen and Murray (1993) have suggested the methods which involve calculation for vibration in floor and include design conditions.

The vibration detection thresholds of people show differences according to their activity. Figure 5.1 presents these thresholds as a function of frequency of floor for various occupancy areas. For instance, while people in offices and residences are disturbed by accelerations reaching 0.005 g, the people in an activity are not discomforted by the vibrations almost 10 times more (0.05 g) (American Institute of Steel Construction (AISC), 2016). This chapter presents the evaluation of floor vibration based on measurements and analyses under the walking load on the ground and second floors. It also presents floor vibration calculations and comparisons with limits after modifications applied to reduce the floor vibration.
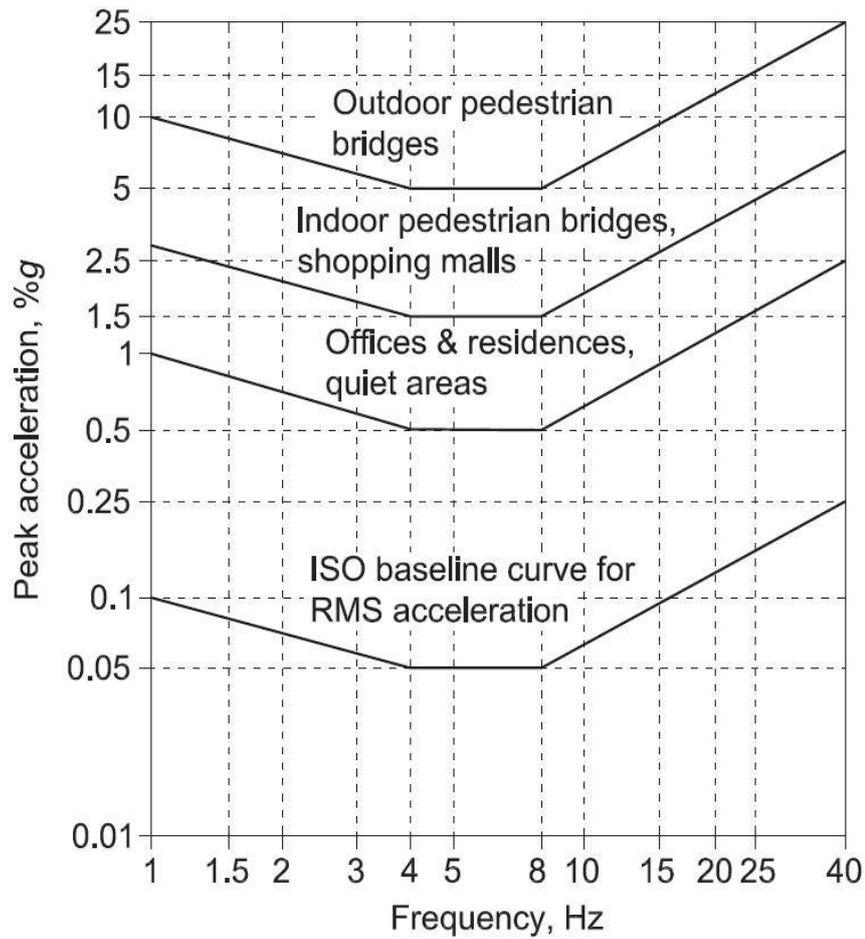
Figure 5.1. Recommended peak acceleration for human comfort vibration due to human activities
(ASIC, 2016)

5.1.1. Vertical Acceleration Records

Within the scope of the study, measurements in the vertical direction were recorded with uniaxial accelerometers installed on the ground and second floor slabs of the investigated RC building. The time variations of these measurements are given in Figs. 5.2 and 5.3, and the hourly maximum values are shown in Figs. 5.4 and 5.5.
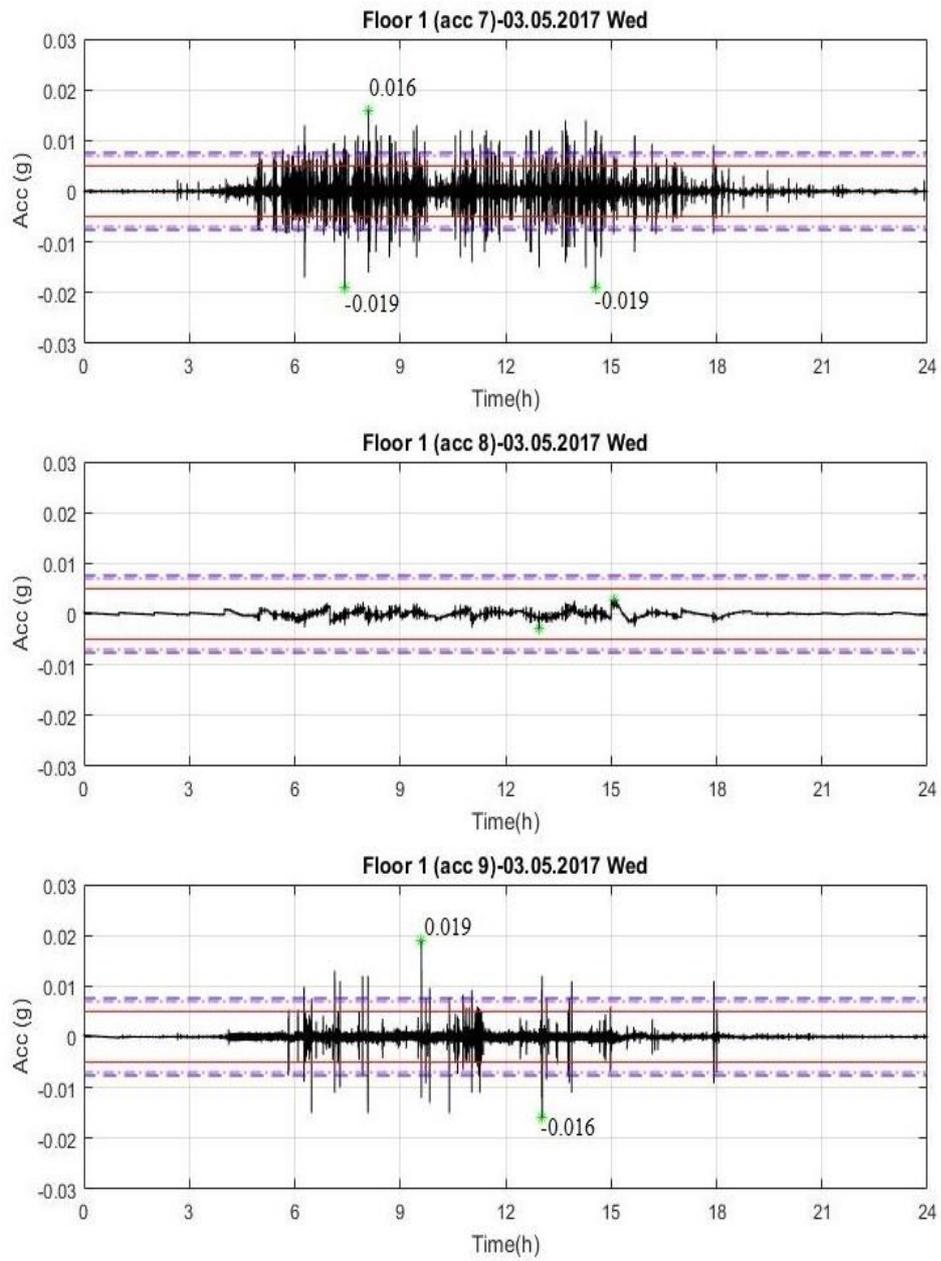
(a)

Figure 5.2. Time history (first day)
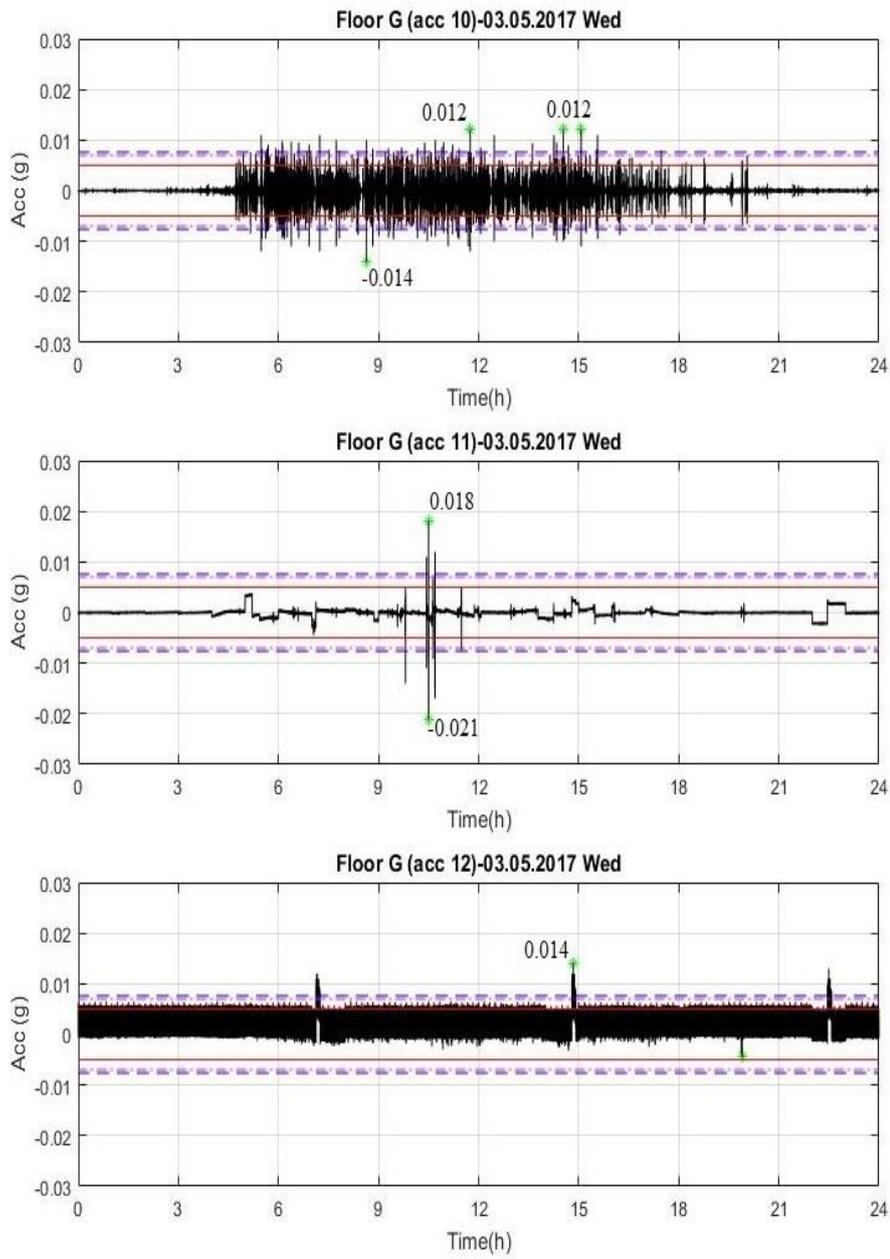
(b)

Figure 5.2. Time history (first day) (continued)
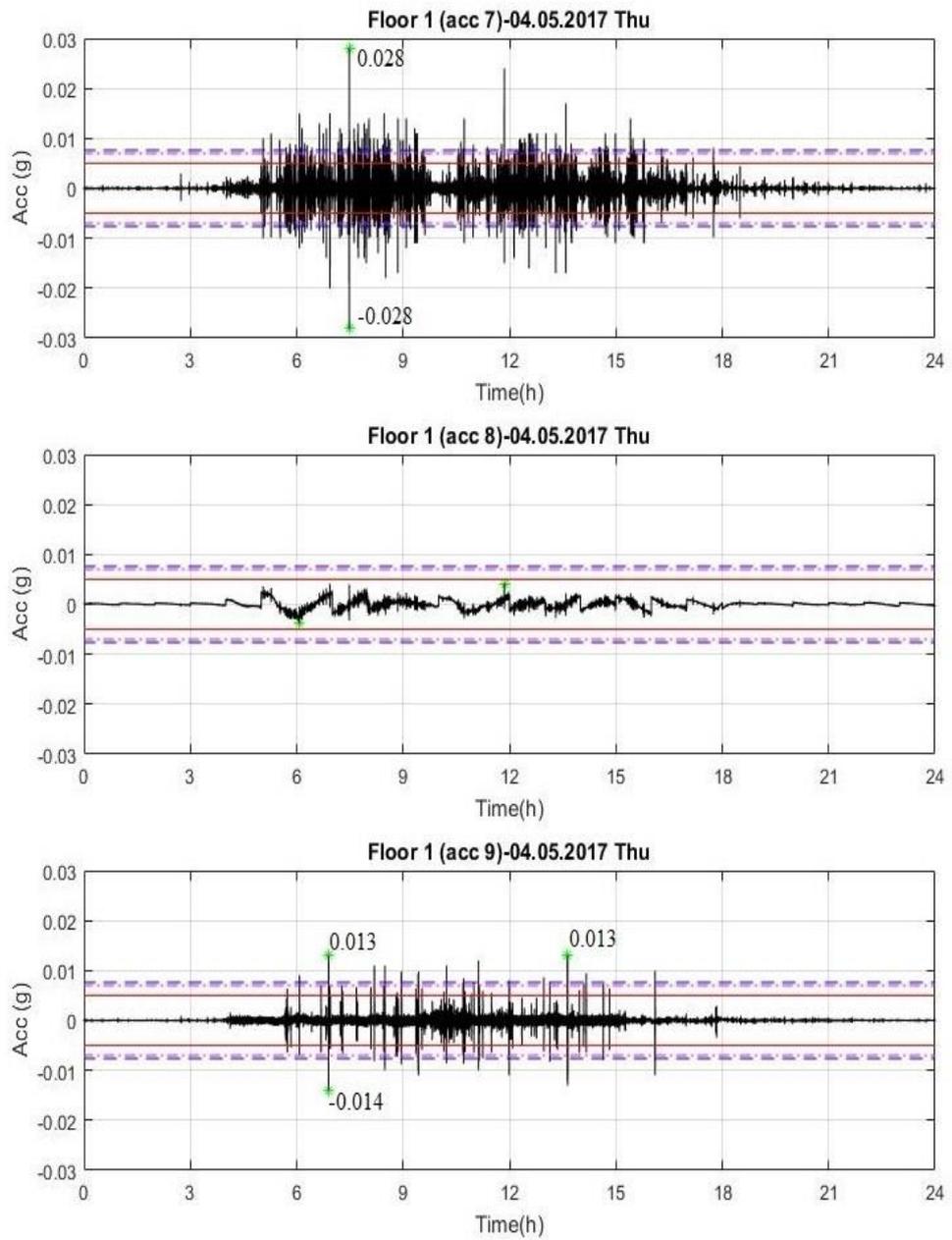
(a)

Figure 5.3. Time history (second day)
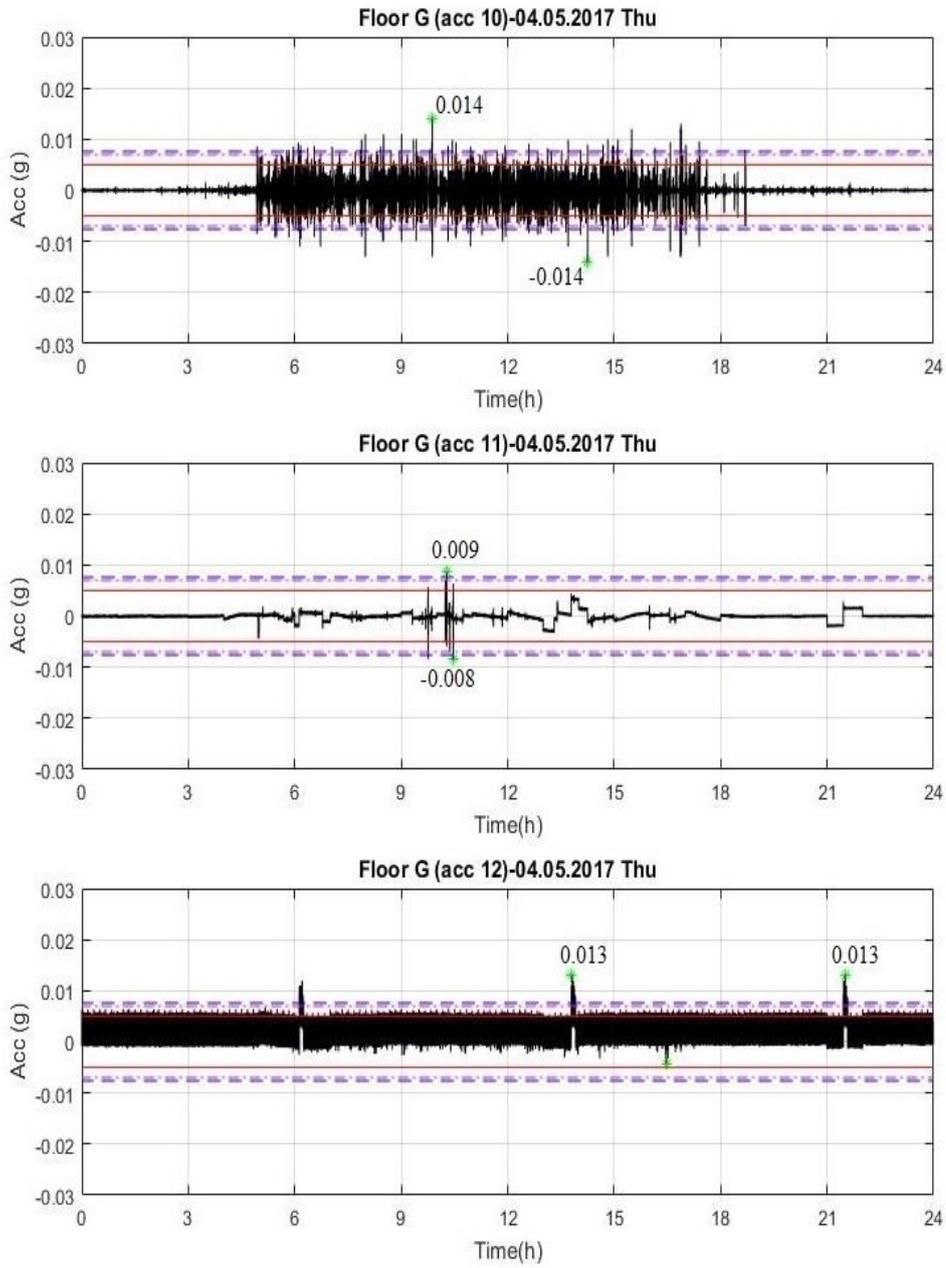
(b)

Figure 5.3. Time history (second day) (continued*)*
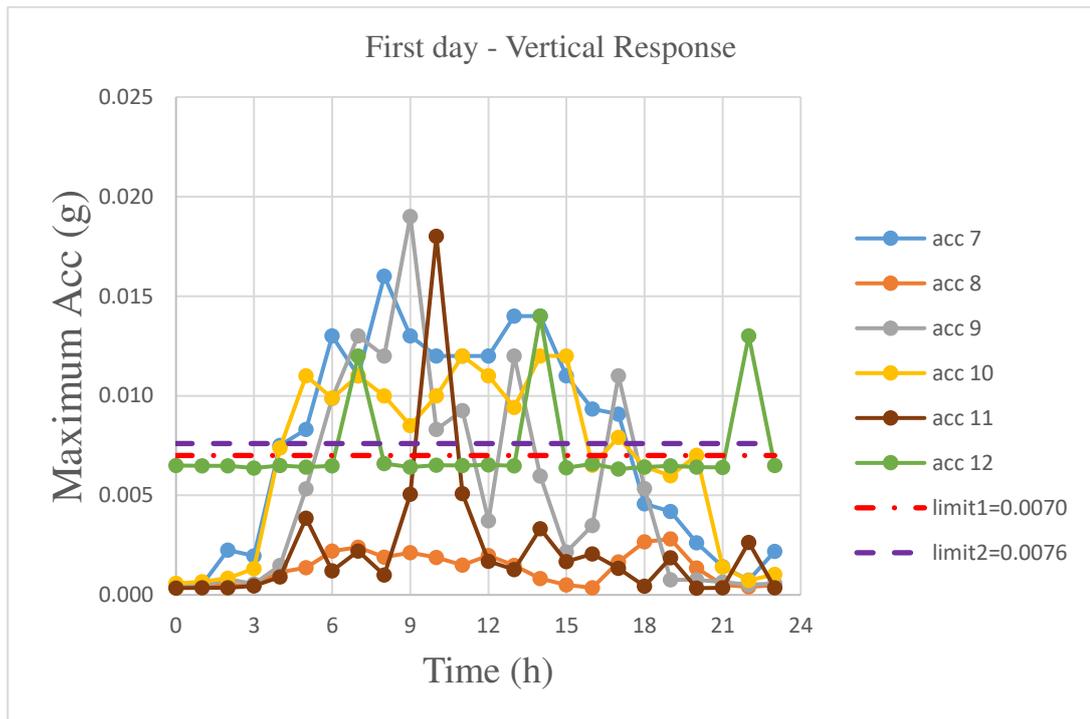
Figure 5.4. Hourly variation of maximum acceleration (03/05/2017)
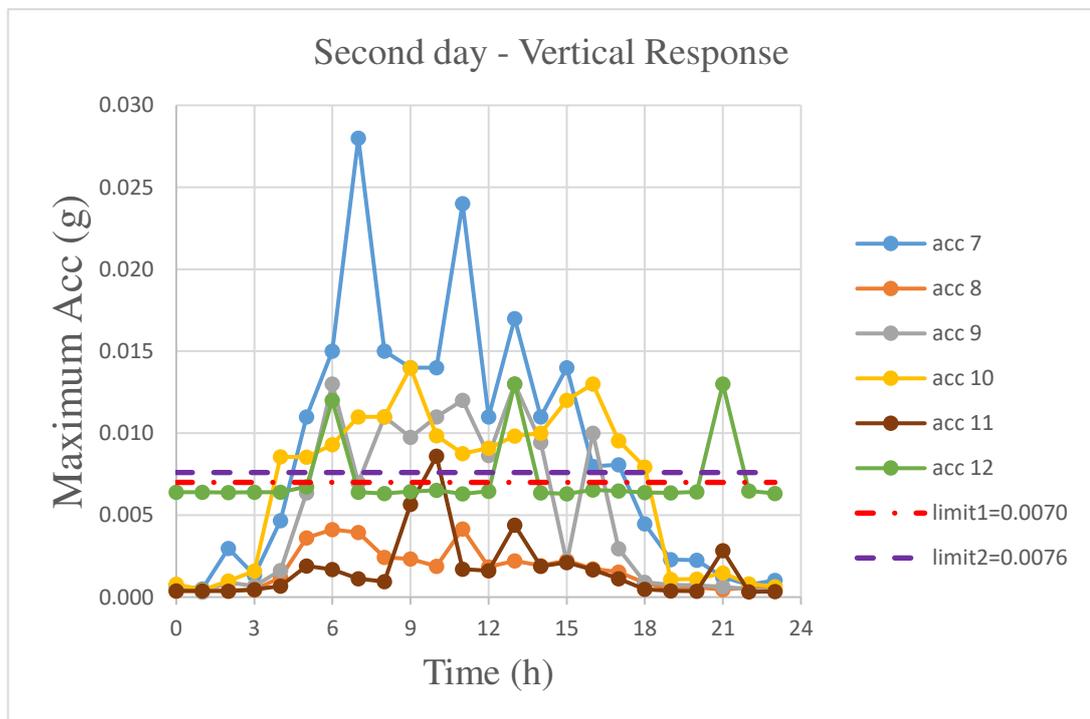
Figure 5.5. Hourly variation of maximum acceleration (04/05/2017)

When the recorded accelerations are examined, it is seen that high values were measured in accelerometers 7, 9, and 10 during working hours. In order to determine whether these acceleration values are tolerable in the conditions of use, the limit values given in the above mentioned design guide were used. First, the frequency of the floor was found from the Fourier analysis of the recorded vertical acceleration (see Fig. 5.6). Then, where this frequency value corresponds to Figure 5.1 was determined and the limit value was calculated as 0.0076 g and 0.0070 g (see Figs. 5.4 and 5.5). These comparison revealed that, accelerations recorded at accelerometers 7, 9, and 10 exceeded this limit value during working hours. Therefore, it is concluded that the existing flooring system does not satisfy the comfort conditions of AISC (2016).
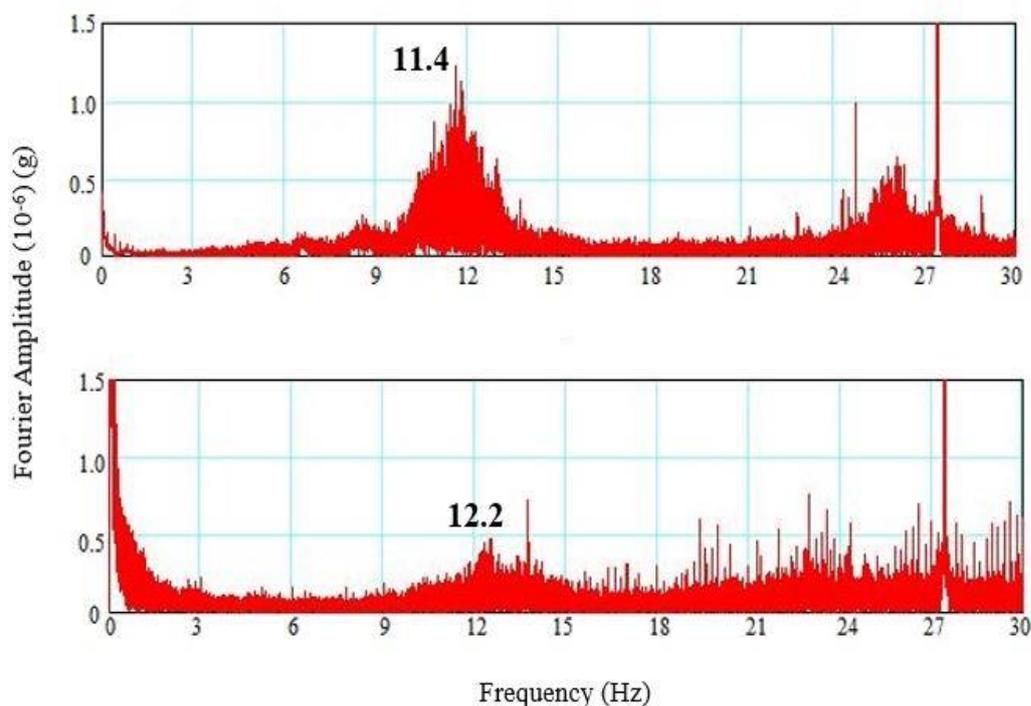
Figure 5.6. Floor frequency for the ground and second floors

5.1.2. Finite Element Model Analysis

Finite element analysis can be employed to estimate vibration response. Firstly, the part of the structure being evaluated is defined in terms of its geometry, mass, stiffness, and damping. Secondly, dynamic properties such as natural frequencies and mode shapes are predicted using eigenvalue analysis. This step was performed in the previous chapter. Thirdly, human-induced loads are presented by a Fourier series or effective impulse as described below. So, in this part of the study, floor vibrations were determined analytically and compared to the tolerance limits to determine whether or not vibrations are excessive.

Finite element model of the slabs of the building was prepared using SAP2000. This part of the study is conducted to obtain a time history plot of floor acceleration for a person walking across the concrete slab that is 4.45 m by 4.80 m in plan. A graph of the vertical accelerations at the middle of the slab was obtained to make sure that the maximum acceleration is calculated. The dynamic effects of a person that weighs approximately 735 N (Lee et al., 2015) walking across the middle of the slab were modeled. The person is assumed to walk with a frequency of 2 Hz (Arup, 2004; Saunier et al., 2011) which means the footfall impacts the slab at every half a second. The forward speed was assumed as 1.5 m/s which results in a stride length of 0.75 m. The peak load was assumed to be 1.4 times the weight (approximately 1 kN) and the duration of impact was taken as 0.45 seconds (Saunier et al., 2011). Therefore, a pulse load of 1 kN lasting 0.45 seconds spaced at 0.75 m apart every half a second was applied. On the plan view, the path of the walk was defined with a line through the middle of the slab. Nodes were added at every 0.75 m which correspond to the stride length. The first step was to define a time history function for the footfall. A new user-defined function was added. Figure 5.7 shows this footfall pulse. The second step was to define a separate load pattern for each footstep. After this step, the footfall loads were assigned to different joints to define the walking path. Modal damping was also set 2 percent (see Table 4.1). The values obtained from the result of walking load

analysis are summarized in Table 5.1. Directions of walking on the floor system are given in Figure 5.8.
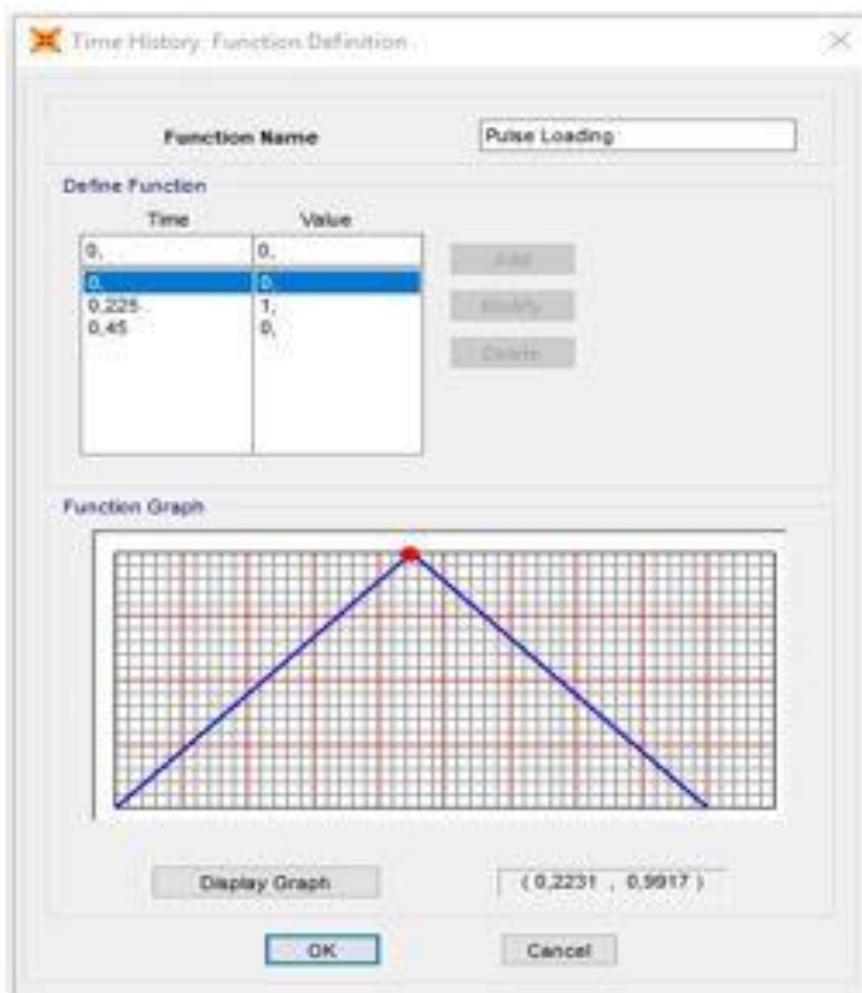
Figure 5.7. Pulse loading (for every footstep (0.75m every 0.5s))

Direction of walking

(a)

Figure 5.8. Different walking load paths

71

Direction of walking

(b)

Figure 5.8. Different walking load paths (continued)

72

Table 5.1.a. *Vibration calculation results for walking load (ground slab) (Analysis-1)*

Model	Location	Middle Point of the slab*	Floor Properties d=14 cm, fn=13 Hz, Acc limit=0.81(%g)						Direction of Walking
			One Person		Two Person		One - Two Person		
			Max (%g)	Min (%g)	Max (%g)	Min (%g)	Max (%g)	Min (%g)	
1	-0.88	353	0.12	-0.10	0.24	-0.20	0.23	-0.19	→
		699	0.00	0.00	0.00	0.00	0.00	0.00	
		977	0.00	0.00	0.00	0.00	0.00	0.00	
2	-0.88	353	0.02	-0.02	0.04	-0.04	0.04	-0.03	↓
		699	0.02	-0.03	0.04	-0.06	0.04	-0.06	
		60	0.01	0.01	0.01	0.01	0.01	0.01	
3	-0.88	353	0.00	0.00	0.00	0.00	0.00	0.00	→
		6	0.13	-0.13	0.26	-0.26	0.24	-0.25	
		977	0.00	0.00	0.00	0.00	0.00	0.00	
4	-0.88	353	0.13	-0.11	0.25	-0.21	0.24	-0.20	→
		699	0.00	0.00	0.00	0.00	0.00	0.00	
		977	0.00	0.00	0.00	0.00	0.00	0.00	
5	-0.88	353	0.00	0.00	0.00	0.00	0.00	0.00	→
		699	0.00	0.00	0.00	0.00	0.00	0.00	
		60	0.00	0.00	0.00	0.00	0.00	0.00	
6	-0.88	353	0.00	0.00	0.00	0.00	0.00	0.00	→
		6	0.14	-0.13	0.29	-0.25	0.27	-0.24	
		977	0.00	0.00	0.00	0.00	0.00	0.00	
7	-0.88	525	0.12	-0.10	0.23	-0.20	0.22	-0.19	↓
		699	0.00	0.00	0.00	0.00	0.00	0.00	
		977	0.00	0.00	0.00	0.00	0.00	0.00	
8	-0.88	525	0.00	0.00	0.00	0.00	0.00	0.00	↓
		699	0.00	0.00	0.00	0.00	0.00	0.00	
		977	0.00	0.00	0.00	0.00	0.00	0.00	
9	-0.88	525	0.00	0.00	0.00	0.00	0.00	0.00	↓
		24	0.12	-0.13	0.25	-0.26	0.23	-0.24	
		977	0.00	0.00	0.00	0.00	0.00	0.00	

*It refers to the midpoint of the slabs with accelerometers

Table 5.1.b. *Vibration calculation results for walking load (second slab) (Analysis-1)*

Model	Location	Middle point of the slab	Floor Properties d=14 cm, fn=13 Hz, acc limit=0.81(%g) One Person		Two Person		One - Two Person		Direction of Walking
			Max (%g)	Min (%g)	Max (%g)	Min (%g)	Max (%g)	Min (%g)	
1	5.12	24	0.37	-0.30	0.74	-0.60	-1.51	-2.18	
		417	0.00	0.00	0.00	0.00	0.00	0.00	→
		709	0.00	0.00	0.00	0.00	0.00	0.00	
2	5.12	24	0.06	-0.05	0.13	-0.11	0.12	-0.10	
		417	0.06	-0.09	0.12	-0.18	0.12	-0.17	↓
		60	0.02	0.02	0.03	0.04	0.03	0.03	
3	5.12	24	0.00	0.00	0.00	0.00	0.00	0.00	
		417	0.24	-0.24	0.48	-0.47	0.45	-0.44	→
		709	0.00	0.00	0.00	0.00	0.00	0.00	
4	5.12	24	0.32	-0.27	0.65	-0.53	0.61	-0.50	
		417	0.00	0.00	0.00	0.00	0.00	0.00	→
		709	0.00	0.00	0.00	0.00	0.00	0.00	
5	5.12	24	0.00	0.00	0.00	0.00	0.00	0.00	
		417	0.00	0.00	0.00	0.00	0.00	0.00	→
		709	0.00	0.00	0.00	0.00	0.00	0.00	
6	5.12	24	0.00	0.00	0.00	0.00	0.00	0.00	
		417	0.21	-0.19	0.43	-0.38	0.40	-0.36	→
		709	0.00	0.00	0.00	0.00	0.00	0.00	
7	5.12	14	0.37	-0.26	0.74	-0.53	0.69	-0.49	
		417	0.00	0.00	0.00	0.00	0.00	0.00	↓
		709	0.00	0.00	0.00	0.00	0.00	0.00	
8	5.12	525	0.00	0.00	0.00	0.00	0.00	0.00	
		699	0.00	0.00	0.00	0.00	0.00	0.00	↓
		977	0.00	0.00	0.00	0.00	0.00	0.00	
9	5.12	24	0.00	0.00	0.00	0.00	0.00	0.00	
		672	0.25	-0.26	0.50	-0.51	0.47	-0.48	↓
		709	0.00	0.00	0.00	0.00	0.00	0.00	

5.1.3. AISC Calculations

In Turkey, there is no design guide provides design criteria for floor vibrations. Therefore, the assessment will be produced in this part of the thesis according to the AISC (2016) design guide. First, the system's approximate peak acceleration ratio is calculated and then compared with the threshold values to determine whether the functionality of the vibration level is acceptable. The necessary parameters regarding the vibration calculation in the guide are given below. The recommended values for frequencies and dynamic coefficients are given in Table 5.2.

Table 5.2. *Common forcing frequency (f) and dynamic coefficients* (α_i) (AISC, 2016)*

Harmonic	Person Walking		Aerobics Class		Group Dancing	
i	f (Hz)	α_i	f, Hz	α_i	f, Hz	α_i
1	1.6–2.2	0.5	2.0–2.75	1.5	1.5–2.7	0.5
2	3.2–4.4	0.2	4.0–5.5	0.6	3.0–5.4	0.05
3	4.8–6.6	0.1	6.0–8.25	0.1	-	-
4	6.4–8.8	0.05	-	-	-	-

* Dynamic coefficient – peak sinusoidal force/weight of person (s).

High frequency floors (> 9 Hz) do not undergo resonance owing to walking; therefore, the peak acceleration of the floor can be determined from Equation 5.1.

$$\frac{\alpha_p}{g} = \frac{2\pi R R_M I_{eff}}{W} \sqrt{\frac{1 - e^{-4\pi h\beta}}{h\pi\beta}} \qquad (5.1)$$

$$= \left(\frac{154.2}{W}\right)\left(\frac{f_{step}^{1.43}}{f_n^{0.3}}\right)\sqrt{\frac{1 - e^{-4\pi h\beta}}{h\pi\beta}} \qquad (in\ lb)$$

where,

α_p/g : Peak acceleration as a fraction of the acceleration due to gravity

R : Calibration factor = 1.3

R_M : Higher mode factor = 2.0

I_{eff} : Effective impulse, ($I_{eff} = \left(\dfrac{f_{step}^{1.43}}{f_n^{1.30}}\right)\left(\dfrac{Q}{17.8}\right)$)

W : Effective weight of the floor

f_n : Natural frequency of floor structure

f_{step} : Step frequency, ($f_{step} = 2\ Hz\ for\ walking$)

β : Damping ratio

h : Step frequency harmonic matching the natural frequency, from Table 5.3.

Bodyweight, Q, was assumed 75.6 kg (≈168 lb) in determining I_{eff}.

Table 5.3. *Harmonic matching the natural frequency of high-frequency floors (AISC, 2016)*

f_n, Hz	h
9–11	5
11–13.2	6
13.2–15.4	7

As seen in the above equations, the most significant parameter for vibration serviceability is the natural frequency of the floor. The floors are generally plate elements working in two directions; their stiffness changes with support conditions, thickness and material properties. Therefore, the natural frequency will be different for various flooring systems. An analytical model requires to be established using appropriate software and support conditions in order to identify the natural frequency of the flooring systems. The criteria point out that the floor system is adequately provided that the peak acceleration, α_p, caused by walking activity obtained from Equation 5.1 does not exceed the acceleration limit, α_0/g, for the comfortable occupancy. Figure 5.1 can also be utilized to assess a floor system provided that the original ISO plateau between 4 Hz and almost 8 Hz is widened from 3 Hz to 20 Hz.

The floor deflection values calculated from the finite element model created by using SAP2000 are given in Figure 5.9. As seen from the figures, the maximum deflection

under dead loads is determined as 2.1 mm and 2.5 mm for ground and second floors, respectively. These deflection values were used to determine the frequencies of the floor according to AISC (2016) design guide.
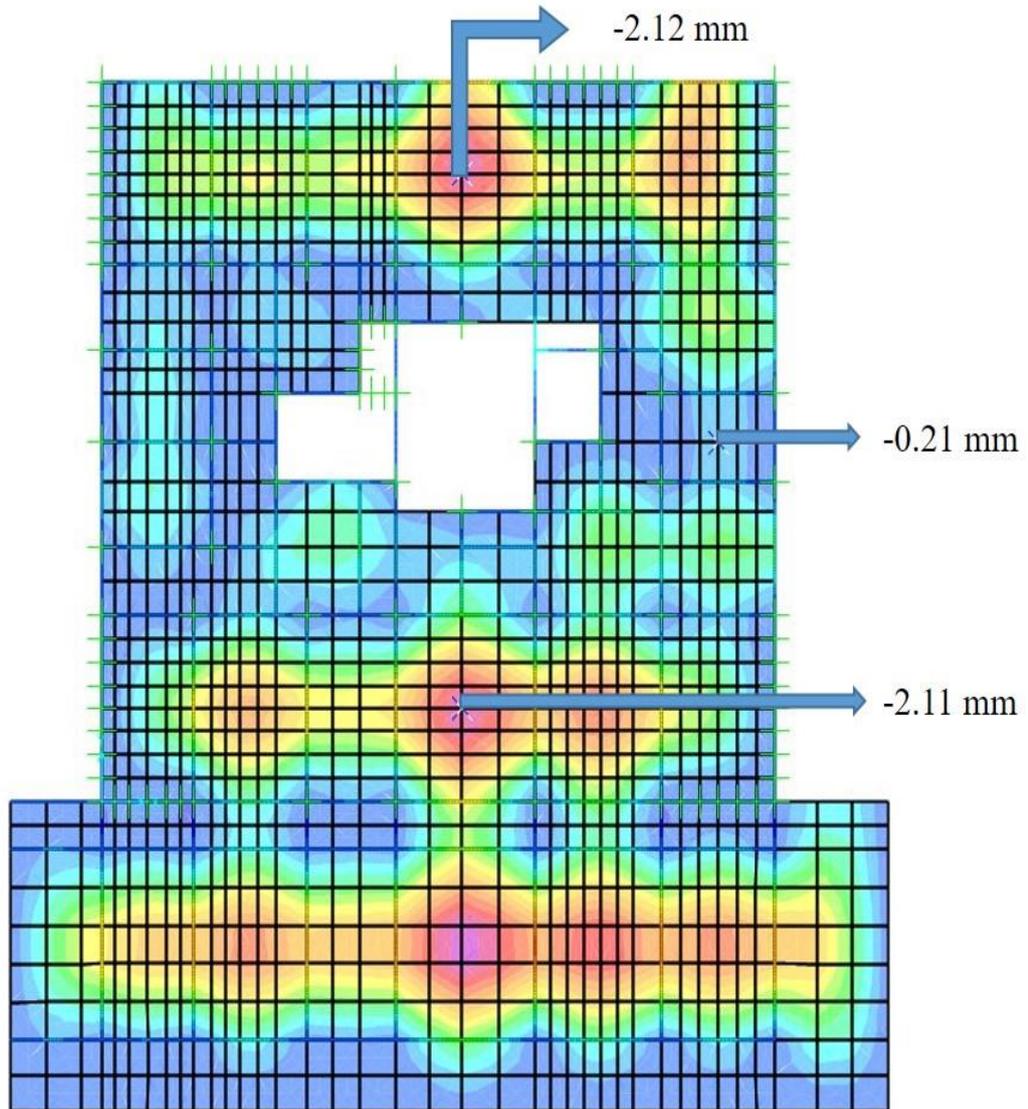
(a) ground floor

Figure 5.9. Deflection values
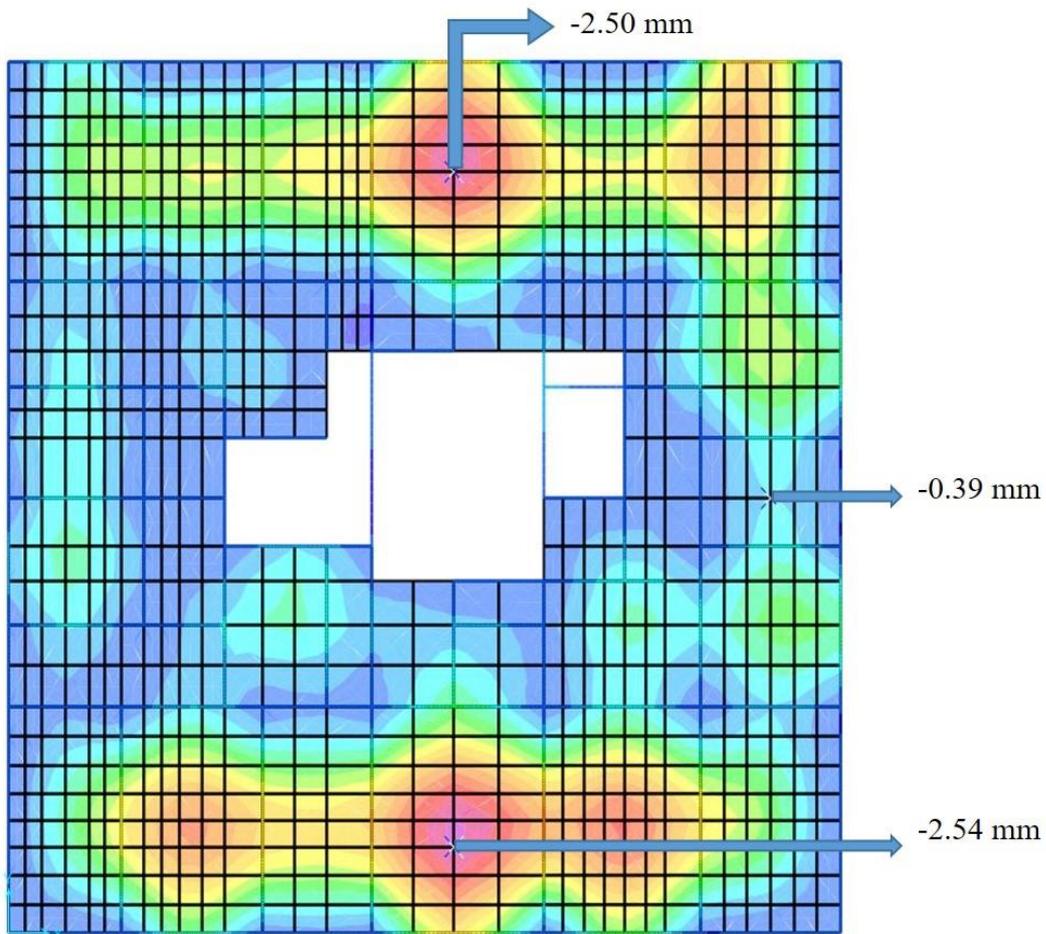
(b) second floor

Figure 5.9. Deflection values (continued)

The load at floors are calculated as below;

Floor: $0.14 \text{ m} \times 2.5 \text{ t/m}^3 = 0.35 \text{ t/m}^2$

Levelling: $0.05 \text{ m} \times 2.2 \text{ t/m}^3 = 0.11 \text{ t/m}^2$

Cladding: $0.02 \text{ m} \times 2.7 \text{ t/m}^3 = 0.054 \text{ t/m}^2$

Plaster: $0.02 \text{ m} \times 2.0 \text{ t/m}^3 = 0.04 \text{ t/m}^2$

Total weight: $0.554 \text{ t/m}^2 \times 4.45 \text{ m} \times 4.80 \text{ m} = 11.83 \text{ t}$ (for ground and second floors)

When the deflection value acquired from the analytical model is substituted in Equation 5.2., the corresponding frequencies of the floor system becomes:

$$f_n = 0{,}18\sqrt{\frac{g}{\Delta}} = 0{,}18\sqrt{\frac{g}{2.12}} = 12.2 \; Hz \tag{5.2.1}$$

$$f_n = 0{,}18\sqrt{\frac{g}{\Delta}} = 0{,}18\sqrt{\frac{g}{2.54}} = 11.2 \; Hz \tag{5.2.2}$$

These frequencies were similar to those from the Fourier analysis of the vertical acceleration. After determining the natural frequency and floor load, the acceleration ratio is calculated from Equation 5.1. For this case, the following values for the floor are utilized;

d = 140 mm (thickness of slabs)

For ground floor (one person):

Natural frequency of the slab: f_n = 12.2 Hz

Step frequency: f_{step} = 2.0 Hz

Recommended limit value: α_0/g = 0.76

Bodyweight: Q = 75.6 kg (≈168 lb)

Weight of the slab: W = 118.3 kN (≈26595 lb)

Damping ratio: β = 0.02

Step frequency harmonic matching: h = 6

$$\frac{\alpha_p}{g} = \left(\frac{154.2}{26595}\right)\left(\frac{2^{1.43}}{12.2^{0.3}}\right)\sqrt{\frac{1 - e^{-4\pi*6*0.02}}{6*\pi*0.02}}$$

$$\frac{\alpha_p}{g} = 0.0106$$

The calculated peak acceleration is greater than the acceleration limit of 0.0076 g, obtained from Figure 5.1. This indicated that the floor does not satisfy vibration requirements.

The case for one person in the second floor leads to:

Natural frequency of the slab: f_n = 11.2 Hz

Step frequency: f_{step} = 2.0 Hz

Recommended limit value: α_0/g = 0.70

$$\frac{\alpha_p}{g} = \left(\frac{154.2}{26595}\right)\left(\frac{2.0^{1.43}}{11.2^{0.3}}\right)\sqrt{\frac{1 - e^{-4\pi*6*\beta}}{6*\pi\beta}}$$

$$\frac{\alpha_p}{g} = 0.0109$$

For this case, the peak acceleration is greater than the acceleration limit of 0.0070 g, extracted from Figure 5.1. Therefore, the second floor vibration level is also above the limit.

As a result of the calculations made according to AISC (2016), the floor acceleration ratios due to human movements were determined as 0.011 g for one person. As shown in Figure 5.1, 0.0076 g and 0.0070 g acceleration ratios are limit values for frequencies of 12.2 Hz and 11.2 Hz, respectively, when the slab is used as an office. When this situation is considered, it is concluded that neither one of the flooring systems satisfies the vibration criteria required in office type buildings under the situation for one walking person.

5.2. Reduction of Floor Vibration by Stiffening the Slabs

The results obtained from the analytical model reveal that the floor acceleration values for the examined slabs do not satisfy the limit values for two or more walking people. Therefore, to keep them below the thresholds the floors need to be made stiffer. A simple option to ensure this can be to increase the thickness of the slabs. The floor

80

acceleration values obtained for the case of increased slab thickness (d=180 mm) are summarized in Table 5.4.

Table 5.4.a. Vibration calculation results for walking load (ground slab) (Anlaysis-2)

Model	Kotu	Point	Floor Properties d=18 cm, fn=15.1 Hz, acc limit=0.94(%g)					
			One Person		Two Person		One - Two Person	
			Max (%g)	Min (%g)	Max (%g)	Min (%g)	Max (%g)	Min (%g)
1	-0.88	353	0.08	-0.09	0.15	-0.18	0.15	-0.17
		699	0.00	0.00	0.00	0.00	0.00	0.00
		977	0.00	0.00	0.00	0.00	0.00	0.00
2	-0.88	353	0.02	-0.02	0.04	-0.03	0.03	-0.03
		699	0.01	-0.01	0.03	-0.02	0.03	-0.02
		60	0.00	0.00	0.00	0.00	0.00	0.00
3	-0.88	353	0.00	0.00	0.00	0.00	0.00	0.00
		6	0.06	-0.08	0.13	-0.16	0.12	-0.15
		977	0.00	0.00	0.00	0.00	0.00	0.00
4	-0.88	353	0.08	-0.08	0.17	-0.17	0.16	-0.16
		699	0.00	0.00	0.00	0.00	0.00	0.00
		977	0.00	0.00	0.00	0.00	0.00	0.00
5	-0.88	353	0.00	0.00	0.00	0.00	0.00	0.00
		699	0.00	0.00	0.00	0.00	0.00	0.00
		60	0.00	0.00	0.00	0.00	0.00	0.00
6	-0.88	353	0.00	0.00	0.00	0.00	0.00	0.00
		6	0.08	-0.07	0.16	-0.14	0.15	-0.14
		977	0.00	0.00	0.00	0.00	0.00	0.00
7	-0.88	525	0.09	-0.09	0.18	-0.19	0.17	-0.18
		699	0.00	0.00	0.00	0.00	0.00	0.00
		977	0.00	0.00	0.00	0.00	0.00	0.00
8	-0.88	525	0.00	0.00	0.00	0.00	0.00	0.00
		699	0.00	0.00	0.00	0.00	0.00	0.00
		977	0.00	0.00	0.00	0.00	0.00	0.00
9	-0.88	525	0.00	0.00	0.00	0.00	0.00	0.00
		24	0.07	-0.08	0.13	-0.16	0.13	-0.15
		977	0.00	0.00	0.00	0.00	0.00	0.00

Table 5.4.b. Vibration calculation results for walking load (second slab) (Anlaysis-2)

Model	Kotu	Point	Floor properties d=18 cm, fn=15.1 Hz, acc limit=0.94(%g)					
			One Person		Two Person		One - Two Person	
			Max (%g)	Min (%g)	Max (%g)	Min (%g)	Max (%g)	Min (%g)
1	5.12	24	0.08	-0.06	0.15	-0.13	0.15	-0.12
		417	0.00	0.00	0.00	0.00	0.00	0.00
		709	0.00	0.00	0.00	0.00	0.00	0.00
2	5.12	24	0.02	-0.02	0.04	-0.03	0.03	-0.03
		417	0.01	-0.01	0.03	-0.02	0.03	-0.02
		60	0.00	0.00	0.00	0.00	0.00	0.00
3	5.12	24	0.00	0.00	0.00	0.00	0.00	0.00
		417	0.07	-0.06	0.14	-0.12	0.14	-0.12
		709	0.00	0.00	0.00	0.00	0.00	0.00
4	5.12	24	0.07	-0.07	0.14	-0.15	0.14	-0.14
		417	0.00	0.00	0.00	0.00	0.00	0.00
		709	0.00	0.00	0.00	0.00	0.00	0.00
5	5.12	24	0.00	0.00	0.00	0.00	0.00	0.00
		417	0.00	0.00	0.00	0.00	0.00	0.00
		709	0.00	0.00	0.00	0.00	0.00	0.00
6	5.12	24	0.00	0.00	0.00	0.00	0.00	0.00
		417	0.07	-0.06	0.15	-0.12	0.14	-0.11
		709	0.00	0.00	0.00	0.00	0.00	0.00
7	5.12	14	0.08	-0.08	0.17	-0.16	0.16	-0.15
		417	0.00	0.00	0.00	0.00	0.00	0.00
		709	0.00	0.00	0.00	0.00	0.00	0.00
8	5.12	525	0.00	0.00	0.00	0.00	0.00	0.00
		699	0.00	0.00	0.00	0.00	0.00	0.00
		977	0.00	0.00	0.00	0.00	0.00	0.00
9	5.12	24	0.00	0.00	0.00	0.00	0.00	0.00
		672	0.07	-0.08	0.15	-0.16	0.14	-0.15
		709	0.00	0.00	0.00	0.00	0.00	0.00

Besides the calculations using the analytical model, floor accelerations were also calculated using AISC Design Guide (2016) for the case of increased slab thickness (d=180 mm). The results for one walking people cases are given below.

For ground floor (one people):

$$\frac{\alpha_p}{g} = \left(\frac{154.2}{31406}\right)\left(\frac{2.0^{1.43}}{13.92^{0.3}}\right)\sqrt{\frac{1 - e^{-4\pi*7*\beta}}{7*\pi\beta}}$$

$$\frac{\alpha_p}{g} = 0.0082$$

The peak acceleration is less than the acceleration limit, α_0/g, of 0.0094 g. The floor is determined to be satisfactory.

For second floor (one people):

$$\frac{\alpha_p}{g} = \left(\frac{154.2}{31406}\right)\left(\frac{2.0^{1.43}}{13.92^{0.3}}\right)\sqrt{\frac{1 - e^{-4\pi*7*\beta}}{7*\pi\beta}}$$

$$\frac{\alpha_p}{g} = 0.0083$$

The peak acceleration is less than the acceleration limit, α_0/g, of 0.0094 g. The floor is determined to be satisfactory.

The floor acceleration for the ground and second floors does not meet the limit values considering two or more persons are walking.

5.3. Discussion of Results

As a result of the calculations both AISC (2016) and the analytical model, the estimated peak acceleration ratio due to human movement were compared with the limits. The floor acceleration limit value for office buildings is 0.005 g in the 4–8 Hz range. The frequencies of the floors that we examined were calculated as 12.2 Hz and 11.2 Hz so the limit values of acceleration ratio for these frequencies values were determined as 0.0076 g and 0.0070 g, respectively. In this case, the existing floor system was found to not meet the serviceability conditions for the case of two or less walking people. Therefore, the floors should be made stiffer to mitigate vibration effects and keep them below limit values. Increasing the thickness of floor can be an alternative solution. However, while this process is made, considering the weakness of the beams in the system, strengthening of the beams was also recommended for this building. In the case of increased slab thickness, it was seen that the new floor system is more convenient for the examined office building.

CHAPTER 6

CONCLUSION

6.1. Introduction

In this study, ambient vibration records were used to estimate the dynamic properties of the building and to determine the acceleration of the floor on the ground and second floors. In addition, the results from both the finite element analyses and measurements were compared with the limits given in AISC Vibrations of Steel-Framed Structural Systems Due to Human Activity Design Guide Series-11 (2016) to determine whether the building satisfies floor vibration requirements. Due to the flexible floor system, it has been observed that permissible floor vibration levels have been exceeded in the current building. The floor vibration levels were shown to reduce when slabs were made stiffer.

6.2. Conclusion

In this study, a six-story reinforced concrete office building in Ankara, Turkey was investigated. The dynamic properties (natural frequencies, mode shapes, damping ratios) were determined by using experimental and theoretical modal analysis methods. When the results were considered, it was seen that there were some differences between the analytical model and the experimental results. The exterior infill walls represented through diagonal strut elements were added to the analytical model, considering that these differences were due to the inadequate of the stiffness. The modulus of elasticity and dimensions of these elements were also evaluated according to various regulations such as TEC (2007), FEMA 356 (2000), Eurocode 6 (2005). The fist mode in the Y direction was found the same as that obtained from experimental measurements. Also, it was seen that there was an improvement in other modes as well. As a result, information about the dynamic characteristics of the

structure and the current state of the structure were identified using ambient vibration records. Furthermore, a more accurate analytical model of existing buildings was obtained using these records.

Vibration analysis of the ground and second floor slabs of the investigated building were performed, and the suitability of these slabs was investigated according to the vibration limit values given in the literature. According to the AISC Steel Design Guide Series-11, the acceleration of the vibration movement occurred in the slabs under the effect of walking people was found as 1.06 and 1.09 percent of g, respectively, for one person. These values increased as the number of existing people increased on the slabs and they exceeded the limit values of 0.76 (for ground floor) and 0.70 (for second floor) percent of g. Therefore, these slabs were found to be inconvenient for office buildings in terms of floor vibrations. Hence, thickness of the slabs should be increased in order to mitigate vibration impacts and keep them under the limit values. After increasing the slab thickness it was shown that the value of vibration acceleration was below the limit values.

REFERENCES

AISC, Steel Design Guide Series-11, 2016, Vibrations of Steel-Framed Structural Systems Due to Human Activity, American Institute of Steel Construction, Chicago, IL.

Allen, D. E., 1990, Building Vibration from Human Activities, Concrete International: Design & Construction, 12(6), 66-73.

Allen, D. E., and Rainer, J. H., 1976, Vibration Criteria for Long-Span Floors, Canadian Journal of Civil Engineering, 3(2), 165-173.

Allen, D. E., Murray, T. M., 1993, Design Criterion for Vibrations Due to Walking, Engineering Journal, AISC, 30 (4), 117-129.

ARTeMIS Extractor, 2019, Structural Vibration Solutions A/S, NOVI Science Park, Niels Jernes Vej 10, DK-9220 Alborg East, Denmark

Arup, O., 2004, Hospital Floor Vibration Study, Comparison of Possible Hospital Floor Structures with Respect to NHs Vibration Criteria, London.

ASCE, 2000, FEMA 356 Prestandard and Commentary for the Seismic Rehabilitation of Buildings, ASCE for the Federal Emergency Management Agency, Washington, D.C., November.

Bachmann, H., and Ammann, W., 1987, Vibrations in structures induced by man and machines, Structural Engineering Document No.3e, International Association for Bridge and Structural Engineering (IABSE), Zürich, Switzerland.

Baspolat, E., Bayraktar, A., Başağa, H. B., Türker, T., 2013, Deriner Beton Kemer Barajının Deneysel Dinamik Özelliklerinin Belirlenmesi, 2nd Türkiye Deprem Mühendisliği ve Sismoloji Konferansı, Hatay, Türkiye, 1-10.

Bayülke, N., 2003. Betonarme yapının dolgu duvarı, TMH, 426/4.

Brincker, R., Zhang, L., Andersen, P., 2000, Modal Identification from Ambient Responses using Frequency Domain Decomposition, 18th International Modal Analysis Conference, San Antonio, USA, 4062, 625-630.

Brincker, R., Zhang, L., Andersen, P., 2001, Modal identification of output-only systems using frequency domain decomposition, Smart Materials and Structures, 10, 441-445.

Carder, D. S., 1936, Observed Vibrations of Buildings, Bulletin of the Seismological Society of America, 26, 245-277.

Celebi, M., 2013, Seismic Monitoring of Structures and New Developments, Earthquake and Health Monitoring of Civil Structures.

Celebi, M., and Safak, E., 1991, Seismic Response of Transamerica Building I: Data and Preliminary Analysis, J. Struct. Eng., 117(8), 2389-2404.

Celik, O. C., Sucuoglu, H., Akyuz, U., 2015, Forced Vibration Testing and Finite Element Modeling of a Nine-Story Reinforced Concrete Flat Plate-Wall Building, Earthquake Spectra, 31, 1069-1081.

Celik, O.C., 2016. Effect of AAC Infill Walls on Structural System Dynamics of a Concrete Building, Journal of Earthquake Engineering, 20:5, 738-748.

CEN, 2005, Eurocode 6: design of masonry structures – part 1-1: common rules for reinforced and unreinforced masonry structures, EN 1996-1-1:2005, Brussles.

Chopra, A. K., 1995, Dynamics of Structures, Prentice Hall, Upper Saddle River, New Jersey.

Chrysostomou, C.Z., and Asteris, P.G., 2012. On the in-plane properties and capacities of infilled frames, Engineering Structures, 41,385-402.

Chung, L., Park, T., Woo, S. S., 2016, Vertical Shaking Accident and Cause Investigation of 39story Office Building, Journal of Asian Architecture and Building Engineering, 15 (3), 619-625.

Clinton, J. F., Bradford, S. C., Heaton, T. H., Favela, J., 2006, The Observed Wander of the Natural Frequencies in a Structure, Bulletin of the Seismological of America, 96(1), 237-257.

Crawford, R., Ward, H. S., 1964, Determination of the Natural Periods of Building, Bulletin of the Seismological Society of America. 54, 1743-1756.

CSI, 2019, CSI Analysis Reference Manual for SAP2000, Computers and Structures, Inc., Berkeley, California.

Cunha, A., and Caetano, E., 2005, From Input-Output to Output-Only Modal Identification of Civil Engineering Structures, IOMAC, Denmark.

Davenny, B., 2010, Footfall Induced Vibrations Healthcare Facilities, Health Care DesignMagazine,https://www.healthcaredesignmagazine.com/architecture/fo otfall-induced-vibrations-healthcare-facilities. Retrieved Date: 23 March 2014, time: 2.54 pm

Debney, P., and Willford, M., 2009, Footfall Vibration and Finite Element Analysis, Sound & Vibration, 11-14.

Dhanasekar, M., and Page, A. W., 1986, The influence of brick masonry infill properties on the behavior of infilled frames, Proc. Instn Civ. Engrs., Part 2, 81, 593-605.

Foutch, D. A., Housner, G. W., Jennings, P. C., 1975, Dynamic Responses of Six Multistory Buildings During the San Fernando Earthquake, California Institute of Technology Earthquake Engineering Research Laboratory, Report No. EERL 75-02. Pasadena, California.

Gajalakshmi, G., Mohaideen, J. A., Kumar, A. R. S., 2015, Analysis of Harmonic Behavior of Human Rhythmic Activity in A RCC Roof Slab, International Journal of Innovative Science, Engineering & Technology, 2 (5), 628-636.

Gentile, C., and Sais, A., 2007, Ambient Vibration Testing of Historic Masonry Towers for Structural Identification and Damage Assessment, Journal of Construction and Building Materials, 21, 1311-1321.

Guralp Systems, 2009, Data Acquisition System User Manual, England.

ISO, 1989, Evaluation of Human Exposure to Whole-Body Vibration-Part:2: Human Exposure to Continuous and Shock-Induced Vibration in Buildings (1 to 80 Hz), ISO 2631-2, International Standards Organization, Geneva, Switzerland.

Ivanovic, S. S., Trifunac, M. D., Novikova, E. I., Gladkov, A. A., Todorovska, M. I., 2000, Ambient Vibration Tests of a Seven Story Reinforced Concrete Building in Van Nuys, California, Damaged by the 1994 Northridge Earthquake, Soil Dynamics and Earthquake Engineering, 19, 391-411.

Jacobsen, N. J., Andersen, P., Brincker, R., (2006), Using Enhanced Frequency Domain Decomposition as a Robust Technique to Harmonic Excitation in Operational Modal Analysis, Proceedings of ISMA2006: International Conference on Noise & Vibration Engineering, Leuven, Belgium.

Japan Institute of Architects and Japan Aseismic Safety Organization, Earthquake-resistant Design for Architects, Revised edition, 2015.

Kumar, P., and Kumar, A., 2014, Human Induced Vibration in Structures, Int. J. Mech. Eng. & Rob. Res., 1 (1), 44-54.

Lee, P. J., Lee, B. K., Griffin, M. J., 2015, Evaluation of Floor Vibrations Induced by Walking Barefoot in Heavyweight Buildings, Acta Acustica united with Acustica, 101(6), 1199-1210, November.

Lenzen, K. H., 1966, Vibration of Steel Joist-Concrete Slab Floors, Engineering Journal, AISC, 3, 133-136.

Li, W. W., Wong, C. T., Leung, M. K., Fung, S. C., 2011, Floor Vibration due to Human Rhythmic Activities: Tin Shui Wai Public Library Cum Indoor Recreation Centre, Procedia Engineering, 14, 3285-3292.

Magalhaes, F., Brincker, R., Cunha, A., 2010, Damping Estimation Using Free Decays and Ambient Vibration Tests, Mechanical Systems and Signal Processing, 24(5), 1274-1290

Mainstone, R. J., and Weeks, G. A., 1970, The influence of a bounding frame on the racking stiffness and strengths of brick walls, Proc. 2nd Int. Conf. on Brick Masonry, Stoke-on-Trent, England, 165-171.

Mehrabi, A.B., Shing, P.B., Schuller, M.P., Noland, J.L., 1996. Experimental evaluation of masonry-infilled RC frames, Journal of Structural Engineering, 122(3), 228-237.

Michel, C., Gueguen, P., Bard, P. Y., 2008, Dynamic parameters of structures extracted from ambient vibration measurements: an aid for the seismic vulnerability assessment of existing buildings in moderate seismic hazard region, Soil Dynamics and Earthquake Engineering, 28(8), 593-604.

Murray, T. M., 1981, Acceptability Criterion for Occupant-Induced Floor Vibrations, Engineering Journal, AISC, 18, 62-70.

Murray, T. M., 1991, Building Floor Vibrations, Engineering Journal, AISC, 28, 102-109.

Murray, T. M., 2001, Tips for Avoiding Office Building Floor Vibration, Modern Steel Construction.

Naeim, F., 1991, Design Practice to Prevent Floor Vibrations, Structural Steel Educational Council, Technical Information and Product Service, California, USA.

Rea, D., and Bouwkamp, J. G., 1971, Dynamic Properties of Timber School Buildings, Bulletin of the Seismological Society of America, 4 (61), 961-974.

Reiher, H., and Meister, F. J., 1931, The effect of Vibration on People, Translated from Forsch. Geb. Ing. Wes: 2(11) 381-6, by U.S. Air Material Command, Translation F-TS-616-RE, Wright Field, Ohio, AMC, 1946.

Safak, E., and Cakti, E., 2014, Simple Techniques to Analyze Vibration Records from Buildings, 7th European Workshop on Structural Health Monitoring, Nantes, France.

Safak, E., and Celebi, M., 1990a, New Techniques in Record Analyses: Torsional Vibrations, In Proceedings of the Fourth U. S. National Conference on Earthquake Engineering, May 20-24, Palm Springs, California, 2, 411-420.

Sampaio, R. A., and Souza, R. M., 2015, Vibration Analysis of a Residential Building, MATEC Web of Conference, 24, 09007.

Sanuier, N., El Husseini, A., Ismail, K., Morency, C., Auberlet, J. M., Sayed, T., 2011, Pedestrian Stride Frequency and Length Estimation in Outdoor Urban Environments using Video Sensors.

Sattar, S., and Liel, A.B., 2010. Seismic performance of reinforced concrete frame structures with and without masonry infill walls, Proceedings of the 9th US National and 10th Canadian Conference on Earthquake Engineering, Toronto, Canada.

Shabbir, F., and Omenzetter, P., 2008, Forced Vibration Testing of a Thirteen Storey Concrete Building, In Proceedings of the New Zealand Society for Earthquake Engineering Annual Conference, New Zealand.

Skolnik, D., Lei, Y., Yu, E., Wallace, J. W., 2006, Identification, Model Updating, and Response Prediction of an Instrumented 15-Story Steel-Frame Building, Earthquake Spectra, 3 (22), 781-802.

Smith, V. K., and Korman, M. S., 2012, Floor Vibration Response to Irish Dancing, The Journal of the Acoustical Society of America, 132 (3).

Soyoz, S., Taciroglu, E., Orakcal, K., Nigbor, R., Skolnik, D., Lus, H., Safak, E., 2013, Ambient and Forced Vibration Testing of a Reinforced Concrete Building before and after Its Seismic Retrofitting, Journal of Structural Engineering, 139(10), 1741-1752.

Stafford, S.B., and Carter, C., 1969. A method of analysis for infilled frames, ICE Proceedings, 44(1), 31-48.

Trifunac, M. D., 1970a, Ambient Vibration Test of a 39-Story Steel Frame Building, Report EERL 70-02, Earthq. Eng. Res. Lab., Calif. Institute of Tech., Pasadena, California, USA.

Trifunac, M. D., 1970b, Wind and Microtremors Induced Vibrations of a 22-Story Steel Frame Building, Report EERL 70-011, Earthq. Eng. Res. Lab., Calif. Institute of Tech., Pasadena, California, USA.

Trifunac, M. D., 1972, Comparison between Ambient and Forced Vibration Experiments, Earthquake Engineering and Structural Dynamics, 1, 133-150.

Trifunac, M. D., Ivanovic, S. S., Todorovska, M. I., 2001, Apparent Periods of A Building I: Fourier Analysis, Journal of Structural Engineering, 127 (5), 517-526.

Turkish Earthquake Code, 2007, Ministry of Public Works and Settlement, Specification for Structures to be Built in Disaster Areas, Government of Republic of Turkey, Ankara.

Turkish Standards Institute, 2000, Requirements for Design and Construction of Reinforced Concrete Structures, TS 500, Ankara, Turkey.

Udwadia, F. E., and Trifunac, M. D., 1973, Ambient Vibration Test of Full-Scale Structure, Proc. 5th World Conference on Earthquake Engineering, Rome, Italy.

Ventura, C. E., Finn, W. D. L., Lord, J. F., Fujita, N., 2003, Dynamic Characteristics of a Base Isolated Building from Ambient Vibration Measurements and Low Level Earthquake Shaking, Soil Dynamics and Earthquake Engineering, 23, 313-322.

Ventura, C. E., Laverick, B., Brincker, R., Andersen, P., 2003, Comparison of Dynamic Characteristics of Two Instrumented Tall Buildings, In Proceedings of IMAC-21: A Conference on Structural Dynamics, the Hyatt Orlando, Kissimmee, Florida, 236-242.

Ventura, C. E., Lord, J. F., Simpson, R. D., 2002, Effective Use of Ambient Vibration Measurements for Modal Updating of a 48 Storey Building in Vancouver, Canada, International Conference on Structural Dynamic Modeling-Test, Analysis, Correlation and Validation Instituto de Engenharia Macanica, Madeira Island, Portugal.

Ventura, C.E., and Horyna, T., 2000, Measured and Calculated Modal Characteristics of the Heritage Court Tower in Vancouver, B.C., INTERNATIONAL MODAL ANALYSIS CCONFERENCE-XVIII: A Conference on Structural Dynamics, 1070-1074.

Ward, H. S., and Crawford, R., 1966, Wind Induced Vibrations and Building Modes, Bulletin of the Seismological Society of America, 50, 793-813.

Yu, E., Skolnik, D., Whang, D. H., Wallace, J. W., 2008, Forced Vibration Testing of a Four-Story Reinforced Concrete Building, Earthquake Spectra, 4 (24), 969-995.

APPENDICES

A. The cross sectional dimensions of the columns

Location	ID	Section	L (m)	ID	Section	L (m)
Basement Floor	K100 – S1	40 x 40	2.97	K100 – S28	50 x 45	2.97
	K100 – S2	40 x 40	2.97	K100 – S29	60 x 45	2.97
	K100 – S3	40 x 40	2.97	K100 – S30	60 x 50	2.97
	K100 – S4	40 x 40	2.97	K100 – S31	55 x 50	2.97
	K100 – S5	40 x 40	2.97	K100 – S32	55 x 55	2.97
	K100 – S6	40 x 40	2.97	K100 – S33	55 x 55	2.97
	K100 – S7	40 x 40	2.97	K100 – S34	40 x 40	2.97
	K100 – S8	35 x 40	2.97	K100 – S35	55 x 60	2.97
	K100 – S9	55 x 60	2.97	K100 – S36	55 x 55	2.97
	K100 – S10	60 x 60	2.97	K100 – S37	30 x 30	2.97
	K100 – S11	50 x 60	2.97	K100 – S38	50 x 60	2.97
	K100 – S12	60 x 55	2.97	K100 – S39	50 x 60	2.97
	K100 – S13	55 x 60	2.97	K100 – S40	65 x 85	2.97
	K100 – S14	40 x 40	2.97	K100 – S41	55 x 65	2.97
	K100 – S15	35 x 30	2.97	K100 – S42	80 x 85	2.97
	K100 – S16	55 x 55	2.97	K100 – S43	40 x 40	2.97
	K100 – S17	60 x 45	2.97	K100 – S44	35x 40	2.97

	K100 – S21	60 x 50	2.97	K100 – S45	50 x 60	2.97
	K100 – S22	60 x 45	2.97	K100 – S46	60 x 60	2.97
	K100 – S23	55 x 50	2.97	K100 – S47	60 x 70	2.97
	K100 – S24	40 x 40	2.97	K100 – S48	75 x 90	2.97
	K100 – S25	55 x 60	2.97	K100 – S49	40 x 45	2.97
	K100 – S26	55 x 55	2.97	K100 – S50	40 x 45	2.97
	K100 – S27	50 x 60	2.97			
Ground Floor	K200 – S1	35 x 40	3.00	K200 – S28	50 x 45	3.00
	K200 – S2	35 x 40	3.00	K200 – S29	50 x 45	3.00
	K200 – S3	35 x 40	3.00	K200 – S30	45 x 50	3.00
	K200 – S4	35 x 40	3.00	K200 – S31	55 x 50	3.00
	K200 – S5	30 x 40	3.00	K200 – S32	50 x 50	3.00
	K200 – S6	30 x 40	3.00	K200 – S33	55 x 50	3.00
	K200 – S7	40 x 40	3.00	K200 – S34	40 x 35	3.00
	K200 – S8	35 x 30	3.00	K200 – S35	35 x 40	3.00
	K200 – S9	50 x 60	3.00	K200 – S36	50 x 50	3.00
	K200 – S10	55 x 60	3.00	K200 – S37	30 x 30	3.00
	K200 – S11	50 x 60	3.00	K200 – S38	50 x 55	3.00
	K200 – S12	60 x 50	3.00	K200 – S39	50 x 55	3.00
	K200 – S13	50 x 60	3.00	K200 – S40	65 x 75	3.00
	K200 – S14	40 x 35	3.00	K200 – S41	55 x 55	3.00

	K200 – S15	35 x 30	3.00	K200 – S42	70 x 75	3.00
	K200 – S16	50 x 55	3.00	K200 – S43	40 x 35	3.00
	K200 – S17	50 x 45	3.00	K200 – S44	35 x 40	3.00
	K200 – S21	50 x 45	3.00	K200 – S45	40 x 40	3.00
	K200 – S22	50 x 45	3.00	K200 – S46	40 x 40	3.00
	K200 – S23	55 x 50	3.00	K200 – S47	40 x 40	3.00
	K200 – S24	40 x 40	3.00	K200 – S48	40 x 60	3.00
	K200 – S25	35 x 40	3.00	K200 – S49	40 x 35	3.00
	K200 – S26	50 x 50	3.00	K200 – S50	40 x 40	3.00
	K200 – S27	45 x 50	3.00			
First Floor	K300 – S1	30 x 40	3.00	K300 – S28	50 x 45	3.00
	K300 – S2	50 x 45	3.00	K300 – S29	50 x 45	3.00
	K300 – S3	30 x 35	3.00	K300 – S30	45 x 50	3.00
	K300 – S4	30 x 35	3.00	K300 – S31	50 x 45	3.00
	K300 – S5	30 x 35	3.00	K300 – S32	50 x 45	3.00
	K300 – S6	27 x 35	3.00	K300 – S33	50 x 50	3.00
	K300 – S7	27 x 35	3.00	K300 – S34	35 x 25	3.00
	K300 – S8	30 x 30	3.00	K300 – S35	30 x 30	3.00
	K300 – S9	50 x 50	3.00	K300 – S36	50 x 50	3.00
	K300 – S10	50 x 50	3.00	K300 – S37	30 x 30	3.00
	K300 – S11	50 x 50	3.00	K300 – S38	50 x 50	3.00

	K300 – S12	50 x 50	3.00	K300 – S39	50 x 50	3.00
	K300 – S13	50 x 50	3.00	K300 – S40	50 x 50	3.00
	K300 – S14	35 x 27	3.00	K300 – S41	50 x 50	3.00
	K300 – S15	30 x 30	3.00	K300 – S42	50 x 50	3.00
	K300 – S16	50 x 50	3.00	K300 – S43	35 x 30	3.00
	K300 – S17	50 x 45	3.00	K300 – S44	30 x 30	3.00
	K300 – S21	50 x 45	3.00	K300 – S45	30 x 30	3.00
	K300 – S22	50 x45	3.00	K300 – S46	30 x 30	3.00
	K300 – S23	50 x 50	3.00	K300 – S47	30 x 35	3.00
	K300 – S24	35 x 27	3.00	K300 – S48	30 x 35	3.00
	K300 – S25	30 x 30	3.00	K300 – S49	30 x 35	3.00
	K300 – S26	50 x 50	3.00	K300 – S50	35 x 30	3.00
	K300 – S27	45 x 50	3.00			
Second Floor	K400 – S1	30 x 40	3.00	K400 – S28	50 x 45	3.00
	K400 – S2	50 x 45	3.00	K400 – S29	50 x 45	3.00
	K400 – S3	30 x 35	3.00	K400 – S30	45 x 50	3.00
	K400 – S4	30 x 35	3.00	K400 – S31	50 x 45	3.00
	K400 – S5	30 x 35	3.00	K400 – S32	50 x 45	3.00
	K400 – S6	27 x 35	3.00	K400 – S33	50 x 50	3.00
	K400 – S7	27 x 35	3.00	K400 – S34	35 x 25	3.00
	K400 – S8	30 x 30	3.00	K400 – S35	30 x 30	3.00

	K400 – S9	50 x 50	3.00	K400 – S36	50 x 50	3.00
	K400 – S10	50 x 50	3.00	K400 – S37	30 x 30	3.00
	K400 – S11	50 x 50	3.00	K400 – S38	50 x 50	3.00
	K400 – S12	50 x 50	3.00	K400 – S39	50 x 50	3.00
	K400 – S13	50 x 50	3.00	K400 – S40	50 x 50	3.00
	K400 – S14	35 x 27	3.00	K400 – S41	50 x 50	3.00
	K400 – S15	30 x 30	3.00	K400 – S42	50 x 50	3.00
	K400 – S16	50 x 50	3.00	K400 – S43	35 x 30	3.00
	K400 – S17	50 x 45	3.00	K400 – S44	30 x 30	3.00
	K400 – S21	50 x 45	3.00	K400 – S45	30 x 30	3.00
	K400 – S22	50 x 45	3.00	K400 – S46	30 x 30	3.00
	K400 – S23	50 x 50	3.00	K400 – S47	30 x 35	3.00
	K400 – S24	35 x 27	3.00	K400 – S48	30 x 35	3.00
	K400 – S25	30 x 30	3.00	K400 – S49	30 x 35	3.00
	K400 – S26	50 x 50	3.00	K400 – S50	35 x 30	3.00
	K400 – S27	45 x 50	3.00			
Third Floor	K500 – S1	30 x 40	3.10	K500 – S28	50 x 45	3.10
	K500 – S2	50 x 45	3.10	K500 – S29	50 x 45	3.10
	K500 – S3	30 x 35	3.10	K500 – S30	45 x 50	3.10
	K500 – S4	30 x 35	3.10	K500 – S31	50 x 45	3.10
	K500 – S5	30 x 35	3.10	K500 – S32	50 x 45	3.10

	K500 – S6	27 x 35	3.10	K500 – S33	50 x 50	3.10
	K500 – S7	27 x 35	3.10	K500 – S34	35 x 25	3.10
	K500 – S8	30 x 30	3.10	K500 – S35	30 x 30	3.10
	K500 – S9	50 x 50	3.10	K500 – S36	50 x 50	3.10
	K500 – S10	50 x 50	3.10	K500 – S37	30 x 30	3.10
	K500 – S11	50 x 50	3.10	K500 – S38	50 x 50	3.10
	K500 – S12	50 x 50	3.10	K500 – S39	50 x 50	3.10
	K500 – S13	50 x 50	3.10	K500 – S40	50 x 50	3.10
	K500 – S14	35 x 27	3.10	K500 – S41	50 x 50	3.10
	K500 – S15	30 x 30	3.10	K500 – S42	50 x 50	3.10
	K500 – S16	50 x 50	3.10	K500 – S43	35 x 30	3.10
	K500 – S17	50 x 45	3.10	K500 – S44	30 x 30	3.10
	K500 – S21	50 x 45	3.10	K500 – S45	30 x 30	3.10
	K500 – S22	50 x 45	3.10	K500 – S46	30 x 30	3.10
	K500 – S23	50 x 50	3.10	K500 – S47	30 x 35	3.10
	K500 – S24	35 x 27	3.10	K500 – S48	30 x 35	3.10
	K500 – S25	30 x 30	3.10	K500 – S49	30 x 35	3.10
	K500 – S26	50 x 50	3.10	K500 – S50	35 x 30	3.10
	K500 – S27	45 x 50	3.10			
Fourth Floor	K600 – S1	30 x 40	2.60	K600 – S28	50 x 45	2.60
	K600 – S2	50 x 45	2.60	K600 – S29	50 x 45	2.60

K600 – S3	30 x 35	2.60	K600 – S30	45 x 50	2.60
K600 – S4	30 x 35	2.60	K600 – S31	50 x 45	2.60
K600 – S5	30 x 35	2.60	K600 – S32	50 x 45	2.60
K600 – S6	27 x 35	2.60	K600 – S33	50 x 50	2.60
K600 – S7	27 x 35	2.60	K600 – S34	35 x 25	2.60
K600 – S8	30 x 30	2.60	K600 – S35	30 x 30	2.60
K600 – S9	50 x 50	2.60	K600 – S36	50 x 50	2.60
K600 – S10	50 x 50	2.60	K600 – S37	30 x 30	2.60
K600 – S11	50 x 50	2.60	K600 – S38	50 x 50	2.60
K600 – S12	45 x 50	2.60	K600 – S39	45 x 50	2.60
K600 – S13	50 x 45	2.60	K600 – S40	50 x 50	2.60
K600 – S14	35 x 27	2.60	K600 – S41	50 x 50	2.60
K600 – S15	30 x 30	2.60	K600 – S42	50 x 50	2.60
K600 – S16	50 x 50	2.60	K600 – S43	35 x 30	2.60
K600 – S17	50 x 45	2.60	K600 – S44	30 x 30	2.60
K600 – S21	50 x 45	2.60	K600 – S45	30 x 30	2.60
K600 – S22	50 x 45	2.60	K600 – S46	30 x 30	2.60
K600 – S23	50 x 50	2.60	K600 – S47	30 x 35	2.60
K600 – S24	35 x 27	2.60	K600 – S48	30 x 35	2.60
K600 – S25	30 x 30	2.60	K600 – S49	30 x 35	2.60
K600 – S26	50 x 50	2.60	K600 – S50	35 x 30	2.60

	K600 – S27	45 x 50	2.60			
Fifth Floor	K700 – S1	30 x 40	2.90	K700 – S28	50 x 45	2.90
	K700 – S2	50 x 45	2.90	K700 – S29	50 x 45	2.90
	K700 – S3	30 x 35	2.90	K700 – S30	45 x 50	2.90
	K700 – S4	30 x 35	2.90	K700 – S31	50 x 45	2.90
	K700 – S5	30 x 35	2.90	K700 – S32	50 x 45	2.90
	K700 – S6	27 x 35	2.90	K700 – S33	50 x 50	2.90
	K700 – S7	27 x 35	2.90	K700 – S34	35 x 25	2.90
	K700 – S8	30 x 30	2.90	K700 – S35	30 x 30	2.90
	K700 – S9	50 x 50	2.90	K700 – S36	50 x 50	2.90
	K700 – S10	50 x 50	2.90	K700 – S37	30 x 30	2.90
	K700 – S11	50 x 50	2.90	K700 – S38	50 x 50	2.90
	K700 – S12	45 x 50	2.90	K700 – S39	45 x 50	2.90
	K700 – S13	50 x 45	2.90	K700 – S40	50 x 50	2.90
	K700 – S14	35 x 27	2.90	K700 – S41	50 x 50	2.90
	K700 – S15	30 x 30	2.90	K700 – S42	50 x 50	2.90
	K700 – S16	50 x 50	2.90	K700 – S43	35 x 30	2.90
	K700 – S17	50 x 45	2.90	K700 – S44	30 x 30	2.90
	K700 – S21	50 x 45	2.90	K700 – S45	30 x 30	2.90
	K700 – S22	50 x 45	2.90	K700 – S46	30 x 30	2.90
	K700 – S23	50 x 50	2.90	K700 – S47	30 x 35	2.90

ID	Section	L (m)	ID	Section	L (m)
K700 – S24	35 x 27	2.90	K700 – S48	30 x 35	2.90
K700 – S25	30 x 30	2.90	K700 – S49	30 x 35	2.90
K700 – S26	50 x 50	2.90	K700 – S50	35 x 30	2.90
K700 – S27	45 x 50	2.90			

B. The cross sectional dimensions of the shear walls

ID	Section	Opening	L (m)
P1 – K100	285 x 25	125	2.97
P1 – K200	285 x 25	125	2.97
P1 – K300	285 x 25	125	2.97
P1 – K400	285 x 25	125	2.97
P1 – K500	285 x 25	125	2.97
P1 – K600	285 x 25	125	2.97
P1 – K700	285 x 25	125	2.97
P2 – K100	297 x 25	125	3.00
P2 – K200	297 x 25	125	3.00
P2 – K300	297 x 25	125	3.00
P2 – K400	297 x 25	125	3.00
P2 – K500	297 x 25	125	3.00
P2 – K600	297 x 25	125	3.00
P2 – K700	297 x 25	125	3.00
P3 – K100	354 x 25	125	3.00
P3 – K200	354 x 25	125	3.00
P3 – K300	354 x 25	125	3.00
P3 – K400	354 x 25	125	3.00
P3 – K500	354 x 25	125	3.00
P3 – K600	354 x 25	125	3.00

P3 – K700	354 x 25	125	3.00
P4 – K100	325 x 25	125	3.00
P4 – K200	325 x 25	125	3.00
P4 – K300	325 x 25	125	3.00
P4 – K400	325 x 25	125	3.00
P4 – K500	325 x 25	125	3.00
P4 – K600	325 x 25	125	3.00
P4 – K700	325 x 25	125	3.00
P5 – K100	25 x 493	125	3.10
P5 – K200	25 x 493	125	3.10
P5 – K300	25 x 493	125	3.10
P5 – K400	25 x 493	125	3.10
P5– K500	25 x 493	125	3.10
P5 – K600	25 x 493	125	3.10
P5 – K700	25 x 493	125	3.10
P6 – K100	25 x 470	125	2.90
P6 – K200	25 x 470	125	2.90
P6 – K300	25 x 470	125	2.90
P6 – K400	25 x 470	125	2.90
P6 – K500	25 x 470	125	2.90
P6 – K600	25 x 470	125	2.90
P6 – K700	25 x 470	125	2.90
P7 – K100	25 x 473	125	2.90
P7 – K200	25 x 473	125	2.90
P7 – K300	25 x 473	125	2.90
P7 – K400	25 x 473	125	2.90
P7 – K500	25 x 473	125	2.90
P7 – K600	25 x 473	125	2.90
P7 – K700	25 x 473	125	2.90

P8 – K100	25 x 477	125	2.90
P8 – K200	25 x 477	125	2.90
P8 – K300	25 x 477	125	2.90
P8 – K400	25 x 477	125	2.90
P8 – K500	25 x 477	125	2.90
P8 – K600	25 x 477	125	2.90
P8 – K700	25 x 477	125	2.90